STUDY OF CERTAIN GEOTECHNICAL PROPERTIES OF BEAUMONT CLAY

A Dissertation

By

MOHAMAD TAYEB HUSSAIN AL-LAYLA

Submitted to the Graduate College of
Texas A&M University in
partial fulfillment of the requirement for the degree of

DOCTOR OF PHILOSOPHY

January 1970

Major Subject: Civil Engineering

STUDY OF CERTAIN GEOTECHNICAL PROPERTIES OF BEAUMONT CLAY

A Dissertation

By

MOHAMAD TAYEB HUSSAIN AL-LAYLA

Approved as to style and content by:

Wayne C. Dunlap
Chairman of Committee

Charles H. Samaan Jr.
(Head of Department)

Harry M. Coyle
(Member)

George W. Kunze
(Member)

L. J. Hirsch
(Member)

Karl J. Koenig
(Member)

ABSTRACT

STUDY OF CERTAIN GEOTECHNICAL PROPERTIES
OF THE BEAUMONT CLAY FORMATION
(January 1970)
Mohamad Tayeb Hussain Al-Layla
B.Sc., University of Baghdad
M.S., Texas A&M University
Directed by: Dr. Wayne A. Dunlap

The Beaumont Clay formation is located in southeast Texas in a belt approximately 70-90 miles wide, parallel to the Gulf of Mexico coastline. It was deposited by rivers as levees and deltas during the Pleistocene epoch. During its geological history is was exposed to the surface and apparently subjected to multiple cycles of drying and wetting. This produced an intricate network of closely spaced weak planes known as fissures. Other weak planes, more widely spaced, are joints. These discontinuities are the major factors in controlling the laboratory shear strength.

In general, Beaumont Clay can be described as stiff, overconsolidated, jointed, and fissured with slickensides. The clay content (<2μ fraction) ranges from 56-77 percent. X-ray diffraction analyses of the clay fraction showed that the material contained about 23-47 percent of montmorillonite with illite, kaolinite and quartz being the other predominant minerals present.

The results of unconsolidated undrained strength tests showed that the shear strength, c_u, obtained from specimens oriented in a horizontal direction was 1.26 of that obtained from specimens oriented in a vertical direction. Comparison of these tests with similar tests on remolded specimens indicated that Beaumont Clay is insensitive.

The consolidated undrained tests revealed that the effective angle of shearing resistance, ϕ', was equal in the horizontal and vertical directions. However, the cohesion intercept, c', was higher in the specimens oriented in a horizontal direction than in the vertical direction. The relation between A_f (pore pressure coefficient at failure) and O.C.R. (over-consolidation ratio) is presented.

The residual angle, ϕ_r', ranged from 8-11^o for Beaumont Clay. A correlation was found to exist between the liquid limit and the residual strength.

The effective angle of shearing resistance, ϕ_d, obtained in the direct shear tests was about 4^o higher than obtained from triaxial drained tests.

All the specimens tested in this study failed at rather small strain. In general, they showed plastic type of failure rather than brittle.

ACKNOWLEDGMENTS

I wish to express my appreciation to Dr. Wayne A. Dunlap, the Chairman of my Graduate Committee, for his assistance and constructive suggestions.

I am indebted to the members of my Graduate Committee: Drs. Harry M. Coyle, Teddy J. Hirsch, Karl J. Koenig and George W. Kunze. Their guidance and advice throughout my academic and research programs were very valuable.

Thanks is extended to Professor Spencer J. Buchanan and his associates for providing the testing samples. The co-operation of all members of the Soil Physics Division of Texas A&M University was helpful.

I am grateful to Mr. Robert E. Bigham and Mr. Lionel J. Milberger for their help.

Acknowlegment is given to the Civil Engineering Department of Rice University for permitting me to borrow their direct shear machine.

Special thanks is due to Mrs. Sherry Teel and Mrs. Sandra Stevens for their expert typing of this manuscript.

And finally, a hearty appreciation is given to my family, without whose generous help I would not have had the opportunity to continue my education.

TO

MY PARENTS

TABLE OF CONTENTS

Chapter

Page

LIST OF TABLES

LIST OF FIGURES

CHAPTER I

INTRODUCTION

A study of the geotechnical properties of Beaumont Clay, which occupies the coastal area of southeast Texas, has both economic and academic value. There has been, and will continue to be, extensive construction activity within the Beaumont formation area. Thus, the fact that little is known about this soil makes this study significant and gives it economic value. From an academic viewpoint, the study is important because there is little information published about soil formations which have stress histories similar to that of Beaumont Clay.

Beaumont Clay gained its present properties as a result of numerous cycles of drying and wetting. Consequently, the clay is desiccated, fissured, and jointed. As a result of these characteristics, the soil engineer faces several difficulties in dealing with problems in Beaumont Clay. Slope failures are frequently encountered and particularly along the Houston ship channel (20)[1]. Settlement predictions, especially of heavy structures as in the case of the San Jacinto Monument (18), are difficult. Caving of shafts drilled for underreamed footings often occurs in certain layers. These and many other problems

---

[1] Numerals in parentheses refer to corresponding items in the list of references. The citations on the following pages follow the style of the Journal of the Soil Mechanics and Foundation Division, American Society of Civil Engineers.

probably can be treated in better fashion if the geotechnical properties are well defined.

For a better understanding of the strength properties of Beaumont Clay--and thus its behavior--the strength parameters of the soil should be defined in terms of effective stress rather than total stress. Indeed, the shear strength and the deformation characteristics of soil are controlled by effective stress rather than total stress (9, 56). The validity of the principal of effective stress in the field of soil mechanics has been demonstrated by several investigators (7, 8, 43).

In this study the strength properties of Beaumont Clay were investigated by means of compression tests (both triaxial and unconfined) and direct shear tests.

In triaxial compression, unconsolidated undrained tests, consolidated undrained tests with pore water pressure measurement, and consolidated drained tests were used. Moreover, the investigation was extended to study the strength properties in the horizontal direction as well as the strength properties of the clay after being remolded.

The strength parameters from drained tests are used in certain long term stability problems, while the results of consolidated undrained tests with pore water pressure measurement are used in determining the pore water pressure coefficients, and also in defining the strength parameters of soil. The study of strength properties in the horizontal direction is desirable in slope stability problems. Investigation on soil in the remolded state gives an indication of the structural effect on the strength properties.

The direct shear test was used to study the concept of residual strength. This is the lower limit of shearing resistance, which occurs at relatively large deformations. According to Skempton (45), it is the main factor in controlling the long term stability of natural slopes and cuts in stiff, fissured clays. Since the residual strength test is time consuming, it is very desirable to relate the residual angle of shearing resistance to some other soil parameter which is easier to determine in the laboratory.

The consolidation properties were studied on specimens which were oriented in the vertical and horizontal direction as well as on remolded specimens. This helped to investigate the effect of stress history on the clay.

In summary, the specific purposes of this investigation were to determine the following for a representative portion of the Beaumont Clay formation:

a. The cohesion intercept, c', and the angle of shearing resistance, ϕ', in terms of effective stress for both undisturbed and remolded samples.

b. The peak and the residual shear strength as determined by direct shear tests.

c. The pore pressure coefficient, A.

d. The variation of shear strength with orientation of the mass.

e. The consolidation properties and the maximum pressure to which the soil has been subjected in its geological

history.

f. The mineralogical properties of the soil and their influence on the geotechnical behavior of the Beaumont Clay.

CHAPTER II

PRESENT STATUS OF THE QUESTION

Extensive studies have been done on soils which are classified as stiff, over-consolidated, and fissured, but these soils, e.g., the London Clay, gained these properties by an overburden pressure which has since been partially removed. On the other hand Beaumont Clay is also stiff, over-consolidated and fissured but as a result of desiccation rather than overburden pressures.

In stability problems involving soils of this type, important characteristics which should be investigated are shear strength (both peak and residual) and the effect of anisotropy. These topics will be discussed in the following paragraphs.

Shear Strength

The shear strength of a soil can be defined as the shear stress on the plane of failure at the time of failure. The shear strength can be divided into three components: cohesion, dilatancy and friction. In turn, each of these components is probably made up of several terms (30).

Cohesion

Cohesion is the shear resistance which can be mobilized between the adjacent particles without the necessity of a normal pressure. It may be regarded as a physico-chemical force acting between

particles. This force depends upon the number of bonding atoms acting between the adjacent particles and their mutual distance. It is mainly the result of summation of the Van der Waals (or attraction) forces, and Coulombic repulsion forces. The cohesion component can be mobilized at relatively small strains during the shearing process.

The cohesion force is a function of the void ratio or water content in saturated soil (12). As the water content increases, the distance between particles increases, and the attraction force decreases. According to the Terzaghi classical theory of consolidation for normally consolidated soil, the void ratio can be related to the effective consolidation pressure. Thus it may be stated that the available cohesion is proportional to the effective consolidation stress, σ_p', (26), and can be expressed as:

$$c' = \sigma_p' \tan\phi_c' \qquad (1)$$

where: c' = the cohesion in terms of effective stress
ϕ_c' = the angle of cohesion shearing resistance

Dilatancy and Friction

During shear displacement, the moving particles interfere with each other both electrically and physically. The particles may climb over each other in order to move in a horizontal direction. This movement may cause a volume increase tendency, which increases the shearing resistance by requiring additional forces to be overcome. The interference between particles disappears after some straining, and the tendency for volume increase no longer exists; thus the dilatancy component drops out from the shearing resistance. The

tendency of volume increase is usually associated with dense material.

During the particles' movement, interparticle friction starts to mobilize and causes the shearing strength to increase, and reaches its limit with further movement.

Dilatancy and friction are usually treated together because of their close relationship. They are direct functions of the effective force normal to the shear surface. Their contribution to the shear strength of soil can be expressed:

$$s = \sigma_i' \tan\phi' \qquad (2)$$

where: σ_i' = the normal effective stress
ϕ' = the angle of shearing resistance in terms of effective stress

The actual shear resistance, which is measured in the laboratory, is a combination of the three components (cohesion, dilatancy, and friction). Fig. 1 shows each force separately and the addition of all the components to give a stress-strain curve, which can be measured in a shear test.

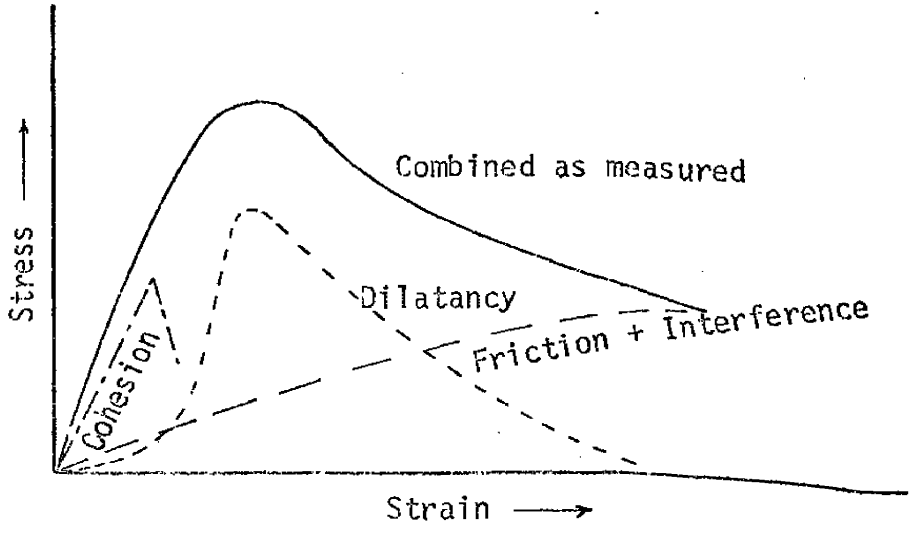

FIG. 1.--COMPONENTS OF SHEAR RESISTANCE (AFTER LAMBE 1960)

The shear strength of soil can be described either in terms of total stress or in terms of effective stress. Bishop and Henkel (9), Lambe (30), Whitman (56) and many others reported that the shear strength of soil is best described in terms of effective stress.

Terzaghi (53) defined the principle of effective stress in the following terms, "The stresses in any point of a section through a mass of earth can be computed from the total principal stresses σ_1, σ_2, σ_3 which act in this point. If the voids of the earth are filled with water under a stress, u, the total principal stresses consist of two parts. One part, u, acts in the water and in the solid in every direction with equal intensity. It is called the neutral stress (or pore-water pressure). The balance, $\sigma_1' = \sigma_1 - u$, $\sigma_2' = \sigma_2 - u$ and $\sigma_3' = \sigma_3 - u$ represents an excess over the neutral stress, u, and it has its seat exclusively in the solid phase of the earth.

"This fraction of the total principal stresses will be called the effective principal stresses. . . A change in the neutral stress, u, produces practically no volume change and has practically no influence on the stress conditions for failure. . . Porous materials (such as sand and clay) react to a change of u as if they were incompressible and as if their internal friction were equal to zero. All the measurable effects of a change in stress, such as compression distortion and a change of shearing resistance are exclusively due to changes in the effective stresses σ_1', σ_2', σ_3'. Hence, every investigation of the stability of a saturated body of soil requires the knowledge of both the total and the neutral stresses."

Bishop and Eldin (8), and Skempton (43) proved the validity of the principal of effective stress in the field of soil mechanics. There are two necessary conditions for the principal of effective stress to be correct in soil and to make the expression $\sigma' = \sigma - u$ correct. First the soil grains must be incompressible, and, second, the yield stress of the soil grains, which control the contact area and intergranular shearing resistance, must be independent of the confining pressure.

Actual soils do not fully satisfy these two conditions. The more correct expression for effective stress can be written as

$\sigma' = \sigma - \kappa u$. Skempton (43) showed that κ can be taken as a constant for a particular soil under a given set of stress conditions. Theoretically κ varies with the stress range and with processes of volume and shear change. It is equal to $(1 - \frac{a \tan\psi}{\tan\phi'})$ for changes in shear strength and to $(1 - \frac{C_s}{C})$ for changes in volume where:

a = the area of contact between the particles, per unit gross area of material
ψ = the angle of intrinsic friction of the solid material
ϕ' = the angle of shearing resistance of the granular material
C_s = the compressibility of the solid substance comprising the particles
C = the compressibility of the soil skeleton

From the above expressions it is clear that κ values are not the same for shear strength and for volume change. Bishop and Blight (7) stated that κ is a function of the stress path being followed and the strain rate being used. Furthermore, they stated that in the range of stress encountered in engineering work the difference in κ values is too small to be observed experimentally.

Terzaghi (53), Bishop and Eldin (8) and Skempton (43) reported that κ can be taken as unity with little error and this approximation is accurate enough for practical purposes.

The well-known Coulomb-Terzaghi equation in the field of soil mechanics is usually used to express shear strength:

$$s = c' + (\sigma - u) \tan\phi' \qquad (3)$$

where: c' = the cohesion intercept
ϕ' = the angle of shearing resistance
σ = the total pressure normal to the plane considered
u = the pore water pressure
s = the shear strength of soil

In dealing with soil mechanics problems and especially with long-term stability, the concept of effective stress becomes important. Bishop and Bjerrum (6) presented several field records showing that the use of effective stress gives more reliable results than total stress in long-term slope stability. Furthermore, they stated that the total stress method ($\phi_u = 0$) can be used in short-term slope stability analysis (end of construction case), where no drainage has taken place, and reliable results can be obtained. However, in over-consolidated fissured clay the $\phi_u = 0$ method can lead to serious problems. Cassel (17), Henkel and Skempton (25), Skempton and LaRochelle (48), Peterson et al. (36), and Mishtak (33) showed that this method often leads to an over-estimation of the factor of safety. This is a result of using the shear strength obtained from small specimens tested in the laboratory. Usually these specimens are not representative of the in situ strength properties (48).

In a stability analysis, two steps are involved: (a) determine the shear strength parameters, c' and ϕ', of the soil and (b) measure or predict the pore pressure. The strength parameters, c' and ϕ', can be determined fairly accurately owing to recent, vast improvements in laboratory techniques.

Consolidated undrained triaxial compression tests with pore pressure measurement provide a basis for estimating the magnitude of pore pressures to be involved in practical problems. However, the pore pressure responds differently according to the type of load applied (9). For this reason, field measurements of pore pressure

are often necessary on many important engineering works (6).

Skempton (42) introduced the pore pressure coefficients, A and B, which forms the basis for estimation of the pore pressures. For saturated soil, the pore pressure change due to a change in total stress may be expressed as:

$$\Delta u = B\,\Delta\sigma_3 + A\,(\Delta\sigma_1 - \Delta\sigma_3) \qquad (4)$$

where: Δu = change in pore pressure
$\Delta\sigma_3$ = change in total minor principal stress
$\Delta\sigma_1$ = change in total major principal stress

A and B are pore pressure coefficients which can be measured in the laboratory. In saturated soil, B usually equals unity. The coefficient A is a function of consolidation pressure, stress history, orientation of particles, and type of test.

Bishop (3) discussed the importance of pore pressure coefficients in practice and demonstrated the usage of them during dam construction and during rapid draw-down.

Henkel proposed another expression for pore pressure (24). He expressed the change in pore water pressure as a function of octahedral stress and octahedral shear, as the following:

$$\Delta u = \beta\,\frac{\Delta\sigma_1+\Delta\sigma_2+\Delta\sigma_3}{3} + a\sqrt{(\Delta\sigma_1-\Delta\sigma_2)^2(\Delta\sigma_2-\Delta\sigma_3)^2(\Delta\sigma_3-\Delta\sigma_1)^2} \qquad (5)$$

where: $\Delta\sigma_1$, $\Delta\sigma_2$, and $\Delta\sigma_3$ are the changes in total stresses
β and a are coefficients to be determined in the laboratory. In a saturated soil, β equals unity.

For the compression test where the cell pressure is kept constant, $\Delta\sigma_2 = \Delta\sigma_3 = 0$ and $\Delta\sigma_1 = (\sigma_1 - \sigma_3)$. The change in pore pressure can be written as:

$$\Delta u = (1/3 + a\sqrt{2})\,(\sigma_1-\sigma_3) \qquad (6)$$

The parameter, a, measures the contribution of the shear stresses to the pore water pressure change.

Henkel's equation has greater general validity than Skempton's equation, owing to the fact that there is a considerable difference in values of A for compression tests and extension tests, whereas corresponding differences in values of a are much smaller.

Anisotropy of Soil

Anisotropy in a soil mass is mainly connected with its structure, which depends on the environmental conditions during which the soil was deposited as well as the stress changes after deposition. Rosenquist (37) demonstrated that clay deposited in salt water acquires an open card house structure with particles randomly oriented. In a fresh water deposit, the structure is somewhat dispersed and a certain degree of parallelism is achieved between the particles. So, in the latter case, the clay will possess some inherent anisotropy. However, during consolidation of a randomly oriented structure under overburden pressure, the isotropic clay may become anisotropic. Consequently, the shear strength of soil may vary with the direction of application of the principal stresses.

Hvorslev (26) investigated the effect of the consolidation process on the orientation of particles in a remolded mass of clay. He concluded that the clay particles in remolded and uniaxially reconsolidated clay have a preferred orientation perpendicular to the direction of the principal consolidation stress. Owing to the orientation of

the particles, the clay may have anisotropic strength, deformation and permeability characteristics.

Bishop (4) reported that the undrained strength of lightly and heavily over-consolidated clay varies with direction of the applied major principal stress. In Weald Clay, which is lightly over-consolidated, the compressive strength with σ_1 horizontal is about 0.75 of the value with σ_1 vertical. In heavily over-consolidated London Clay, the ratio of horizontal to vertical strength is 1.46 as reported by Ward et al. (55). Furthermore, they reported that there is a great reduction in strength for specimens trimmed at an inclination of 45^{o}, with the strength being about 60-90 percent of a vertical sample. This reduction in strength results from weakness along bedding planes which, in specimens trimmed at a 45^{o} orientation, corresponds to the probable direction of the failure surface. Bishop (4) presented the variation of undrained strengths of London Clay graphically as shown in Fig. 2.

Bishop et al. (11) explained the variation in strength with the orientation of samples as being primarily a pore pressure phenomenon. In terms of effective stress, the difference was slight. The A values are 0.42 for the vertical sample and 0.19 for the horizontal sample.

Using vane tests to measure shear strength in the field, Aas (1) found that the ratio between the undrained shear strength acting along the horizontal and vertical failure surface equalled unity in a lightly over-consolidated clay. This ratio varied between 1.5 and 2 in a normally consolidated clay.

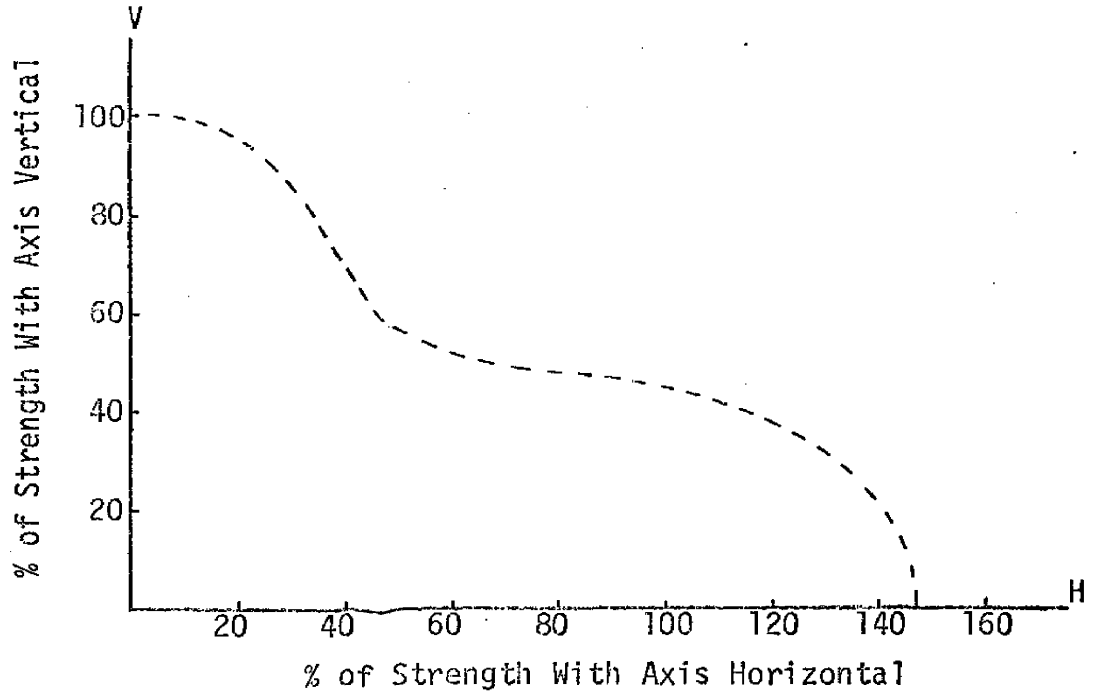

FIG. 2.--VARIATION OF STRENGTH WITH ORIENTATION OF SAMPLE IN LONDON CLAY (AFTER BISHOP 1966)

Lo (10) reported that the ratio between horizontal and vertical undrained shear strength may vary from 0.8 to 0.64 for lightly over-consolidated clay.

It appears that the ratio between the horizontal and the vertical strength varies from one soil to another and with the type of test. Therefore, it is necessary to investigate this point in Beaumont Clay.

Residual Strength

In dealing with the strength of clay and its application to slope stability problems, Terzaghi (52) classified clays in three groups: (a) soft, intact clays free from joints and fissures; (b)

stiff, intact clays free from joints and fissures; and (c) stiff, fissured clays. Terzaghi differentiated between soft and stiff clays on the basis of the liquidity index, (L.I.) and suggested that most stiff clays have a L.I. less than 0.5.

The stability of slopes in soft clay can be determined with reasonable accuracy as reported by Skempton and Golder (47) and by Bishop and Bjerrum (6). For the condition immediately following construction, undrained strengths should be used. Drained strengths should be used for long-term conditions. In stiff, intact clay, Skempton and Brown (46) showed that the same methods can be used and reliable results can be obtained.

In stiff fissured clay, the conventional methods of testing and analysis give unsatisfactory results. Experience shows that the average shear strength along the failure surface is much smaller than the shear strength measured in the laboratory by conventional tests. This discrepancy has been shown by case histories as presented by Skempton (45), Cassel (17), Henkel and Skempton (25), Henkel (23) and many others.

Indeed, the problem of slope stability in stiff fissured clay becomes very important, and a satisfactory solution is needed. This has attracted the attention of many investigators to the subject, which has greatly increased the knowledge regarding slope stability in these clays.

Terzaghi (52) was the first to point out the discrepancy between in situ and laboratory strengths. He explained this discrepancy as a

result of the presence of fissures in the clay. During an excavation or cutting the stress condition changes. The clay tends to swell, the fissures open, water enters the fissures, and a softening process begins. Also non-uniform swelling occurs. This process can affect the clay to a considerable depth, and reduce its strength. Terzaghi suggested neglecting the cohesion portion of the strength in design problems. However, experience shows that there is also a significant difference between the angle of shearing resistance found in the laboratory and the operative angle in the field (45).

Skempton (45) introduced the concept of residual strength, and succeeded in predicting the actual strength which operates in the field by the use of a special drained direct shear test. In drained shear tests, if the sample is strained well beyond failure, its strength will--and ultimately does--reach a certain minimum value. This value is defined as the residual strength, which remains constant with further straining. The residual strength can be expressed by the equation:

$$s_r = c'_r + \sigma' \tan\phi'_r \qquad (7)$$

where: c'_r = the cohesion intercept in terms of the residual strength
ϕ'_r = the angle of residual shearing resistance
s_r = the residual strength

It appears that in many cases the cohesion intercept disappears and the angle of shearing resistance decreases. Skempton (45) reported that in moving from the peak to the residual, the cohesion intercept c' disappears completely. During the same process the angle of shearing resistance also decreases--in some clays by only 1-2^o, but

in others by as much as 10^{o}. Skempton stated that part of the strength decrease from peak to residual was the result of an increase in water content. Also, the development of a thin shear band in which the clay particles are oriented in the direction of shear causes a reduction in shear strength.

Fissures, joints and other discontinuities have a major influence on the behavior of clays by acting as stress concentrators. When the peak strength at any point in a mass is exceeded, the strength at that point decreases. This action places additional stress on other points, and causes the peak to be exceeded at these points also. In this way a progressive failure will start and the strength on the entire slip surface decreases to the residual strength (45). The fissures and joints also act as discontinuous planes of weakness. Skempton and Petley (50) showed that the strength along joints and fissures is less than the peak strength, and it is probably closer to the residual strength.

Skempton (45) reported that the residual strength of a clay, under any given pressure, is independent of stress history of the clay, and it depends on the nature of the particles: the residual strength decreases with increasing clay content. Kenney (27) showed that the residual strength depends upon the amount and the nature of the clay mineral present. He also showed that a significant decrease in residual strength occured with increasing pressure. Morgenstern (34) reported that the residual strength is independent of stress history, original structure and other factors which dominate the path

dependent properties of soils. At residual state a unique structure occurs, and the resistance of clay depends upon this structure and the physical interaction of the clay particles alone.

Bjerrum (13) emphasized the significance of bond strength and its effect on progressive failure, which is initiated by stress concentration at the toe of a slope as a result of the relief of high lateral stresses. Bjerrum classified clays according to bond strength and the recoverable strain. The most dangerous soils from the viewpoint of progressive failure are the over-consolidated clays possessing strong bonds that have been subjected to gradual disintegration by weathering. The least dangerous are the unweathered over-consolidated clays with strong bonds, where the strength of the bond is enough to prevent any liberation of stored strain energy.

Bishop (5) discussed progressive failure and concluded that it is a result of non-uniform mobilization of shear resistance. He posed the question as to whether the average shear strength observed along the failure surface in the field is related to the laboratory shear test. This depends on the difference between the peak and residual strength and on the strain required for this difference to be established. Bishop used the brittleness concept of soil which he expressed as:

$$I_B = \frac{\tau_f - \tau_r}{\tau_f} \qquad (8)$$

where: I_B = the brittleness index
τ_f = the peak strength
τ_r = the residual strength

The I_B value can be used to express the maximum percentage of reduction in strength in passing from the peak state to the residual state.

CHAPTER III

TEST MATERIALS AND METHODS

The samples of Beaumont Clay used in this research were obtained near Baytown, Texas. The location of the area is shown in Fig. 3.

Several logs of borings from the area were examined before choosing the location and the depth of the samples to be tested. It was found that at this location the soil contains a large amount of calcareous nodules, and layers of silty and sandy clay to a depth of approximately 18 feet. From 20-33 feet deep the material is stiff fissured clay. Below 33 feet a layer of silty material is present. The depth selected for borings which would give the best samples to serve the objectives of this study was 20-33 feet.

Shelby tubes were used to obtain continuous cores of 3 and 5 inches in diameter from depths of 20-35 feet and 20-27 feet, respectively. The 3-inch diameter samples were extruded in the field. Visual identification and penetrometer tests were conducted on each sample. The samples were wrapped with aluminum paper, coated with at least two layers of wax and labeled. They were then transported to the Soil Mechanics Laboratory at Texas A&M University. At the laboratory the samples were given at least three additional thick coatings of wax, and stored in the moisture room.

The 5-inch diameter samples were kept in the Shelby tubes, and the ends of each tube were covered with aluminum paper and coated with several layers of wax. The tubes were transported to the

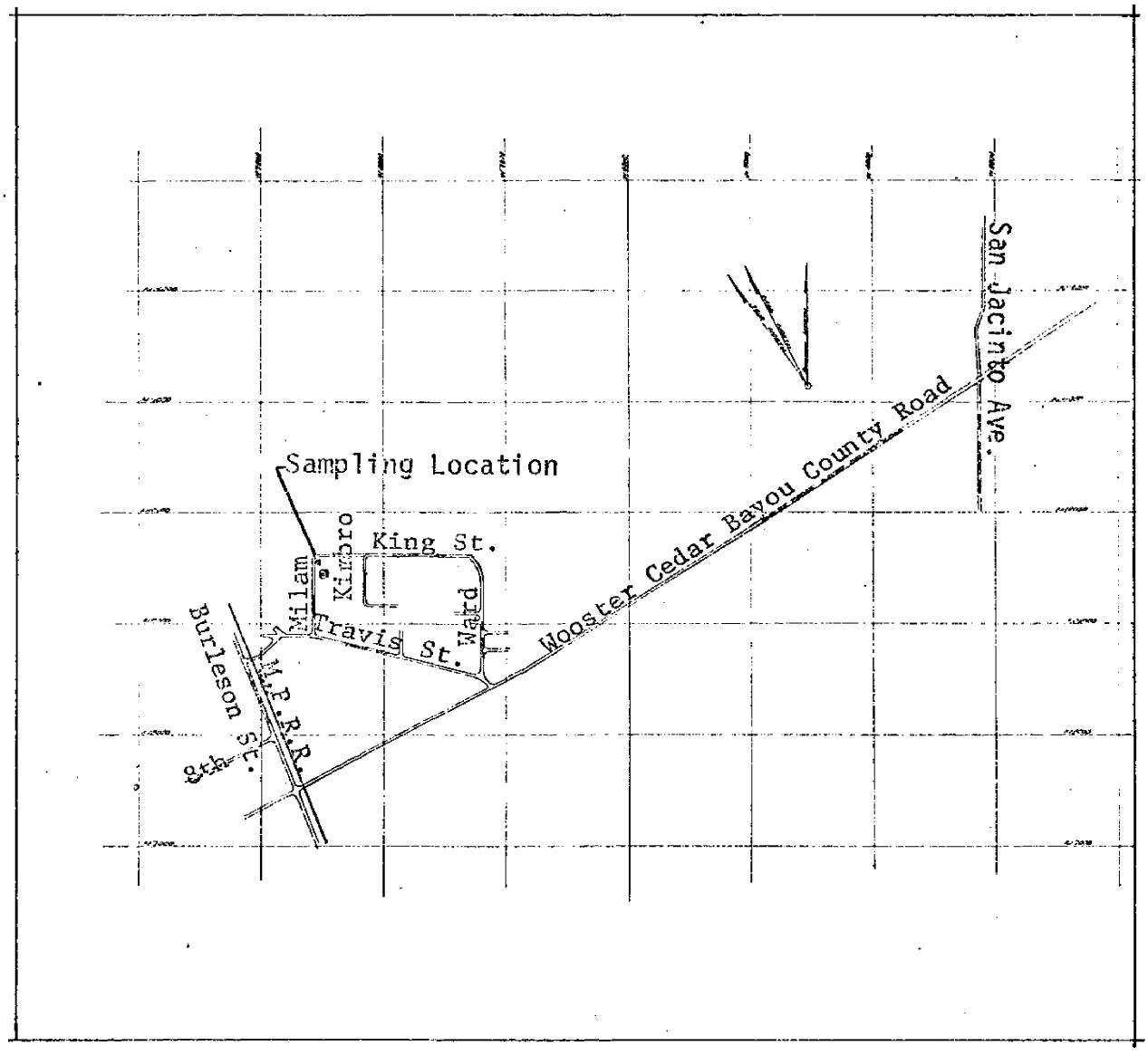

FIG. 3.--THE LOCATION OF THE SAMPLING AREA IN BAYTOWN

laboratory where the samples were extruded and wrapped with two layers of aluminum paper, then coated with at least four layers of wax and stored in the moisture room.

Elevation of the Ground Water Table

The elevation of the water table in the area was measured by observing the levels of the water in the borings one week after sampling. At that time the level of the water was 3-4 feet below the ground surface, a level which remained stable.

Index Properties Tests

The procedures used in finding the index properties of the soil are given by Lambe (29). Tests were conducted to ascertain the following information: natural water content, liquid limit, plastic limit, specific gravity, dry unit weight, and grain size distribution.

X-ray Diffraction Analyses

Three samples were taken from separate zones which appeared to have different characteristics. A fourth sample was collected from the surface of the joints and from different locations near the joints. The latter had the same color as the soil on the surface of the joints.

All samples were prepared for analysis according to the method given by Kunze and Rich (28). Specimens saturated with Mg, K, and Mg-ethylene glycol were prepared in thin films on glass slides.

An American Philips high angle goniometer X-ray diffraction unit was used to obtain diffraction patterns. This instrument is equipped with a proportional counter and a copper target X-ray tube which is operated at 35 kilovolts and 20 milliamperes with one half degree divergence and scatter slits and a 0.006-inch receiving slit. The two theta (2θ) angles of the X-ray diffraction patterns were converted to Angstrom* units. The identifications of clay minerals were made by using the lattice spacing given by Brindley (15). The peak height method was used to estimate the amounts of clay minerals (38).

Consolidation Tests

Consolidation tests were conducted on several specimens. Two of them were performed on specimens oriented in the horizontal direction. One was performed on a remolded specimen, and five of them were performed on specimens oriented in the vertical direction. The specimens used in consolidation tests were 2.5 inches in diameter and 0.568 inches in thickness. They were prepared very carefully, in the moisture room, to avoid any disturbance to the specimen.

The remolded specimen, prepared from an undisturbed specimen, was remolded thoroughly in the moisture room to minimize the loss of water from the specimen. The remolded material was packed in the cutter ring to the exact volume of the undisturbed specimen, and then the consolidation test was performed in the standard manner.

---

*One Angstrom unit equals 10^{-8} cm.

The Casagrande type consolidometer was used in these tests. The procedures for preparing the specimens and conducting the tests are those given by Lambe (29). In analyzing the data the log fitting method was used.

The purpose of the consolidation tests was (a) to estimate the magnitude of the pre-compression load of the soil, (b) to check the consolidation behavior of the material in vertical and horizontal directions, (c) to investigate the effect of soil structure on the coefficient of consolidation (c_v), and (d) to obtain some indication about the stress history of the material.

Direct Shear Tests

Drained direct shear tests were conducted on three groups of samples, with three main purposes in view: (a) to find the peak strength parameters, c' and ϕ'; (b) to find the residual strength parameters, c_r' and ϕ_r'; and (c) to develop the stress-displacement curves.

Apparatus

A strain controlled direct shear machine manufactured by Clockhouse Engineering, Ltd. was used for this test. Fig. 4 is a diagrammatic sketch and Fig. 5 is a photograph of this shear machine. This machine is capable of developing the small, constant rates of strain which are necessary in drained tests. The machine consists of three major parts: the shear box and proving ring, the loading

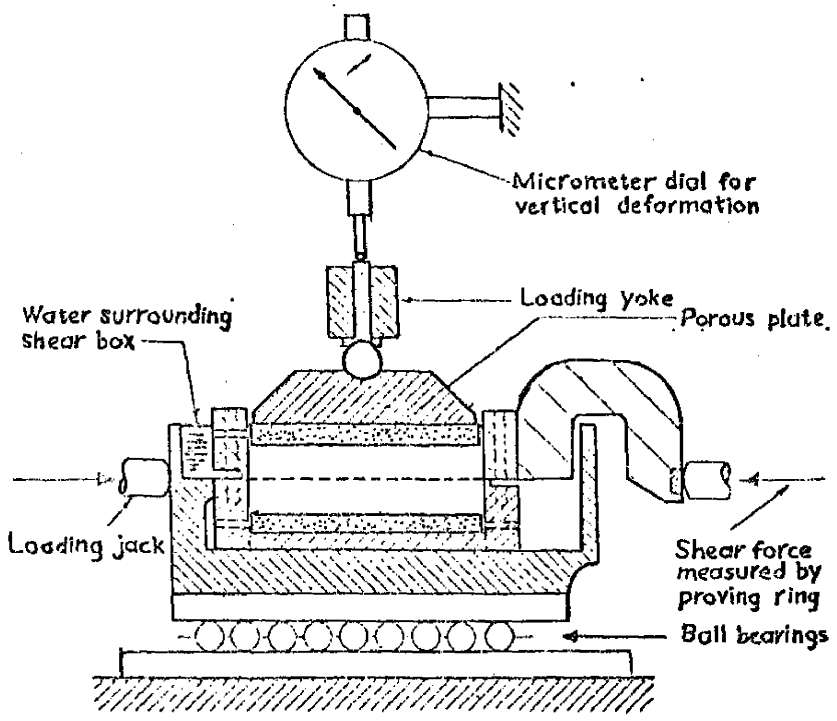

SECTION OF SHEAR BOX

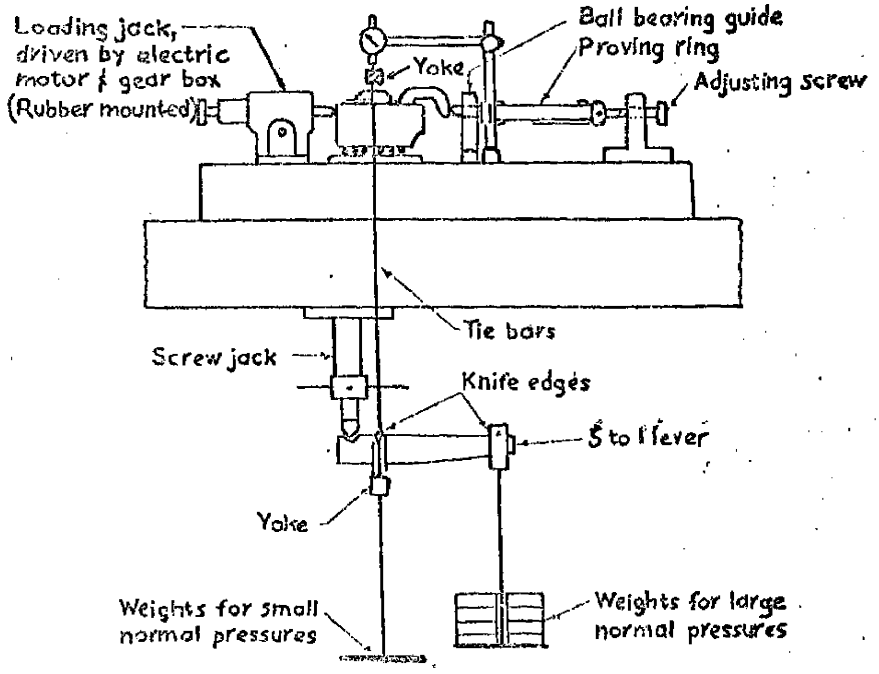

LAYOUT OF LOADING SYSTEM

FIG. 4.--DIAGRAMMATIC SKETCH OF DIRECT SHEAR MACHINE

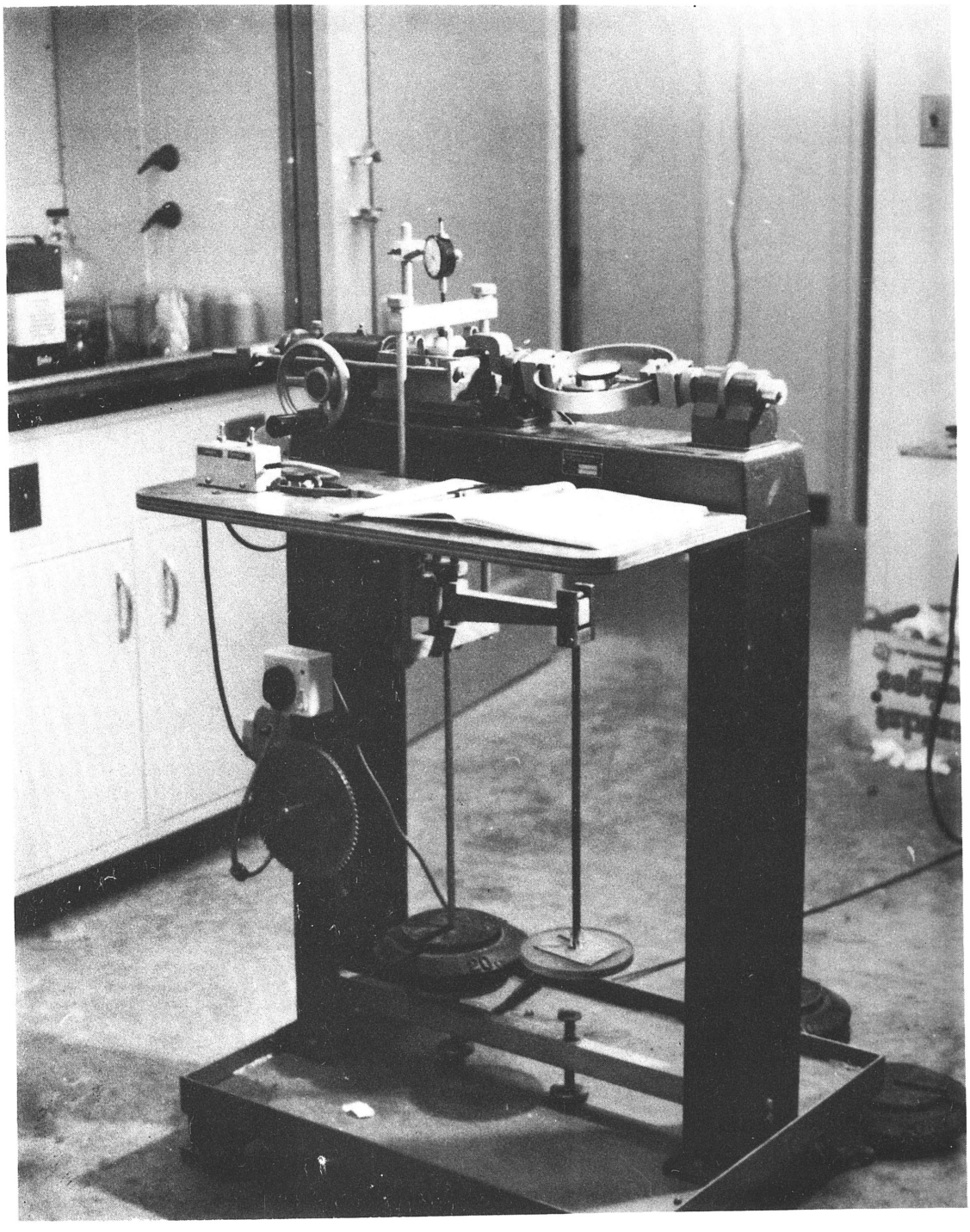

FIG. 5.--PHOTOGRAPH OF DIRECT SHEAR MACHINE

system, and the driving motor with gears. To achieve the purposes of this research, the machine was modified locally so that back and forth shearings were possible.

The shear box itself is of conventional split box design. It is placed in a metal water chamber which slides on two ball-bearing tracks under the action of the horizontal force. The lower part of the box is firmly attached to the moving chamber, whereas the upper part of the box is held stationary by a hooked arm which in turn touches the calibrated proving ring through which the shearing force is measured.

The consolidation load is applied to the sample by a simple lever system, using dead weights. The horizontal force is applied by a loading jack which is operated by an electric motor. The rate of the loading can be varied from 0.05 to 0.00006 inches/minute by arranging the gears. The machine has a capacity of 500 lbs. vertically, corresponding to a normal stress of 71 psi on a 2.5-inch diameter specimen. The horizontal load capacity (or shearing force) of the machine is 1000 lbs.

Test Procedure

A specimen 2.5 inches in diameter and 0.65 inches thick, was prepared in the humid room. A saturated porous stone was placed into the split shear box followed by the specimen, then another saturated porous stone, and finally the top platen. The assembled shear box was next lowered into the water chamber and the lower part fixed

rigidly by means of two bolts inserted between the shear box and the inside wall of the chamber.

As stated before, three groups of samples were used. Each group consisted of three specimens which were consolidated under pressures of 10, 20, and 40 psi. Each particular consolidation load was applied to the specimen for an interval of time sufficient to assure that complete consolidation of the specimen was achieved. A minimum period of 24 hours was used, although most specimens reached secondary consolidation in less than 24 hours.

At the end of the consolidation phase, the specimens were sheared at a constant rate of horizontal movement of 0.007 inches/hour. The method proposed by Gibson and Henkel (21) was used to calculate the rate of shearing. The rate of shearing which was used in the tests was sufficient to assure at least 95 percent dissipation of pore water pressure.

During the shearing processes, the shear force and the vertical movement of the specimens were recorded at arbitrarily chosen intervals. When the shear box reached its limit of travel, it was brought back to its original position using the same rate of shearing. This shearing process was then repeated until the shear strength decreased to a constant value. This usually occurred after the fifth shearing; however, six shear reversals were conducted on each specimen to assure that the residual strength was obtained. The accuracy of the shearing force measurement was 0.13 lbs.

At the end of the shear tests, other tests were performed on each group of samples to determine the liquid limit, plastic limit, specific gravity, and grain size distribution.

Triaxial Compression Tests

One of the major tests in this investigation was the triaxial compression test. The outstanding advantages of the triaxial test are the control of the drainage condition and the measurement of pore pressures. There are two separate stages in the triaxial test: the application of an all around pressure followed by the application of the axial load. The stress caused by the axial load is commonly called the deviator stress, since it is the difference between σ_1 and σ_3, where σ_1 and σ_3 are the major and the minor principal stresses, respectively.

The triaxial test is classified according to the drainage conditions which exist during the two stages of the test. The test can be one of the following:

1. Undrained Test--In this test no drainage is permitted during either stage. This test sometimes is designated as a UU or Q test. It was conducted on both undisturbed and remolded samples in this research.

2. Consolidated Undrained Test--Complete drainage is allowed under the application of the all around pressure. No drainage is permitted during the application of the deviator stress and the excess pore water pressure which is developed in the specimen can be

measured. This test is often designated as a CU or R test. It was also conducted on undisturbed and remolded samples.

3. Drained test--In this test drainage is permitted during both stages. Full consolidation occurs under the all around pressure, and no excess pore water pressure is built up during the application of the deviator stress. Volume change can be measured during the application of the deviator stress. This is often designated as an S test. It was conducted on undisturbed samples only.

Apparatus

The triaxial apparatus consists of several units, which are discussed below:

1. Triaxial compression cell--The triaxial compression cell was designed and manufactured in the Civil Engineering Department, Texas A&M University. It is made of aluminum except for the brass pedestal and the stainless steel piston. In the base there are five conduits, as shown in Fig. 6. Four conduits are provided with zero volume change Circle Seal valves. The fifth conduit is provided with a Klinger "sleeve-packed"valve. Two of the conduits go to the base of the specimen through the pedestal where the one with the Klinger valve connects to a null indicator for pore water pressure measurement and the other connects to a volume change device. Through the volume change device a back pressure can be applied to the specimen. The three other conduits are used to fill the cell with water, to apply cell pressure, and to drain the cell. The pedestal, 1.5 inches in

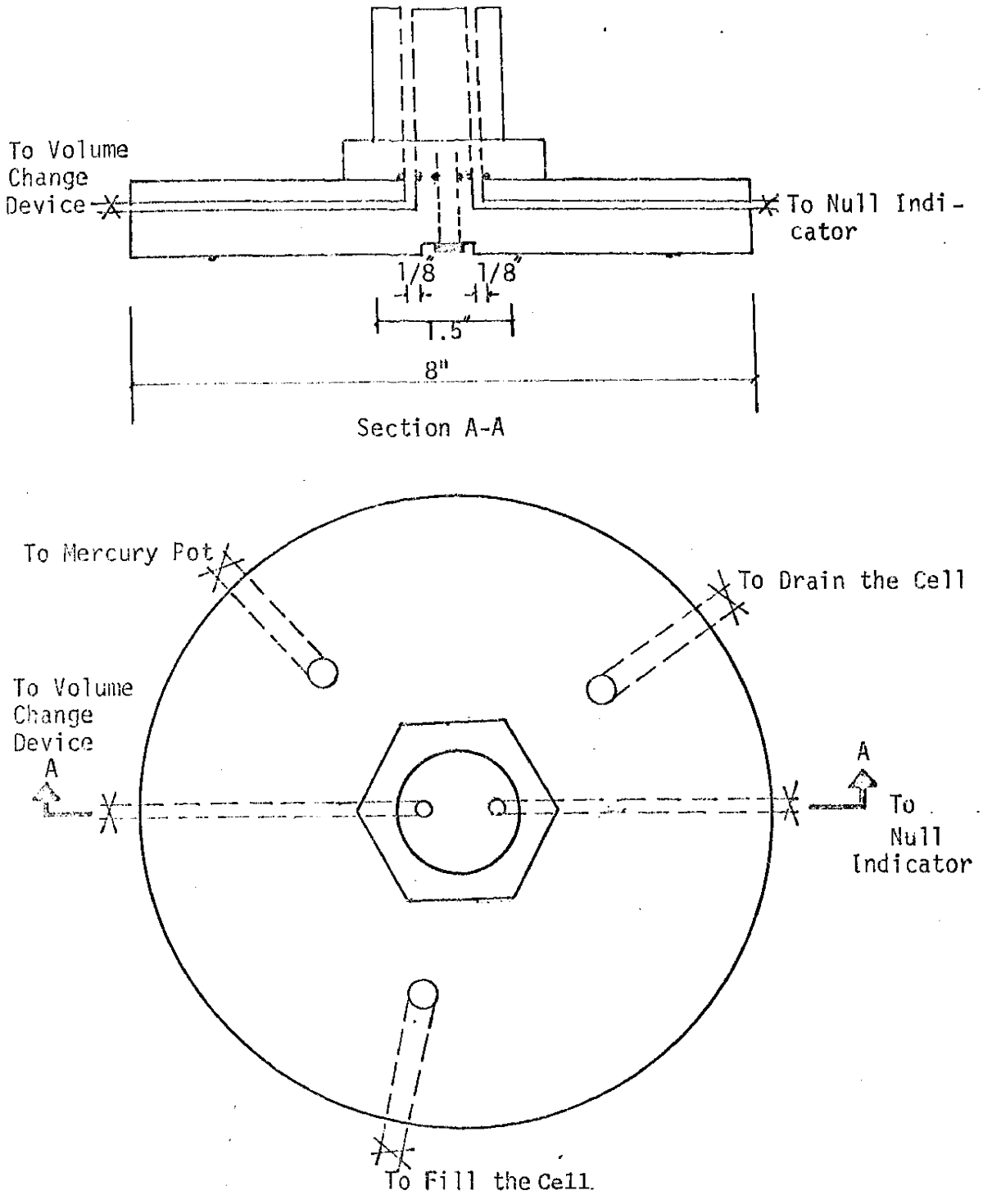

FIG. 6.--SCHEMATIC DIAGRAM FOR THE BASE OF TRIAXIAL COMPRESSION CELL

diameter, is connected to the base of the cell as shown in Fig. 6.

A clear lucite chamber, with a 0.25-inch wall thickness allows chamber pressures up to 100 psi. In the cell head assembly a 0.75-inch diameter stainless steel piston is used to transmit the load to the specimen. It moves practically free of friction along a set of linear ball bushings, which remain constantly lubricated. Leakage between the piston and cell head assembly is controlled by applying a film of Lubriplate grease (manufactured by Fiske Brothers Refining Co.) to the piston and cell head assembly before each test. At the top of the cell is a bleed valve.

2. Pressure Contol System--A self-compensating mercury control system was used to apply the cell and back pressures required throughout the triaxial test. The mercury control system has two outstanding advantages. First, it provides a constant pressure through each stage of the test. Second, it eliminates the possibility of air reaching the specimen through the de-aired water used to saturate the system and fill the triaxial cell. If compressed air were used as the pressure source, the air could dissolve in the water, diffuse through the membrane and reach the specimen.

The mercury control system consists of two "pots," A and B (Fig. 7). Each pot consists of an inner and outer cylinder which are usually filled with mercury and de-aired water. Mercury from the lower pot can be pumped to the upper pot by a control cylinder. The principle of the mercury control system is illustrated in Fig. 7. A single cylinder from each pot can be used to obtain pressure, and

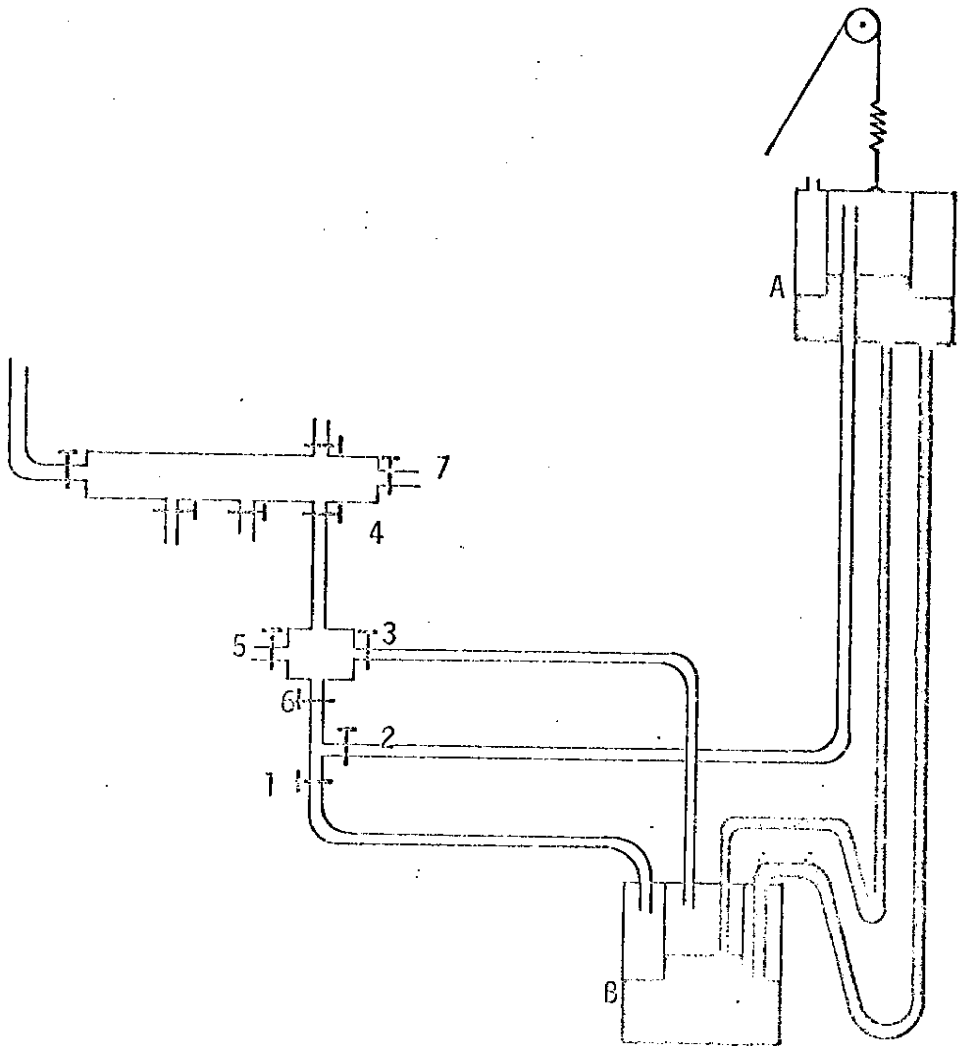

FIG. 7.--THE DOUBLE MERCURY POTS

almost half the pressure capacity of the system can be obtained. This can be done when valves 1, 6, and 5 are opened (Fig. 7). The pressure can be measured on a gauge if valves 4 and 7 are opened, too. To obtain full pressure capacity of the system, valves 1, 2, 3 and 5 are opened and valve 6 is closed.

The pressure of the water in the triaxial cell results from the difference in the level between the mercury surface in the upper and lower pots, minus the head of water from the lower pot to the triaxial cell. The spring carrying the upper pot is attached to a cable which runs over a pulley fixed in the ceiling of the laboratory. The height of the pot can be controlled by a winch. With the height available in the A&M Soil Mechanics Laboratory, a maximum pressure of 95 psi can be obtained. The pressure obtained is self-compensating, as explained below.

When a volume decrease occurs, either due to specimen consolidation or leakage, water will be lost from pot B and the mercury level in this pot will rise to compensate for the water lost. This amount will be replaced from pot A. The drop in mercury in the upper pot reduces its weight, but the pot automatically adjusts its own level due to the movement in the spring, which has appropriate stiffness.

3. Pore Pressure Measurement System--A Bishop type null indicator was used to measure the pore pressure in the specimen. It has a U-tube shape and is shown diagrammatically in Figure 8. The lower part of both arms of the tube is filled with mercury, which stays

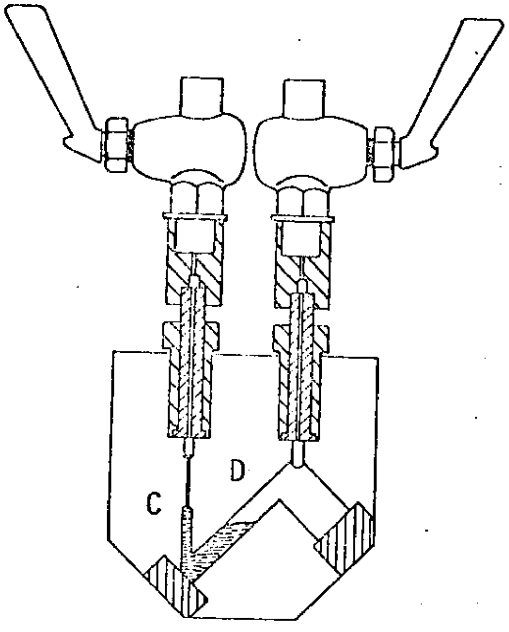

Bishop Null Indicator

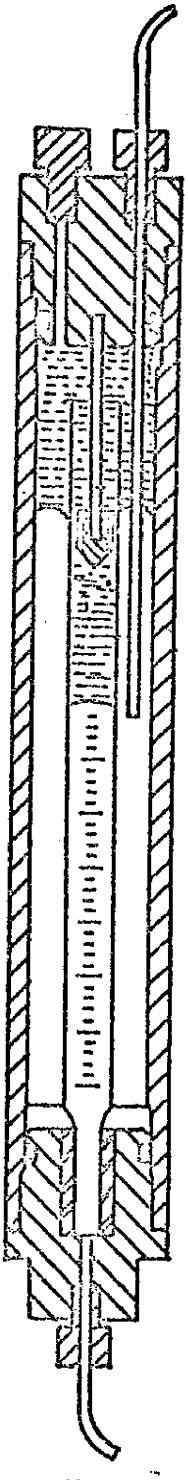

Volume Change Device

FIG. 8.--NULL INDICATOR AND VOLUME CHANGE DEVICES

at the same level in both arms when the null indicator is in use. De-aired water fills the rest of the U-tube.

One end of the null indicator is connected to a valve that leads to the base of the specimen, and the other end is connected to the control cylinder and the pressure gauge as shown in Fig. 9. An increase in pore pressure in the specimen will tend to depress the mercury in Tube C (Fig. 9). This can be immediately balanced by adjusting the piston in the control cylinder to increase the pressure in tube D of the null indicator by an equal amount, which is registered on the pressure gauge. No problems have been found in using the Bishop null indicator, and it is quite simple to operate.

4. Volume Change Device--The volume change of the specimen is found by measuring the volume of water expelled from the pore space of the soil. The device used for this purpose is shown in Fig. 8. It consists of a 25 ml. burette which is placed in a lucite cylinder. A line from the top of the lucite cylinder goes to the pressure control system and to one of the mercury pots. Through this line back pressure can be applied to the specimen. Another line goes from the lower end of the graduated cylinder to the base of the specimen. The system is filled with de-aired water and kerosene which floats on top of the water. Fig. 8 shows the volume change device when it is filled with water and kerosene. The volume change is determined by measuring the displacement of the water-kerosene interface. Usually a red dye is added to the kerosene, so it is easy to see the interface.

In all of the consolidated undrained and drained triaxial tests, a back pressure was applied to the specimens to insure saturation.

5. Compression Testing Machine--A model T56B compression testing machine manufactured by Wykeham Farrance Engineering Ltd. was used in performing the triaxial compression tests. The machine will provide a constant rate of movement for 25 different rates of speed ranging from 0.06 to 0.000024 inches/minutes. For further details on the operation of this machine, the reader is referred to the operations manual published by Wykeham Farrance Engineering Ltd.

6. Miscellaneous Equipment--Several other items of equipment were used in preparing the triaxial specimens. These include:

a. A rotary trimmer and wire saw used to trim the larger specimens down to the 1.5 inch diameter required for triaxial testing.

b. A 1.5-inch diameter by 3.0-inch long split mold used to trim the ends of the specimen to insure a right circular cylindrical specimen.

c. A membrane stretcher used to facilitate placing membranes around the specimens.

d. A lucite tube 1.5 inches in diameter by 3.0 inches long in which the remolded specimens were formed.

Fig. 9 is a schematic diagram of the triaxial test equipment; Fig. 10 is a photograph of the system.

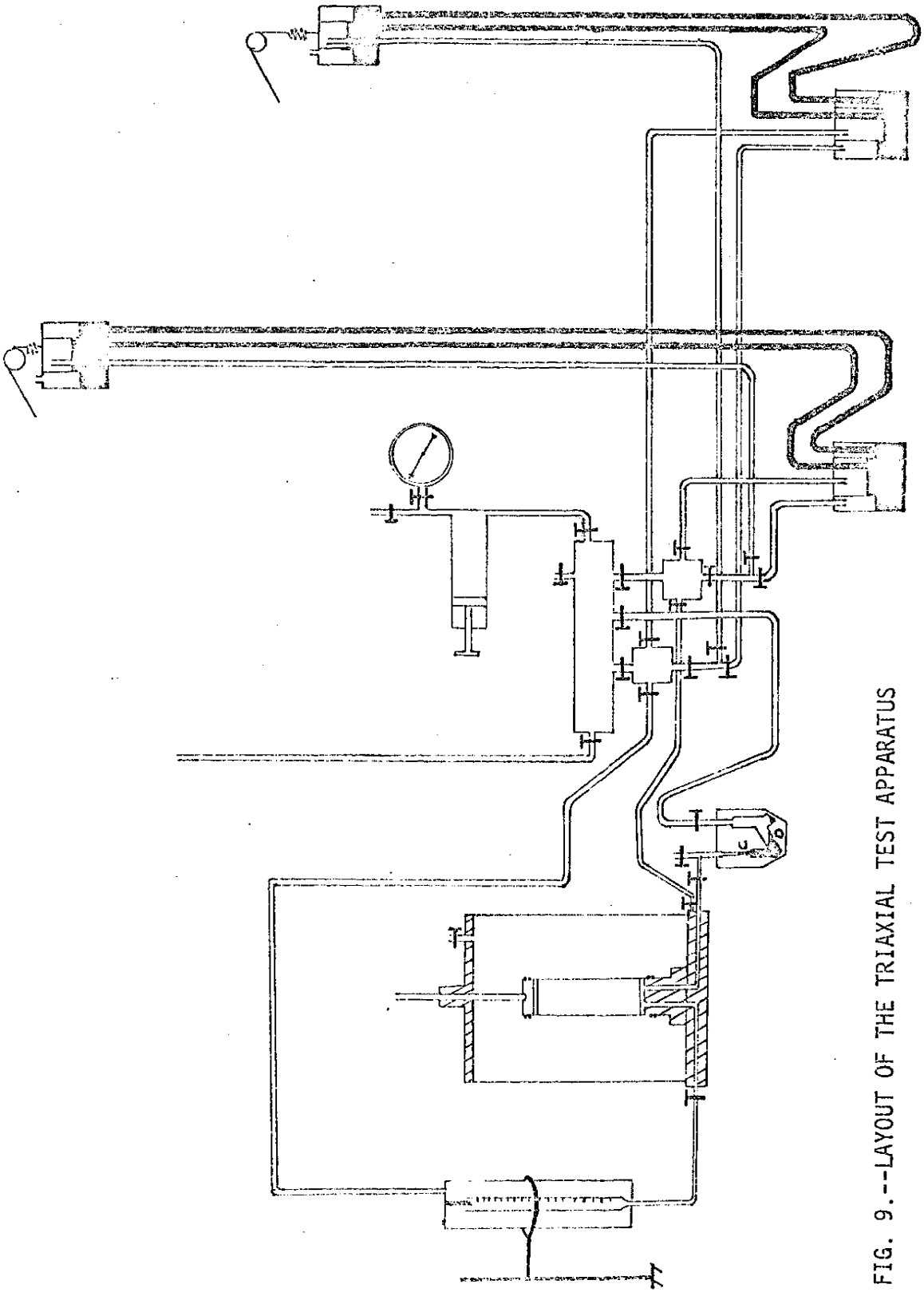

FIG. 9.--LAYOUT OF THE TRIAXIAL TEST APPARATUS

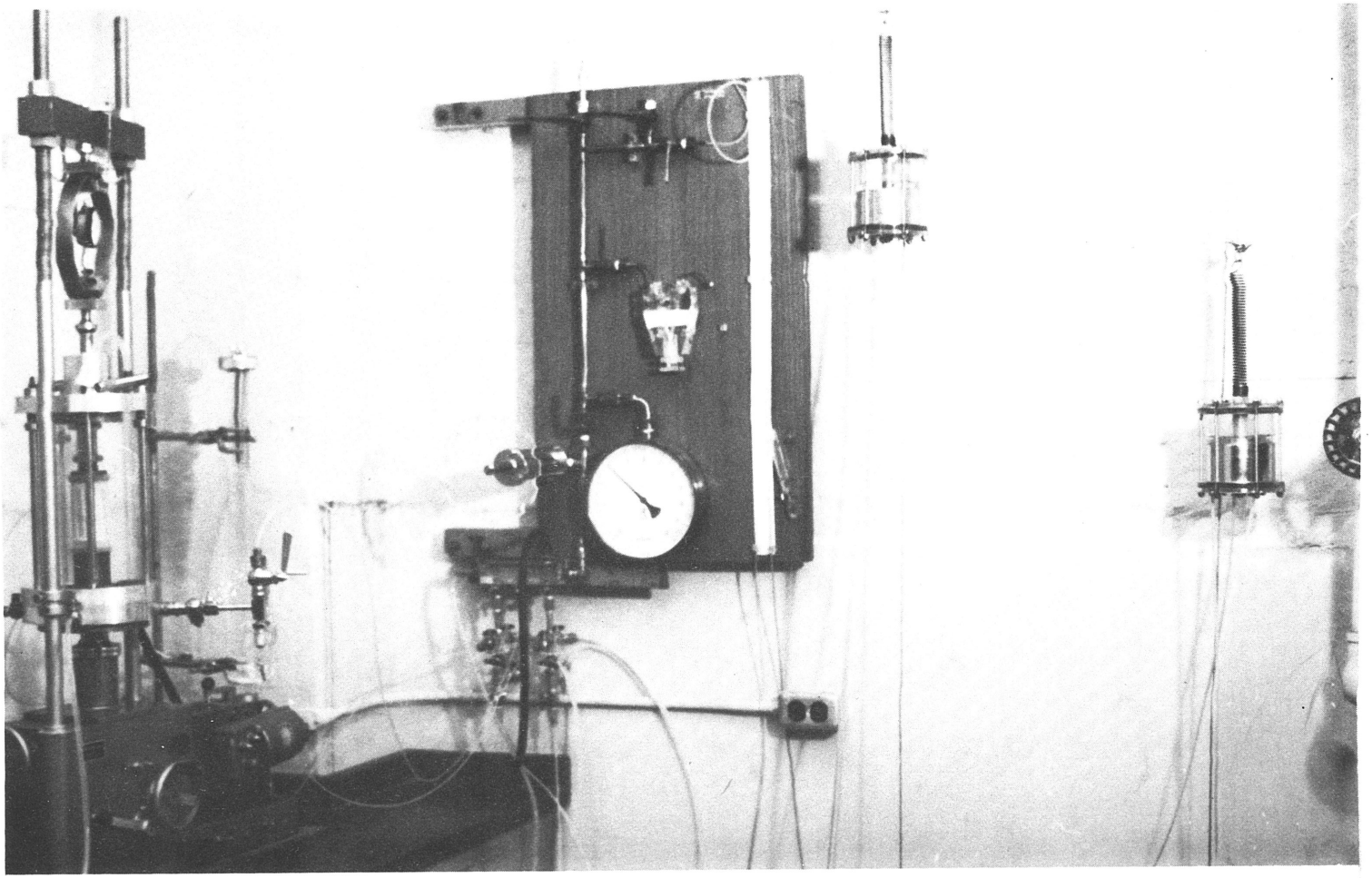

FIG. 10.--PHOTOGRAPH OF THE TRIAXIAL TEST EQUIPMENT

Test Procedure

Both undisturbed and remolded specimens were tested triaxially. The preparation of all specimens was done in the moisture room in order to minimize the evaporation of water from the specimens. For each triaxial test the following measurements were taken. Two samples were taken for the moisture content determination, the weight of the specimen before and after the test was determined, the dimensions were measured, and the shear angle on which each specimen failed was recorded.

Preparation of Undisturbed Specimens.--Cylindrical specimens, 1.5 inches in diameter and 3.0 inches in height, were prepared either from a 3-or 5-inch core. From the 5-inch core four specimens could be prepared from the same depth, while only one specimen could be prepared from the 3-inch core. For this series of tests, the cylindrical specimens were cut with their major axis either in the vertical or in the horizontal direction.

Set-up of the Specimen in the Triaxial Cell.--Before placing the specimen in the cell it was necessary for the base of the cell, the pore water pressure device, volume change device and all the conduits to be saturated with de-aired water. The mercury level in the null indicator was adjusted and the pore water pressure system was checked to make sure it was free of air bubbles.

A saturated porous stone, 1.5 inches in diameter, was place on the pedestal. De-aired water from the volume change device was circulated to assure that no air bubbles were entrapped between the

porous stone and the pedestal. Excess water was blown away from the porous stone surface, and the specimen was placed on the porous stone. Another saturated porous stone was placed at the top of the specimen, then the brass cap. The specimen was then surrounded by saturated filter drain strips. By means of the membrane stretcher, a rubber membrane, 0.008 inches thick, was placed around the specimen. The membrane was gently stroked against the specimen in an upward direction to remove any air trapped between the membrane and the specimen. Two rubber O-rings were used at each end of the specimen, making watertight seals.

The upper part of the cell was then fastened to the base of the cell and the cell was filled with de-aired water. Again, care was taken not to trap air bubbles inside the cell.

A confining pressure of about 10 psi was applied, and the resulting pore water pressure was measured after it had equalized. Then the confining pressure was increased about 3 psi, and again the pore water pressure was measured. This process was repeated again, and if the change in pore water pressure was less than the change in confining pressure, a back pressure was applied through the volume change device. The process of increasing the confining pressure, measuring the resulting pore water pressure, then applying the back pressure was continued until the increment in pore water pressure was equal to the increment in confining pressure. This equalization means that the specimen is fully saturated and $B = 1$, where $B = \frac{\Delta u}{\Delta \sigma}$.

At this stage the desired consolidation pressure was applied by increasing the confining pressure. The valve to the volume change device was opened and drainage of the specimen was allowed to proceed. The specimens were consolidated under 10, 20, 40, and 60 psi, respectively. After the consolidation process was completed, the valve to the volume change device was closed, or in the case of a drained test, it was left open. Then the specimen was ready to be sheared.

Shearing Process of Triaxial Specimens.--The proving ring was positioned and brought into contact with the triaxial cell piston. With the motor drive running, the zero reading of the proving ring and the pore water pressure of the specimen was recorded. The piston was brought into contact with the loading cap of the specimen and the test was started. Readings of the proving ring dial and the pore water pressure were taken at intervals until the specimen failed. The rate of axial strain which was adopted in consolidated undrained tests was 0.00024 inches/minute. In the case of drained tests the method proposed by Gibson and Henkel (21) was used to compute the rate of axial strain; the rate used was 0.000072 inches/minute.

Remolded Specimens.-- The tests on remolded specimens were conducted after the specimen was tested in the undisturbed condition. The specimen was remolded in the moisture room, and it was then placed in the lucite tube in layers about 0.25 inches thick. A steel bar was used to compact the material and care was taken to produce a uniform specimen without entrapped air bubbles. In general the weight of the remolded specimens was about 1 to 4 grams less than the weight

of undisturbed specimens. There was no significant variation in the moisture content between the remolded and the undisturbed specimen. The rest of the procedure for testing remolded specimens was the same as for undisturbed specimens.

Unconsolidated Undrained Tests.--In the case of unconsolidated undrained tests, the same procedure for preparing the specimens described above was used. When setting a specimen in the cell, the porous stones were removed and lucite platens, 1.5 inches in diameter, were used to prevent drainage. The rate of the axial strain was 0.02 inches/minute.

CHAPTER IV

ENGINEERING GEOLOGY OF THE SITE

The Quaternary Coastal Plain of Texas forms a belt which is 70-90 miles wide and parallel to the Gulf of Mexico shoreline. This plain extends from the Sabine River on the east to Almos Creek in Southern Kleberg County (39). In general the coastal plain is flat, featureless and transected by seven major rivers, as shown in Figure 11. It consists principally of fluviatile deposits in the form of levees, flood plain deposits and deltas. A few thin marine deposits are intercolated with the fluviatile materials.

The uppermost part of the Quaternary is composed of a layer of clay approximately 400 feet thick which is referred to as the Beaumont Clay (22) of Pleistocene age. The Beaumont Clay lies unconformably upon the Lissie formation, and is in turn covered by stream deposits and wind-blown sand which are about 15 feet thick. However, in some places the Beaumont Clay is exposed at the surface.

Quaternary Stratigraphy

The stratigraphy of the Coastal Plain consists of the Recent and four Pleistocene formations. From youngest to oldest, the four Pleistocene units are the Beaumont, Upper Lissie, Lower Lissie, and Willis. Each formation rests unconformably upon a weathered and eroded surface. They are similar to each other in their mode of formation. The units dip seaward and extend beneath the Gulf of Mexico

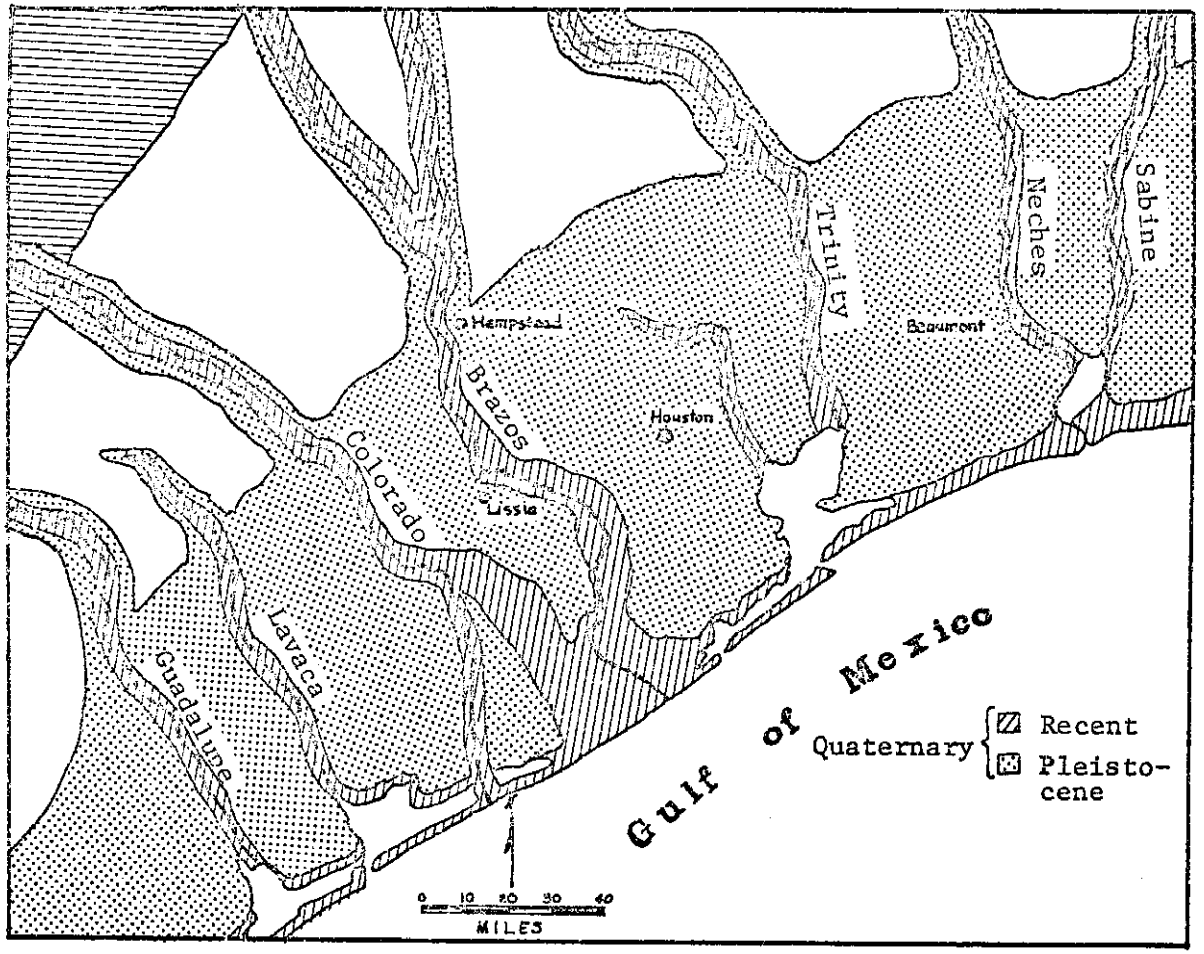

FIG. 11.--THE QUATERNARY COASTAL PLAIN OF SOUTHEAST TEXAS (AFTER BERNARD ET AL. 1962)

as far as the Continental Shelf. The present slope of the depositional surface of each layer as reported by Bernard et al. (2) is as follows:

Beaumont	2 feet per mile
Upper Lissie	2.5 feet per mile
Lower Lissie	3.5 feet per mile
Willis	10 feet per mile

The relationship between these depositonal surfaces reflects net inland uplift and coastal subsidence during Quaternary time. The oldest formation has been subjected to a greater amount of tectonic activity and it therefore has a steeper slope, while the youngest unit has been subjected to a lesser amount of tectonic activity and consequently has a more gentle slope.

Geologic History of Pleistocene of the Gulf Coastal Plain

According to Doering (19) and Bernard et al. (2) the history of the Quaternary is correlated with glacial and interglacial stages. The correlations are based principally on the variation of sea level caused by the advance and retreat of the ice mass. When the sea level dropped down, the rivers cut trenches in their valleys and erosion took place on all the Coastal Plain. During the return of the sea to its former level, the rivers filled their respective trenches and began to contribute material to the processes which were operating along the coast positions.

The Quaternary deposits have been correlated with interglacial stages. Also, the periods of non-deposition or erosion have been correlated with glacial stages when the existing sea level was low. Fig. 12 shows the glacial and interglacial stages and their durations. The lower part of the figure is the Wisconsin glacial stage, shown to an expanded time scale. In order of decreasing age, the glacial stages are the Nebraskan, Kansan, Illinoian, early Wisconsin, and late Wisconsin.

The Beaumont Clay, which is the major concern of this study, was deposited at the beginning of the early Wisconsin stage. The formation consists of tan and brownish-red clay with occasional layers of silt and fine sand. Calcareous nodules are also frequently found. The clay is jointed and badly fissured with slickensided surfaces. Most joints, which are formed in a series of intersecting curved surfaces, are covered with a thin layer of light gray clay. Fig. 13 shows a specimen with a single joint surface; however, several specimens contained more than one joint surface.

The clay was deposited on a broad flat flood plain during periods of overflow. During the dry season the clay shrunk and a net of cracks was opened. As each flood occurred new material was deposited in the cracks and on top of the previous layer. Cyclic deposition and non-deposition coupled with drying continued for a considerable interval of time. This cyclic wetting and drying produced many joint systems which are now visible in the Beaumont Clay. The different colors found on the surfaces of the joints are either due to different

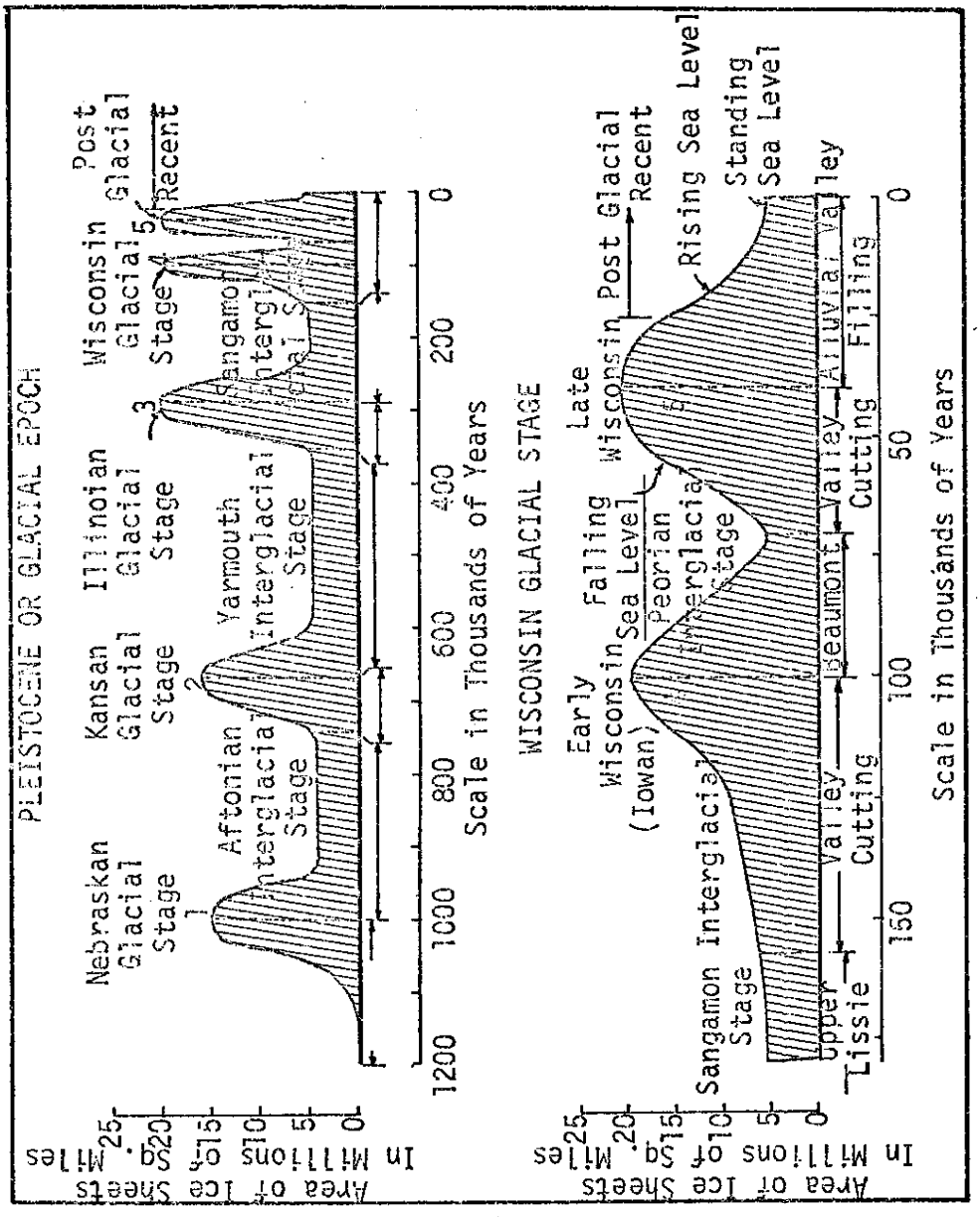

FIG. 12.--CORRELATION OF PLEISTOCENE EVENTS (AFTER BERNARD ET AL. 1962)

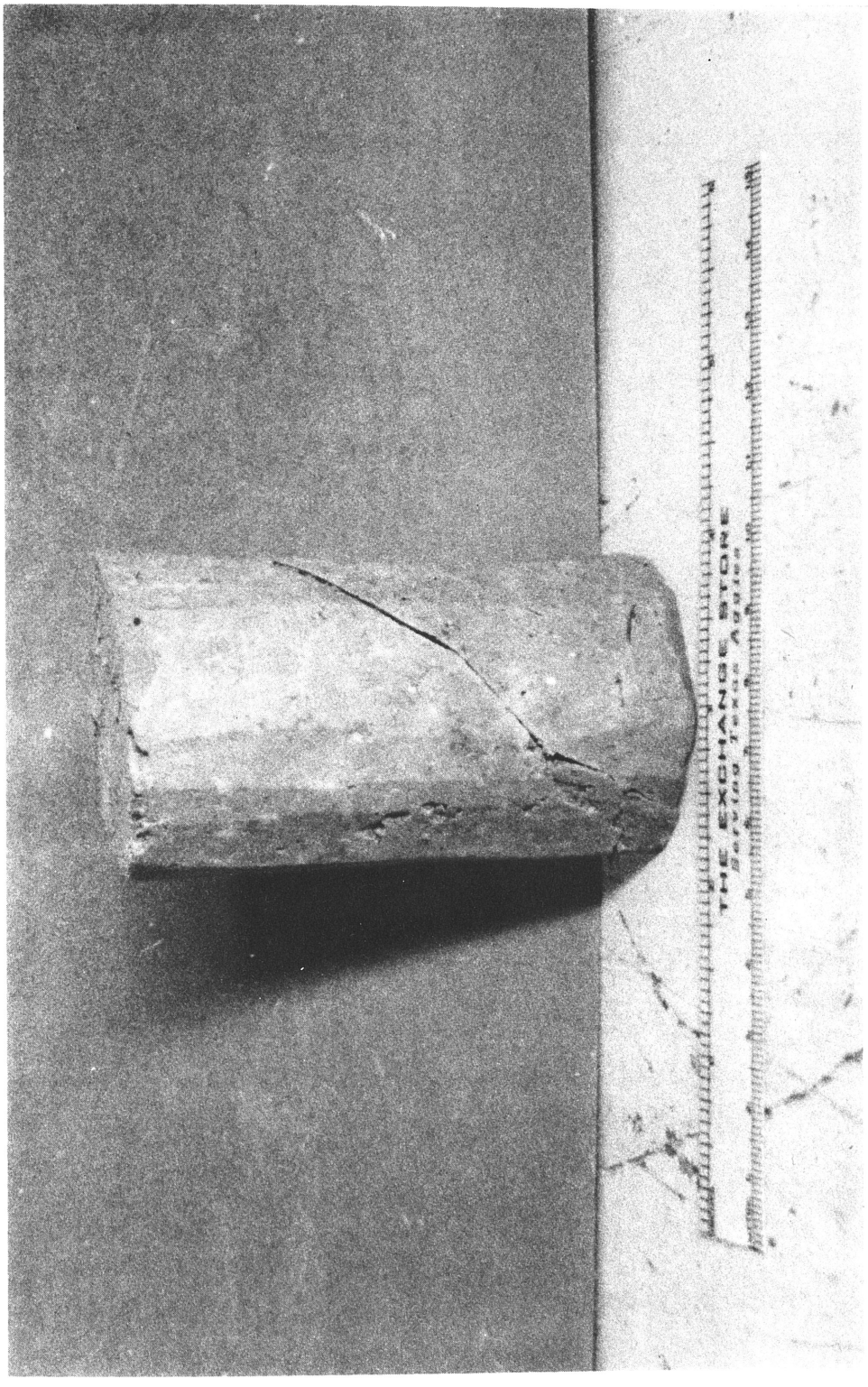

FIG. 13.--SAMPLE WITH JOINTED SURFACE

material deposited on them, or to the fact that these joints served as planes which allowed the circulation of water. The circulating waters may have brought chemical reactions about which changed the color along the joints. Between the joints, the blocks of clay contain randomly oriented fissures. The number of fissures per unit volume is extremely variable. The formation of the fissures occurred when the clay was subjected to repeated cycles of drying and wetting. The variation in the type of clay mineral caused a differential swelling and contraction. These differential movements were accompanied by differential internal strains, which were large enough to cause structural failure and to form the fissures.

The Beaumont Clay is far from being a homogeneous material. Fig. 14 shows a borehole log in the material investigated in this study. It appears that many of the clay layers have been subjected to different degrees of weathering. The variations in degree of weathering have produced layers which show different properties.

The early Wisconsin stage ended when the sea level dropped down about 450 feet below the present sea level. As a result, the water table in the coastal plain dropped down and a large part of the Beaumont Clay was subjected to drying for a long time.

The Effect of Geological Processes on the Engineering Properties of Beaumont Clay

The Beaumont Clay can be described as stiff, over-consolidated, jointed, and fissured with slickensides. The water table in the area

FIG. 14.--LOG OF THE CB-1 BORING

Depth	Penetrometer Reading tsf	Description of Stratum
2		
4		
5	2.0	
6		Tan clay with calcareous nodules. Some of the nodules are as large as 1.5 inches. There are some black specks.
8	1.5	
10	1.6	Tan clay with calcareous nodules. Looks stiff.
12		
14		
15	1.9	Tan clay with calcareous nodules. Slicken sided and stiff.
16		
18		
20	1.0	Tan and yellow slicken sided clay. There is a silty layer about 2-3 inches in thickness.
22	2.2 2.5	Tan clay badly fissured with slicken sides. Very difficult to trim. There are joints and spots of gray color
24		
25		
26	2.2	Tan fissured. Less fissured than the layer above, contains joints with gray surfaces. The green spots are scattered in clay mass.
28	2.2	Red clay, badly fissured with slicken side, jointed, joint surfaces contain fine silt and sand material.
30	2.5	
32	1.5	Tan clay fissured but less than above, lesser number of joints, some gray spots. There are seams of silty clay.
34	1.5	
35		
36	2.2	Tan fissured, occasional silty seams.
38		
40		
42		
44		

where the samples were taken was estimated to be 3-4 feet below the ground surface. The plasticity characteristics of the clay are shown in Fig. 15. The clay is classified according to the Unified Soil Classification System as CH material with liquid limits varying from 60-95 and plastic limits varying from 20-32. The natural water content is a few percent higher than the plastic limit. The content of clay-sized particles (< 2 μ) ranges from 56-77 percent, which gives an activity range of 0.72-1.05. According to Skempton (41) the clay can be classified as inactive to normal. The dry unit weight and the specific gravity ranges from 88-96 pcf and from 2.68 to 2.78, respectively. Fig. 16 shows that the water content of the clay varies several percent within a short distance vertically. The variations in water content reflect variations in liquid limit and corresponding variations in the mineralogical composition of the clay; the latter may have indirectly created fissures as mentioned before.

The degree of fissuring varies with depth. In general, the clay is composed of hard, irregular lumps, which have dimensions of 2-4 mm. across. Fig. 17, which shows a mass of Beaumont Clay before and after being soaked in water, provides an excellent visual indication of the degree of fissuring.

At a depth of 20-23 feet, the clay is tan and brownish-red in color and is badly fissured with slickensides. X-ray diffraction shows that the percentage of montmorillonite at this depth is higher than at other depths and that it is about 47 percent of the total clay fraction. A correspondingly high liquid limit (see Fig. 16) is also

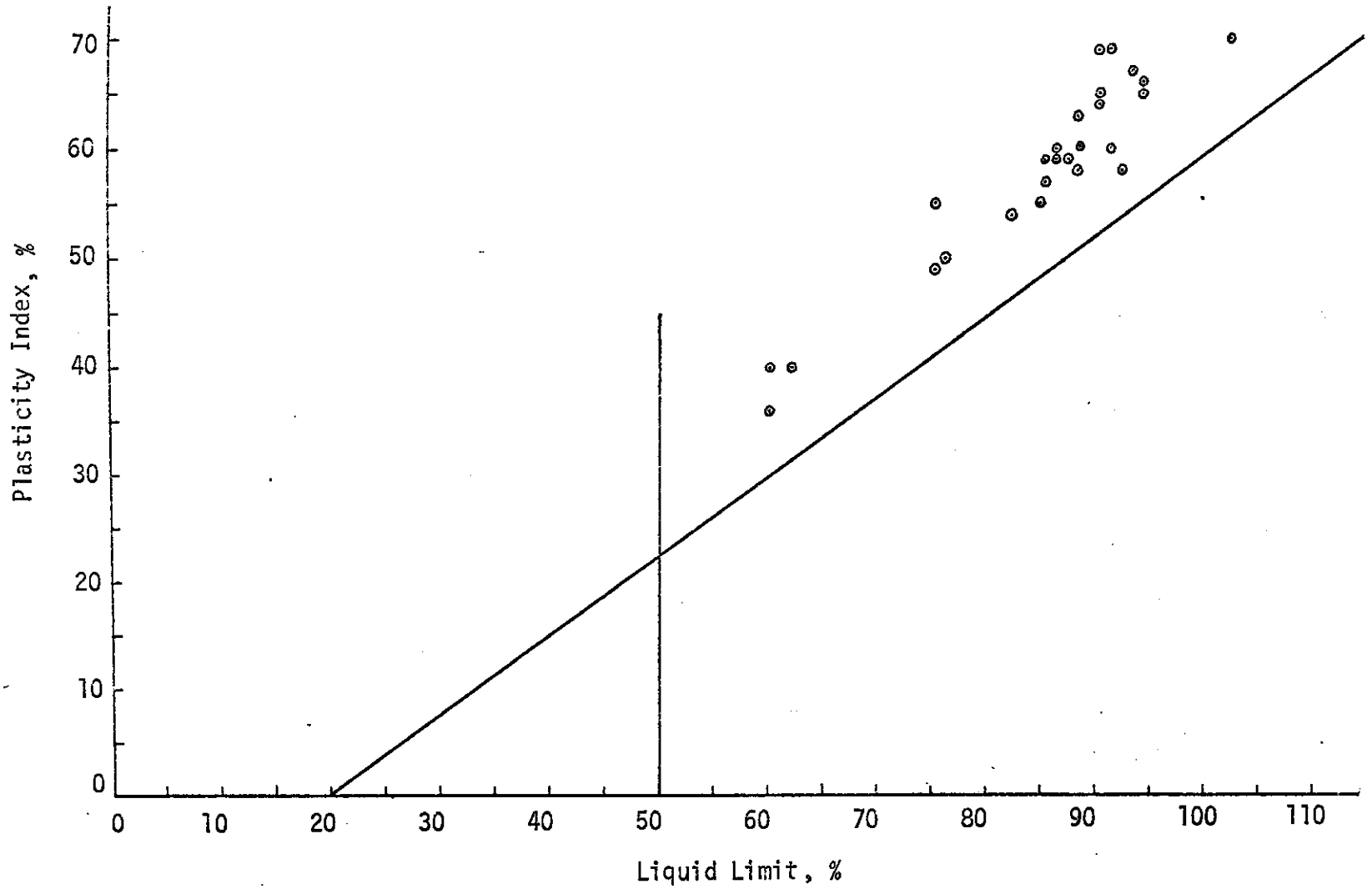

FIG. 15.--PLASTICITY CHART

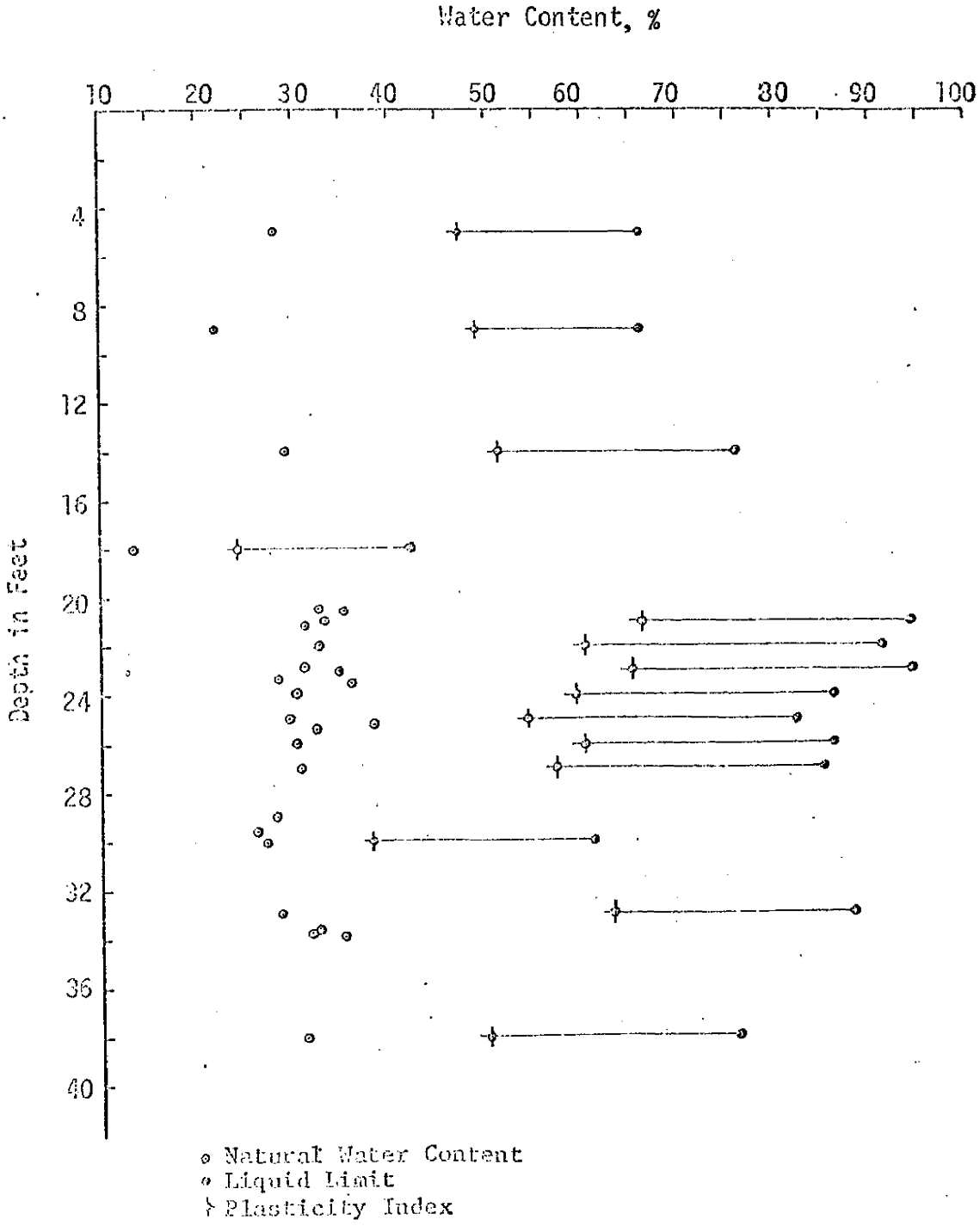

FIG. 16.--VARIATION OF WATER CONTENT, LIQUID LIMIT AND PLASTICITY INDEX WITH DEPTH

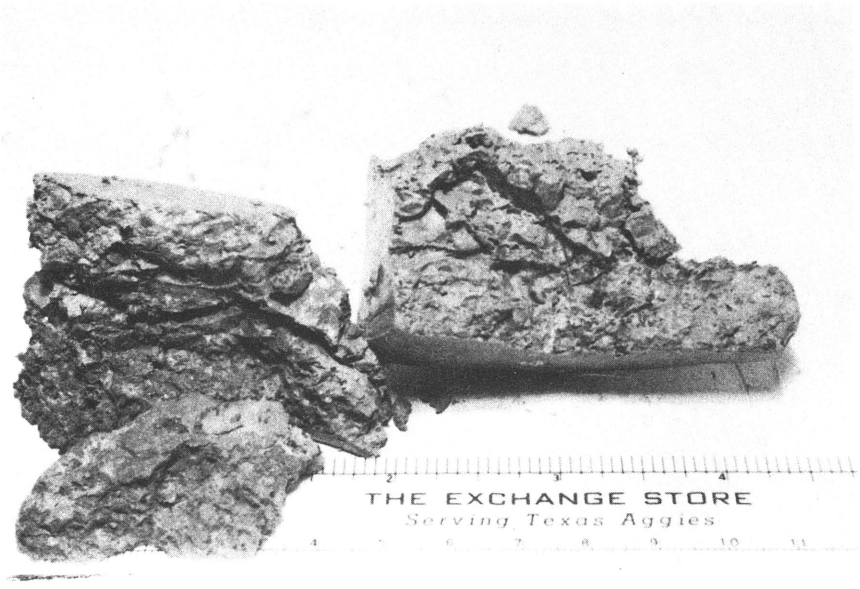

a. The Fissures in Beaumont Clay

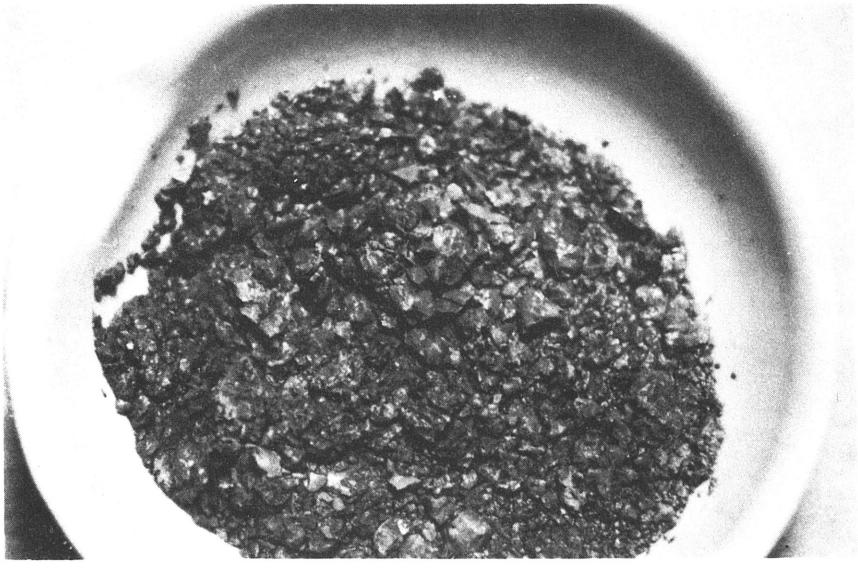

b. The Clay After Soaking in Water

FIG. 17.--PHOTOGRAPH OF FISSURES IN BEAUMONT CLAY

found at this depth.

At a depth of 24-28 feet, the clay is tan, contains fewer fissures, and the lumps are more firmly attached to each other. The clay has light gray spots, and the joints at this depth are smooth and shiny. However, at a depth of 29-31 feet, the color changes from tan to red and the clay is badly fissured and jointed. On the surface of the joints there is a layer of very fine sand and silt. This layer is extremely thin, probably no thicker than 2 or 3 grain diameters of the sand or silt sized particles. A mineralogical analysis shows that the clay minerals are almost the same as in other layers, except there is a lower percentage of montmorillonite and a high percent of illite (see Table 2).

The Beaumont Clay was subjected to repeated cycles of drying and wetting during as well as after it was deposited. Consequently, chemical and physical changes occurred, which affected the engineering properties of Beaumont Clay. Some of the phenomena which resulted from these processes are discussed at length in this paper.

There are numerous active faults within the Houston and Baytown areas. These faults are the result of subsidence of the area due to pumping of water, oil and gas from subsurface formations. The effect of subsidence and faults on the engineering properties of the Beaumont Clay is beyond the scope of this study.

Desiccation

The over-consolidation of the Beaumont Clay was caused by desiccation. When the clay was exposed to the surface, water started moving from the interior of the mass toward the surface where it evaporated. This process reduced the water content and created a capillary pressure or tension in the pore water of the soil (54). Such tension or negative pore pressure increases with decreasing moisture content of the soil. However, the total normal stress remains practically unchanged. Since the total stress is equal to the sum of the pore pressure and effective stress, decreasing the pore pressure causes equivalent increases of the effective stress. This effective stress acts all around the soil and consolidates it, not by increasing the total weight, but by increasing the negative pore pressure. This kind of consolidation gives no preferred particle orientation, and thus causes the clay to be isotropic (26). During the swelling process, the clay is free to swell more in the vertical direction than horizontally. This causes the effective stress to be more in a horizontal direction than in a vertical direction. The swelling process introduces an anisotropic phenomenon to the clay mass. Therefore, the Beaumont Clay can be considered an anisotropic material. Most of the over-consolidated soils which have been studied (e.g., London Clay) were consolidated by overburden pressure which was subsequently removed. Blight (14) showed in the laboratory that the slope of e-log p curve of specimens consolidated by mechanical loading

and by desiccation is different. The void ratios of specimens consolidated by desiccation are higher under similar effective pressures.

Consolidation Curves

For this study, consolidation tests were conducted on specimens oriented in vertical and horizontal directions as well as on remolded specimens. Typical e-log p curves for vertical, horizontal and remolded specimens are shown in Fig. 18. The pre-consolidation pressure for vertical and horizontal specimens, as found by the Casagrande method (16), is about 4.7 tsf. The coefficients of consolidation (c_v) are shown in Table 1. The c_v values for the remolded specimen is smaller than the undisturbed specimens. This difference can be attributed to the effects of fissures and joints, and structures which facilitated the drainage of the water. In general, c_v for horizontal specimens is higher than the vertical. The consolidation tests show that the horizontally oriented specimens deformed less than the vertically oriented under similar pressure. This variation in consolidation behavior of two specimens is the result of higher stresses in the horizontal direction to which the soil has been subjected during the geological history of the material.

There are several interesting features of the e-log p curves obtained from consolidation tests. First, the virgin part of the consolidation curve is parabolic rather than a straight line. Such a curve makes the method of determining the pre-consolidation pressures highly approximate. The second feature is the distinct change

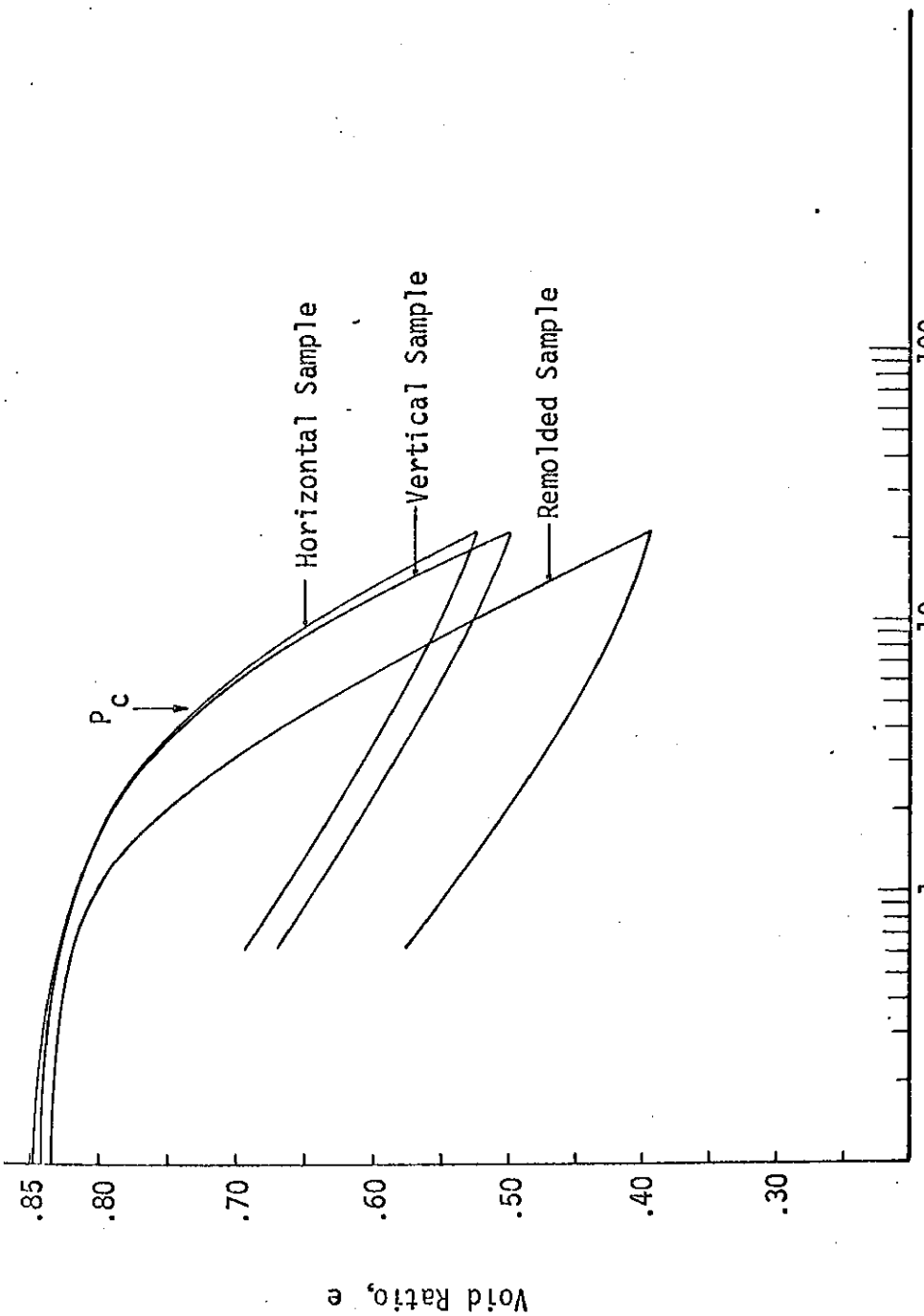

FIG. 18.--CONSOLIDATION CURVES OF BEAUMONT CLAY

TABLE 1.--THE VALUES OF COEFFICIENTS OF CONSOLIDATION (c_v)(in.^{2}/min.)

Depth ft.	Specimen Orientation	Consolidation Pressure tsf. 0.64-1.28	1.28-2.56	2.56-5.12	5.12-10.25	10.24-20.48	Preconsolidation Pressure tsf
19-21	Vertical	12.20×10^{-3}	6.35×10^{-3}	4.42×10^{-3}	1.78×10^{-3}	1.36×10^{-3}	4.65
19-21	Horizontal	9.93×10^{-3}	5.47×10^{-3}	4.07×10^{-3}	2.84×10^{-3}	2.34×10^{-3}	4.30
21-23	Vertical	13.20×10^{-4}	12.00×10^{-4}	4.55×10^{-4}	5.30×10^{-4}	4.67×10^{-4}	4.80
25-27	Vertical	2.84×10^{-3}	1.11×10^{-3}	1.04×10^{-3}	0.77×10^{-3}	0.76×10^{-3}	4.65
25-27	Horizontal	5.30×10^{-3}	2.27×10^{-3}	1.44×10^{-3}	1.22×10^{-3}	1.13×10^{-3}	4.70
25-27	Remolded*	5.68×10^{-4}	4.30×10^{-4}	4.19×10^{-4}	4.82×10^{-4}	5.68×10^{-4}	
29-30	Vertical	14.42×10^{-3}	13.35×10^{-3}	4.55×10^{-3}	2.70×10^{-3}	1.59×10^{-3}	6.40
33-35	Vertical	9.25×10^{-3}	1.89×10^{-3}	0.79×10^{-3}	0.47×10^{-3}	0.29×10^{-3}	6.80

in the curvature of the consolidation curve near the vicinity of the swell pressure. The third point of interest is that the rebound part of the consolidation curve is rather steep. This steep curve can be used as a possible indicator of certain geologic conditions which may have affected this soil. The curve suggests that the clay has weak bonds and the locked-in strain energy is small. Such conditions might be expected if the clay were subjected to weathering after initial deposition.

Initial Suction and Swelling Pressure

The capillary and swelling pressures were assumed to be equal (44). The swelling pressure was measured using two methods. First, the consolidation stages of the triaxial test were used to estimate the swelling pressure of the Beaumont Clay, and it was found to be about 1.40 tsf. Second, in the conventional consolidation test the swelling pressure was estimated to be about 1.10 tsf. The average value was 1.25 tsf.

The suction pressure values can be used to estimate K_o, the coefficient of earth pressure at rest. Skempton (44) reported that K_o for an over-consolidated clay could be estimated from the expression:

$$K_o = \frac{(\frac{P_k}{p}) - A_s}{1 - A_s} \qquad (9)$$

where: P_k = suction pressure
p^k = vertical effective stress in situ and
A_s = $\Delta u/\Delta (\sigma_1 - \sigma_3)$ corresponding to the removal of the deviator stress when $\sigma_1 = \sigma_2 > \sigma_3$

No tests were made to calculate A_s. However, Skempton (44) suggested that A_s for over-consolidated clays is equal to 0.3, and this is a reasonable approximation. If this value is used, then K_o for Beaumont Clay is about 1.5

Mineralogical Analyses

Results for the mineralogical analyses of the Beaumont Clay are shown in Table 2. These analyses show that the Beaumont Clay is composed principally of montmorillonite and illite. The <2μ samples contain an estimated quantity of 23-47 percent montmorillonite. A lower percentage of montmorillonite is accompanied by an increase in illite content, estimated to be from 28-55 percent. The content of kaolinite is estimated to be from 7-18 percent, and the quartz is estimated to be from 8-15 percent. The analyses on material from 2 to 50 μ are also shown in Table 2. These analyses show that the minerals are illite, kaolinite, quartz, feldspar and calcite. Table 2 also shows particle size distribution as it varies with depth.

It was stated that the color of the clay along the joint surfaces is light gray. A mineralogical analyses was performed on this material, and the major clay minerals found are shown in Table 2. No difference in clay minerals was found between this material and the bulk of the sample.

TABLE 2.--PARTICLE SIZE DISTRIBUTION AND MINERALOGICAL COMPOSITION

Depth ft.	Particle Size Distribution Sand % 2-.06mm	Silt % .06-.022mm	Clay % <.002mm	Mineralogical Composition < .002mm Mont. %	Illite %	Kaolinite %	Mineralogical Data on .002-.050mm Minerals found
20-22	4.0	20.0	76	47	28	15	Illite, Kaolinite, Quartz, Feldspar, and Calcite
24-25	4.3	18.7	77	40	32	18	Same as above
29-31	10.3	33.7	56	23	55	7	Same as above
33-35	6.3	33.7	60				
Surface of the Joints	1.4	10.6	88	46	31	15	

CHAPTER V

RESULTS AND DISCUSSION OF RESULTS

Triaxial Tests

Before discussing the results, it is pertinent to mention the two failure criteria commonly used in presenting the results of triaxial tests on soils. These criteria are: the maximum deviator stress, $(\sigma_1 - \sigma_3)$; and the maximum principal effective stress ratio $\frac{\sigma_1'}{\sigma_3'}$. Fundamentally, it is more logical to use the latter. It takes into consideration the effect of pore pressure, which causes σ_3' to vary throughout the test. However, in practice, pore water pressure is not always measured. Thus, it is necessary to define the strength in terms of the maximum deviator stress. In this study, both criteria are used to present the results of the triaxial tests.

In the Beaumont Clay, the principal effective stress ratio reached its maximum value before the maximum deviator stress in most of the specimens as shown in Table 3. This phenomenon is a result of the variation of pore water pressure with strain.

In general, the pore water pressure reached its maximum value before the deviator stress. However, in several cases, and especially at high consolidation pressures, the two criteria coincided at the failure point. When this happened, the pore water pressure reached its maximum value when the maximum deviator stress was obtained. In drained tests, there is obviously no difference between the two criteria.

TABLE 3.--SUMMARY OF TRIAXIAL TESTS

Depth ft.	Specimen Orientation	Core Diameter In.	Water Content, %	Consolidation Pressure, psi	Strength Parameter		Failure Strain, %		A_f	
					c', psi	ϕ'	$\frac{\sigma'_1}{\sigma'_3}$	$\sigma_1 - \sigma_3$	$\frac{\sigma'_1}{\sigma'_3}$	$\sigma_1 - \sigma_3$
20-21.5	Vertical	5	34.7	10			2.71	4.44	.196	.080
20-21.5	Vertical	5	33.8	20			3.83	5.40	.330	.269
20-21.5	Vertical	5	34.7	40	2.9	15.5°	3.13	3.13	.466	.466
20-21.5	Vertical	5	34.7	60			3.73	3.73	.580	.580
20-21.5	Horizontal	5	32.0	10			1.16	1.85	.233	.172
20-21.5	Horizontal	5	31.5	20			1.55	2.15	.258	.210
20-21.5	Horizontal	5	34.6	40	3.5	15.5°	2.34	2.34	.360	.360
20-21.5	Horizontal	5	32.7	60			5.74	4.15	.490	.470
20-22	Vertical	3	30.2	10			3.78	5.93	.077	-.038
20-22	Vertical	3	33.5	20	2.9	16.4°	2.10	6.03	.322	.182
20-22	Vertical	3	33.2	40			4.32	4.91	.378	.373
22-23.5	Vertical	5	34.7	10			1.65	7.36	.320	.138
22-23.5	Vertical	5	34.4	20			2.90	6.25	.471	.409
22-23.5	Vertical	5	33.9	40	1.4	17.3°	3.95	3.95	.543	.543
22-23.5	Vertical	5	35.5	60			4 .76	4.76	.588	.588
22-23.5	Horizontal	5		10			1.35	3.98	.207	.039
22-23.5	Horizontal	5	32.4	20			1.02	1.33	.357	.288
22-23.5	Horizontal	5	30.5	40	4.6	17.0°	2.51	2.51	.408	.408
22-23.5	Horizontal	5	31.8	60			3.40	3.40	.491	.491
33-35	Vertical	3	34.3	10			1.88	5.53	.233	.044
33-35	Vertical	3	33.7	20	2.8	19.5°	1.57	6.10	.374	.238
33-35	Vertical	3	32.6	40			1.95	2.23	.386	.374
33-35	Vertical	3	32.0	40			2.46	2.46	.488	.488

TABLE 3 (Cont'd.)

Depth ft.	Specimen Orientation	Core Diameter In.	Water Content, %	Consolidation Pressure, psi	Strength Parameter		Failure Strain,%		A_f	
					c', psi	ϕ'	$\frac{\sigma'_1}{\sigma'_3}$	$\sigma_1-\sigma_3$	$\frac{\sigma'_1}{\sigma'_3}$	$\sigma_1-\sigma_3$
22-23.5*	Vertical	3	29.3	10			2.76	2.76		
22-23.5*	Vertical	3	30.2	20	3.6	13.0°	1.81	1.81		
22-23.5*	Vertical	3	30.4	40			2.44	2.44		
22-23.5**	Vertical	3	37.4	10			2.94	4.36	.402	.358
22-23.5**	Vertical	3	37.7	20	3.6	12.5°	5.93	7.04	.516	.490
22-23.5**	Vertical	3	37.3	40			6.46	6.93	.677	.659
22-23.5**	Vertical	3	40.8	10			3.91	3.91	.371	.371
22-23.5**	Vertical	3	41.1	20	3.2	12.5°	6.50	6.50	.570	.570
22-23.5**	Vertical	3	41.2	40			6.90	6.90	.803	.803

* Drained test
**Remolded test

Consolidated Undrained Tests

The results of these tests are presented below in Table 4. The strength parameters of vertical and horizontal specimens are given where these data are available.

TABLE 4.--RESULTS OF CONSOLIDATED UNDRAINED TESTS

Depth ft.	Specimen Orientation	c', psi	ϕ'	A_f
20 - 21.5	Vertical	2.90	15.5^o	0.20 - 0.58
20 - 21.5	Horizontal	3.50	15.5^o	0.23 - 0.50
22 - 23.5	Vertical	1.40	17.3^o	0.32 - 0.59
22 - 23.5	Horizontal	4.60	17.0^o	0.21 - 0.49
20 - 22	Vertical	2.90	16.4^o	0.08 - 0.38
33 - 35	Vertical	2.80	19.5^o	0.23 - 0.49

Typical Mohr circles of the specimens are shown in Fig. 19. It was found that the results were quite scattered, and this can be attributed to the different orientation of pre-existing failure planes in the various specimens. These weak planes were noted prior to loading, and their inclination exhibits all degrees of variation, which caused the variation of strength in the specimens. Consequently, it is not easy to draw a Mohr failure envelope for the specimens. In Fig. 20, the results are plotted in terms of half of the deviator stress, $1/2(\sigma_1 - \sigma_3)$, against the mean effective stress, $1/2(\sigma_1' + \sigma_3')$, and a best-fitting line is drawn through the points. The slope of this line, ψ, is related to the slope of the Mohr envelope by the expression:

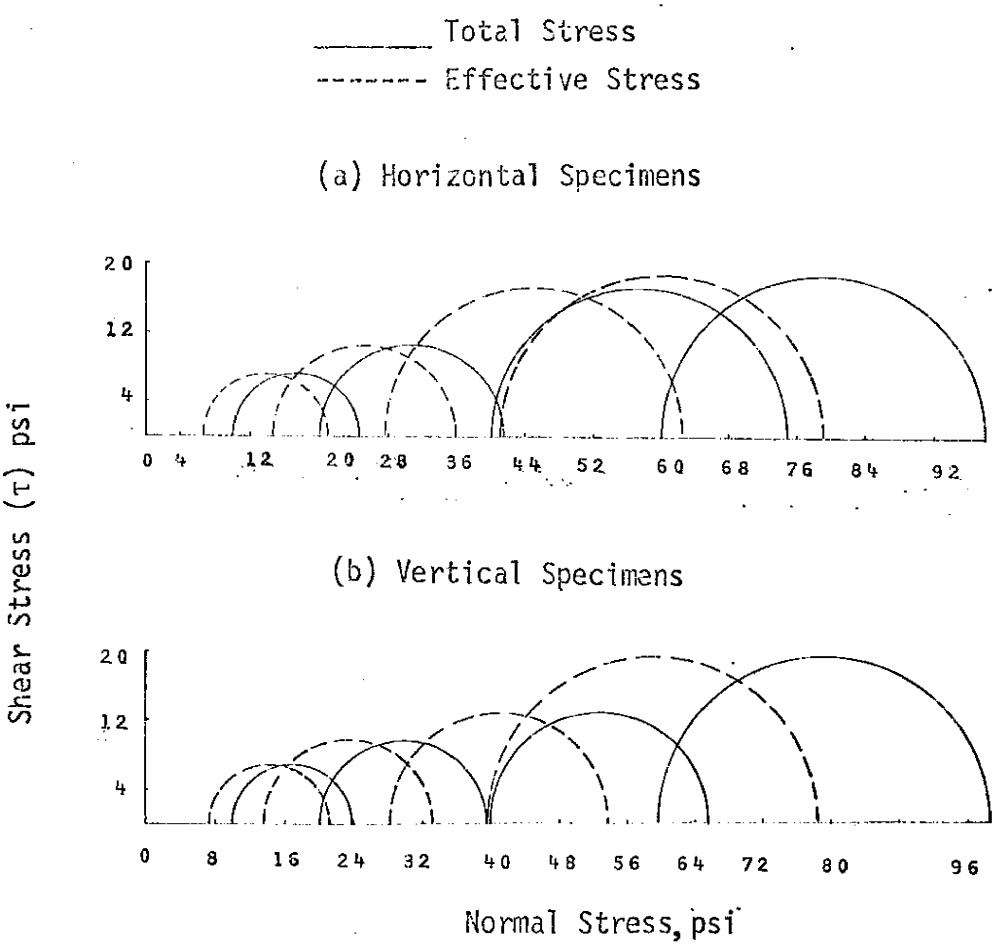

FIG. 19.— MOHR CIRCLES FOR HORIZONTAL AND VERTICAL SPECIMENS

(a) Horizontal Specimens

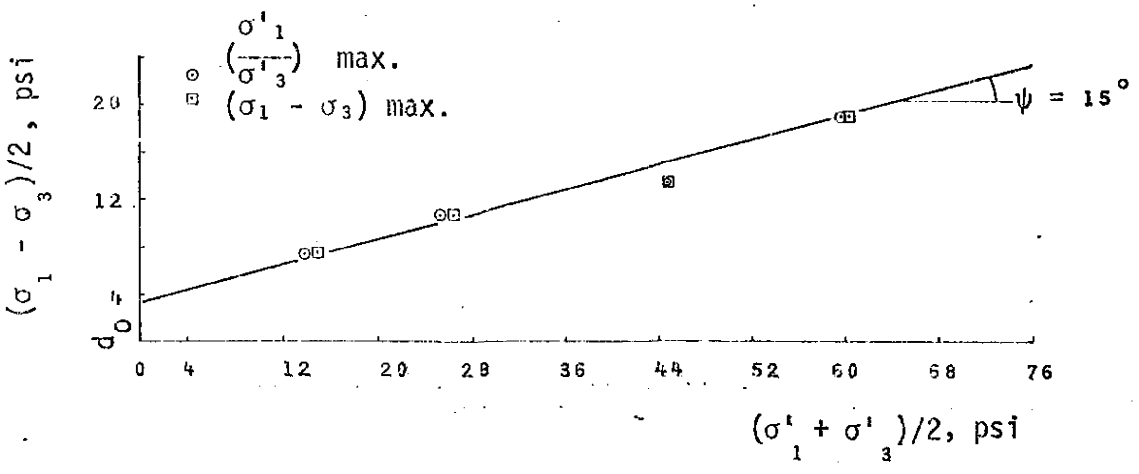

(b) Vertical Specimens

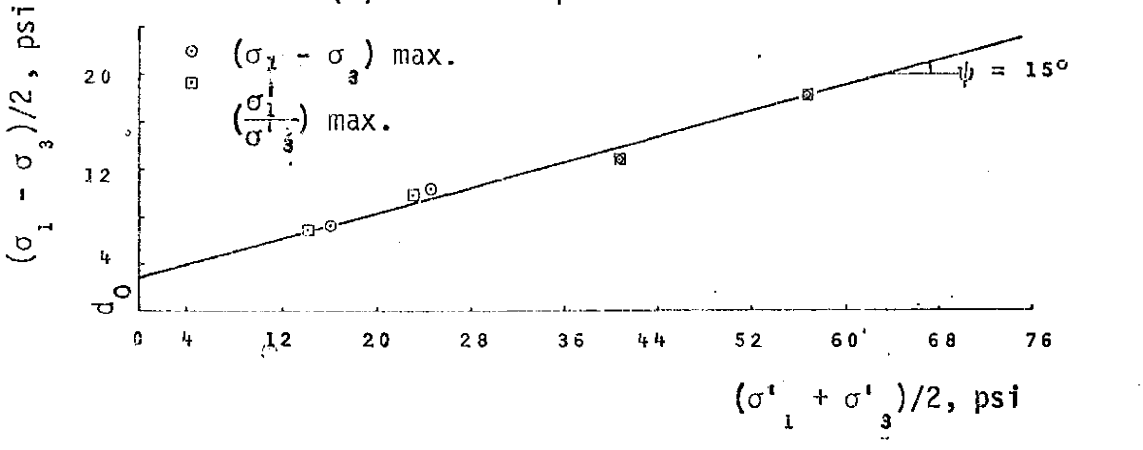

FIG. 20.— RELATIONSHIPS BETWEEN $(\sigma_1 - \sigma_3)/2$ AND $(\sigma'_1 + \sigma'_3)/2$ FOR HORIZONTAL AND VERTICAL SPECIMENS

$$\tan \psi = \sin \phi'$$

The intercept d_o is related to the cohesion by the expression:

$$d_o = c' \frac{\tan \psi}{\tan \phi'}$$

In Fig. 20 the results are presented using both failure criteria, $(\sigma_1 - \sigma_3)_{max.}$ and $(\frac{\sigma_1'}{\sigma_3'})_{max.}$, but no significant difference is found in the strength parameters expressed in the two criteria.

The results in Table 4 indicate that the angle of shearing resistance at a particular depth has the same value in the vertical and horizontal direction. However, the cohesion intercept c' is higher in the horizontal direction than in the vertical. This variation in the cohesion is probably a manifestation of the soil structure. The structure of the clay in the horizontal direction is different than in the vertical direction because of the higher horizontal stress to which the clay has been subjected.

As might be expected, the strength properties of Beaumont Clay vary with depth as shown in Table 4. This variation is mainly associated with the degree of fissuring and the nature of the joints. In the case of smooth joints, the strength tends to be low.

Stress-Strain Curves.--Typical stress-strain curves are presented in Figs. 21 and 22. Most of the specimens reached a maximum stress at rather small strain as shown in Table 5. However, the curves indicate plastic rather than brittle type of failure.

It was observed throughout the preparation of the specimens that most of them contained at least one pre-existing failure plane in addition to the fissures. Fig. 23 shows several triaxial specimens

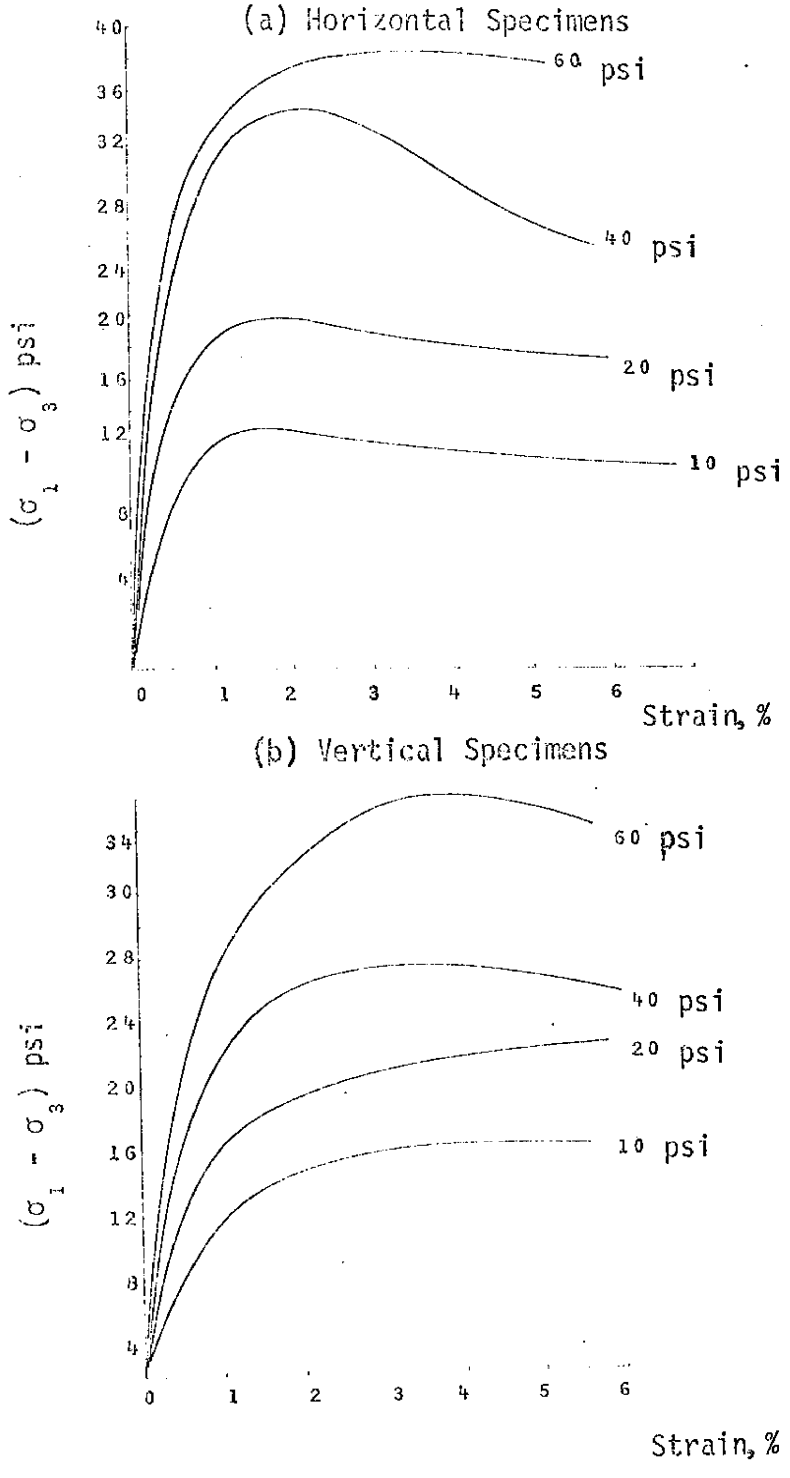

FIG. 21.— STRESS-STRAIN CURVES FOR HORIZONTAL AND VERTICAL SPECIMENS

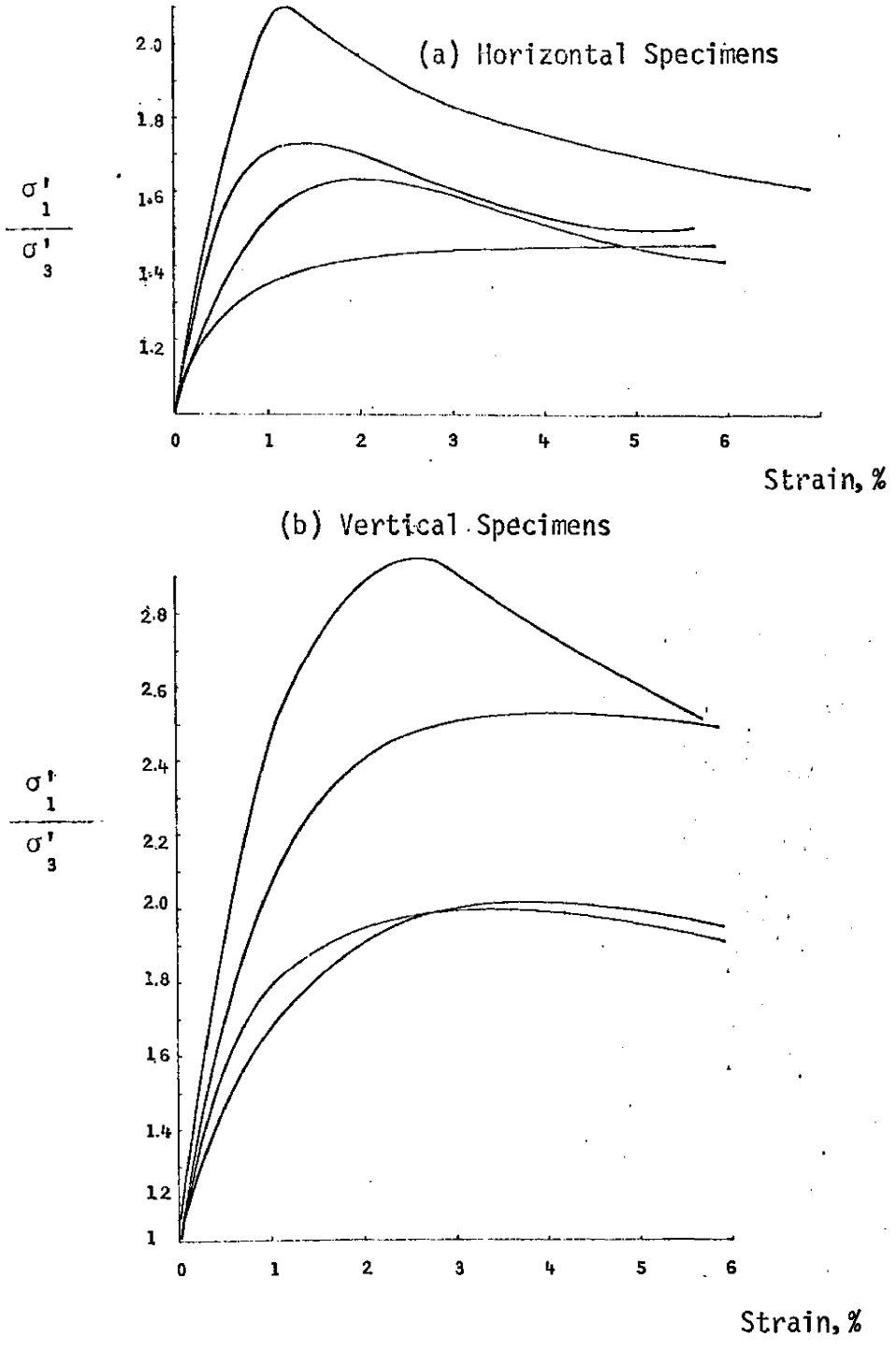

FIG. 22.-- RELATIONSHIPS BETWEEN EFFECTIVE PRINCIPAL STRESS RATIO AND STRAIN, FOR HORIZONTAL AND VERTICAL SPECIMENS

TABLE 5.--FAILURE STRAIN OF CONSOLIDATED UNDRAINED SPECIMENS

Depth ft.	Specimen Orientation	Failure Strain, %
20 - 21.5	Vertical	2.71 - 3.83
20 - 21.5	Horizontal	1.16 - 5.74
20 - 22'	Vertical	2.10 - 4.32
22 - 23.5	Vertical	1.65 - 4.76
22 - 23.5	Horizontal	1.02 - 3.40
33 - 35	Vertical	1.57 - 2.46

after testing. It was found that the discontinuities, which include fissures and joints, are the factors which control the behavior of the specimens under loading and have pronounced effects on the stress-strain curves. It was also observed that the failure of the specimens was slip type rather than plastic, perhaps due to the fact that most of the specimens failed completely or partially on their pre-existing failure planes.

The mechanism of the failure of the specimens is not quite clear. It is well known (5, 45) that the fissures and the joints have a major effect on the mechanism of the failure. The tested specimens were observed closely in the process of loading. It was found that the shear plane, in some cases, went around small pieces of the clay following the fissure surfaces, but in most cases it cut through these pieces. Where there were joints, in general, the specimens failed on these joints. The fissures and the joints affected the peak value of

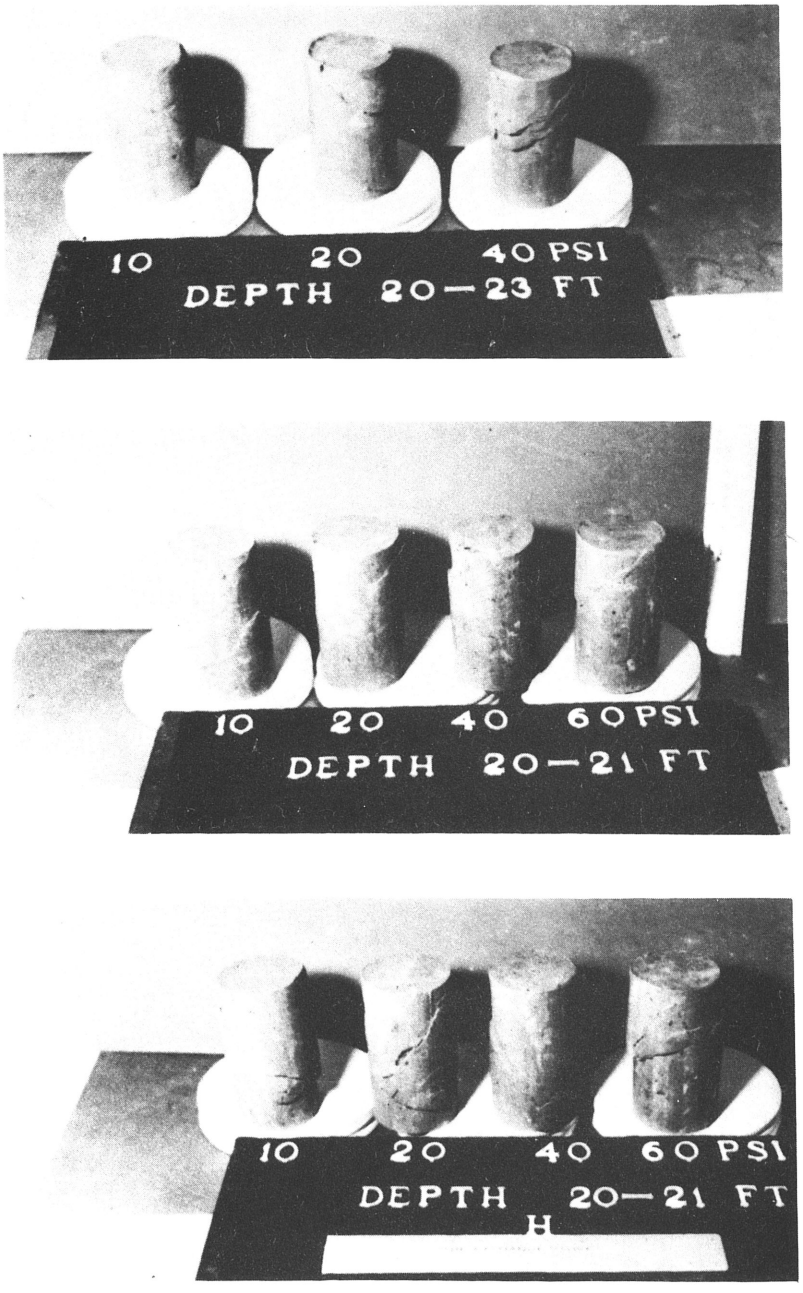

FIG. 23.--SPECIMENS OF BEAUMONT CLAY AFTER THE TEST

the stress-strain curves, and a curve with a sharp peak is very seldom found, while most of the curves do not show any peak.

The stress-strain curves for horizontal specimens are presented in Fig. 21. They show the same type of plastic failure as the vertical specimens; however, the horizontal specimens show a higher strength. In general, as shown in Table 5, the horizontal specimens failed at smaller strains than the vertical ones.

Pore Water Pressure.--Fig. 24 shows the variation of the pore water pressure with strain for different consolidation pressures and for both vertical and horizontal specimens. It appears that there is no significant difference in pore water pressure between the vertical and horizontal specimens, although the pore pressures in horizontal specimens tend to decrease more after passing the peak value than they do in vertical specimens.

In heavily over-consolidated soil, the pore water pressure usually exhibits a large decrease in its value and becomes negative under loading, as reported by Bishop and Henkel (9). It has been shown that Beaumont Clay is an over-consolidated clay; however, the pore water pressures measured in this research do not clearly confirm this phenomenon. In general, the pore water pressure shows a slight decrease in its value after the peak. The measured values of pore water pressure in the tested specimens was confirmed by the volume change measurements in the drained tests. In these specimens the volume decreased throughout the tests, which is equivalent to the behavior of the pore water pressure in the undrained tests. This

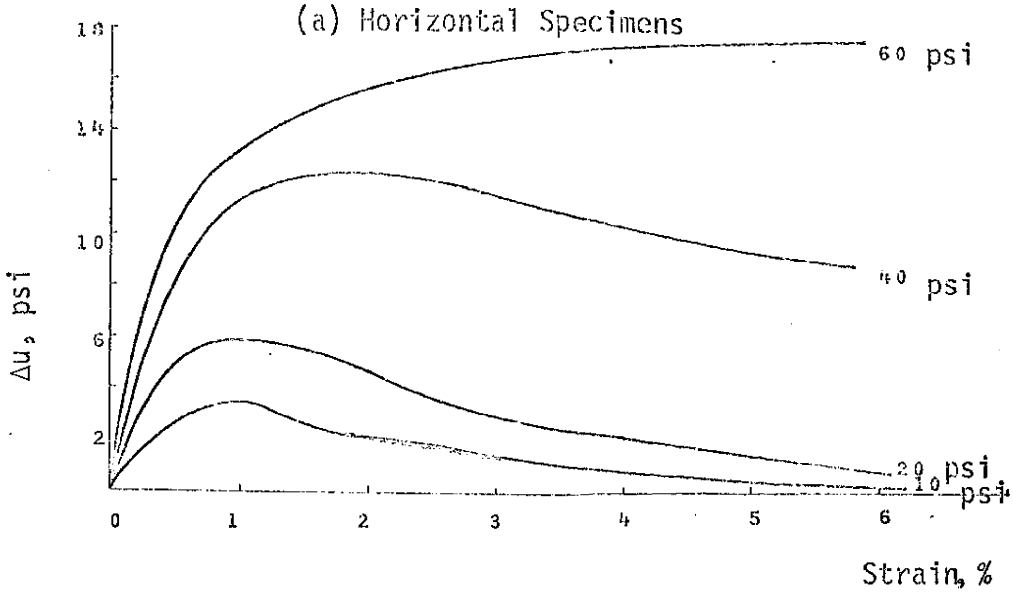

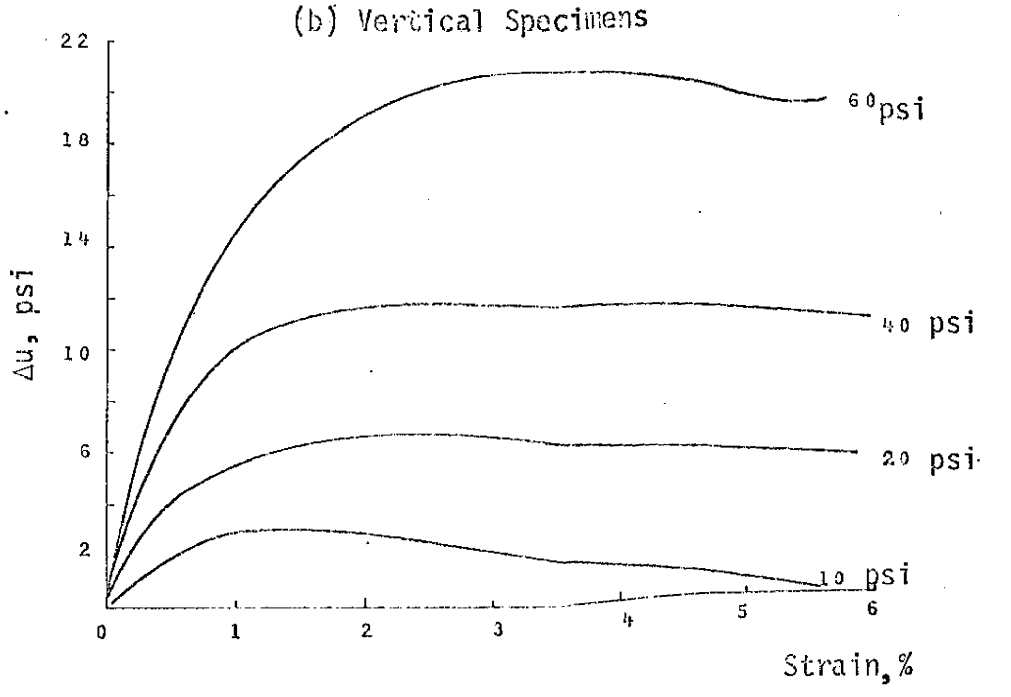

FIG. 24.-- RELATIONSHIPS BETWEEN EXCESS PORE WATER PRESSURE AND STRAIN FOR HORIZONTAL AND VERTICAL SPECIMENS

unique relationship of the pore water pressure with strain is attributed to the fissures and pre-existing failure planes, which control the behavior of the specimens under loading. It is the writer's opinion that the pore water pressure which was measured was the one which existed in the fissures and joints, and probably was different from the one existing in the intact lumps of the clay. Unfortunately, the technique necessary to confirm this opinion is not available.

A question may arise as to whether this behavior was the result of of leakage between the membrane and the rubber O-rings. This point was checked for almost every specimen. The specimen was left under loading conditions at the end of the test for about one hour and during that period the pore water pressure was checked several times, and no variation in its value was found.

Pore Water Pressure Coefficient (A).--Fig. 25 plots the pore water pressure coefficient (A) vs. strain for different consolidation pressures, and for both vertical and horizontal specimens. At consolidation pressures of 10 and 20 psi the A value reaches a maximum then decreases with strain, while at consolidation pressures of 40 and 60 psi the A value stays constant or shows a slight increase with the strain.

The value of A_f (the coefficient of pore water pressure at failure) is a function of consolidation pressure as well as the stress history of the material (42). Fig. 26, which illustrates the relationship between A_f and the over-consolidation ratio (O.C.R.), shows there is a wide variation in the A_f values at the same consolidation

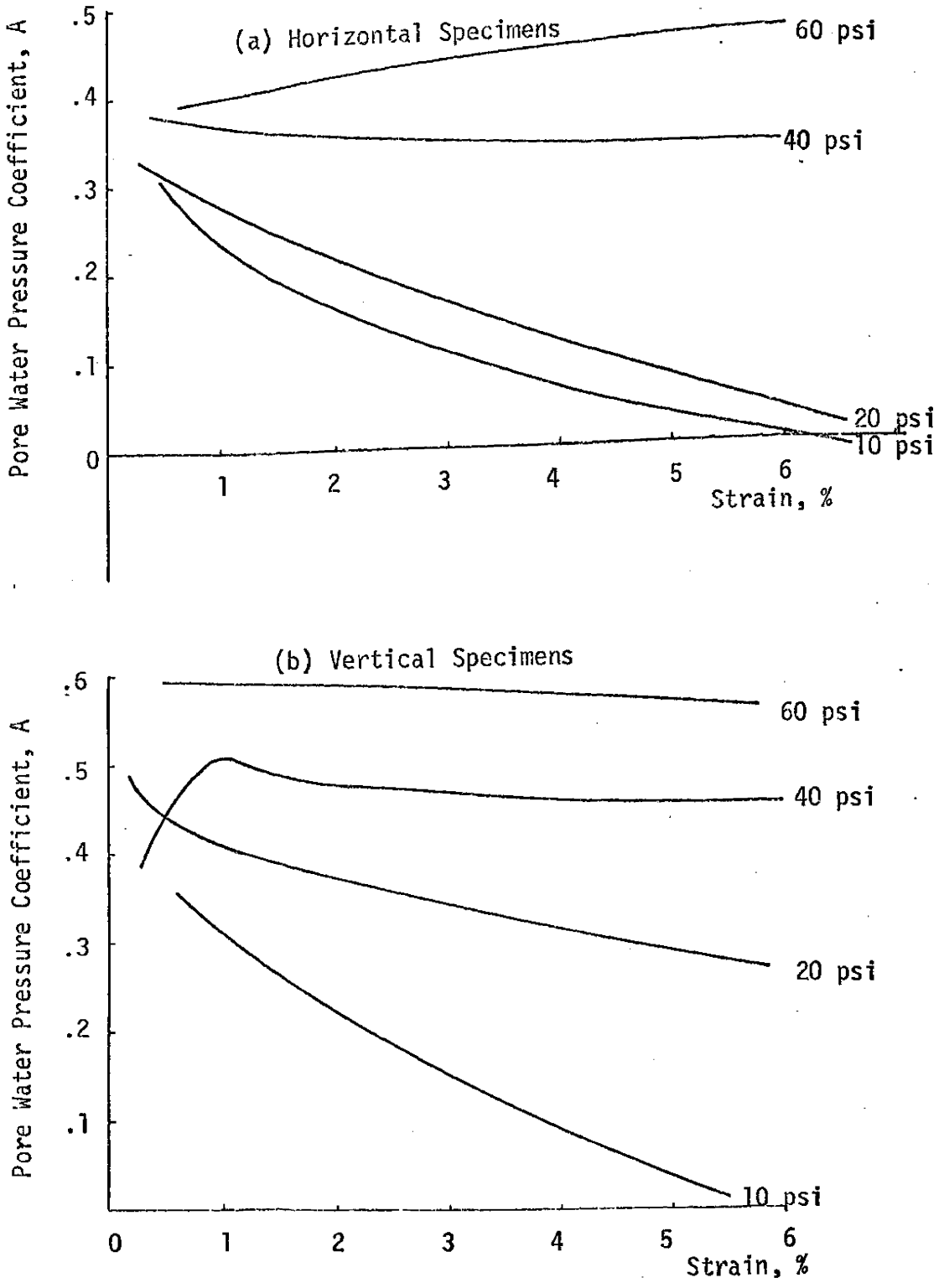

FIG. 25.-- RELATIONSHIPS BETWEEN PORE PRESSURE COEFFICIENT (A) AND STRAIN FOR HORIZONTAL AND VERTICAL SPECIMENS

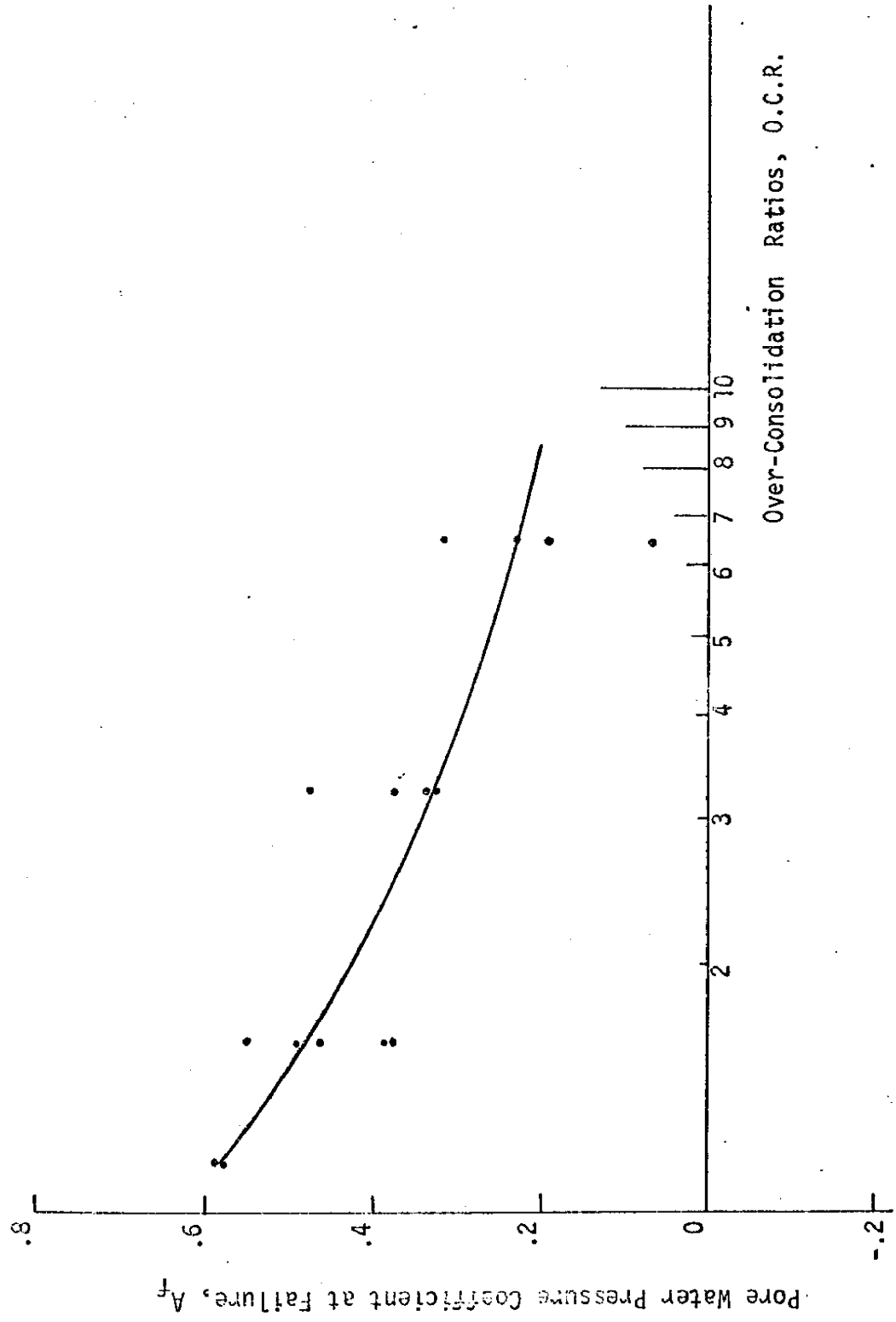

FIG. 26.--RELATIONSHIP BETWEEN A_f AND O.C.R. OF BEAUMONT CLAY

pressure. This variation could be attributed to the degree of fissuring and to the nature of pre-existing joints in the specimens. These discontinuities (fissures and joints) have a major effect on the behavior of the specimens, as stated before, and particularly on the failure strain. Since A_f is a function of failure strain, this could be the major factor which controls A_f values.

For horizontal specimens, A_f in general is less than the value for vertical specimens as shown in Table 4.

Consolidated Undrained Tests on Remolded Specimens

Specimens from depth 22-23.5 feet were remolded, and two series of tests were conducted on them. In the first series, the specimens were remolded at a moisture content of 37.5 percent, which is 2-3 percent higher than the natural water content. In the second series, specimens were remolded at a moisture content of 41 percent. Both series were tested under undrained conditions after consolidation in the triaxial apparatus.

The strength parameters are presented in Table 6 and Fig. 27. These parameters are: $\phi' = 12.5^0$ for both series and $c' = 3.6$ and 3.2 psi for the first and second series, respectively. The variation in the water content does not affect the angle of shearing resistance any significant amount that could be measured in these tests. However, the cohesion intercept is a function of water content for a saturated soil, and it decreases with the higher moisture content, as might be expected.

TABLE 6.--CONSOLIDATED UNDRAINED RESULTS FOR REMOLDED SPECIMENS

Depth ft.	Water Content,%	ϕ'	c', psi	A_f	Failure Strain, %
22 - 23.5	37.5	12.5	3.6	.402 - .677	2.94 - 6.46
22 - 23.5	41.0	12.5	3.2	.37 - .803	3.91 - 6.90

It may be noted from Tables 4 and 6 that the value of ϕ' for the undisturbed specimens at a depth of 22-23.5 feet is approximately 17^{o}, while for the remolded specimens it is 12.5^{o}. This difference is due to the particles' structural arrangement. In the case of remolded specimens, the original structure of the clay is disturbed by remolding. In the sampling processes, the clay may also be disturbed to some extent, and this disturbance may affect the values of the angle of shearing resistance which are measured in the laboratory.

The stress-strain curves, pore water pressure curves, and the coefficients of pore water pressure curves are shown in Figs. 28, 29, and 30, respectively. The stress-strain curves are flatter than the curves for undisturbed specimens, and failure occurs at higher strains than for undisturbed specimens. All the remolded specimens which reached a maximum value and failed showed plastic characteristics during failure.

The coefficient of pore water pressure A_f increases as the moisture content increases, and in general, A_f is higher in remolded specimens than in the undisturbed.

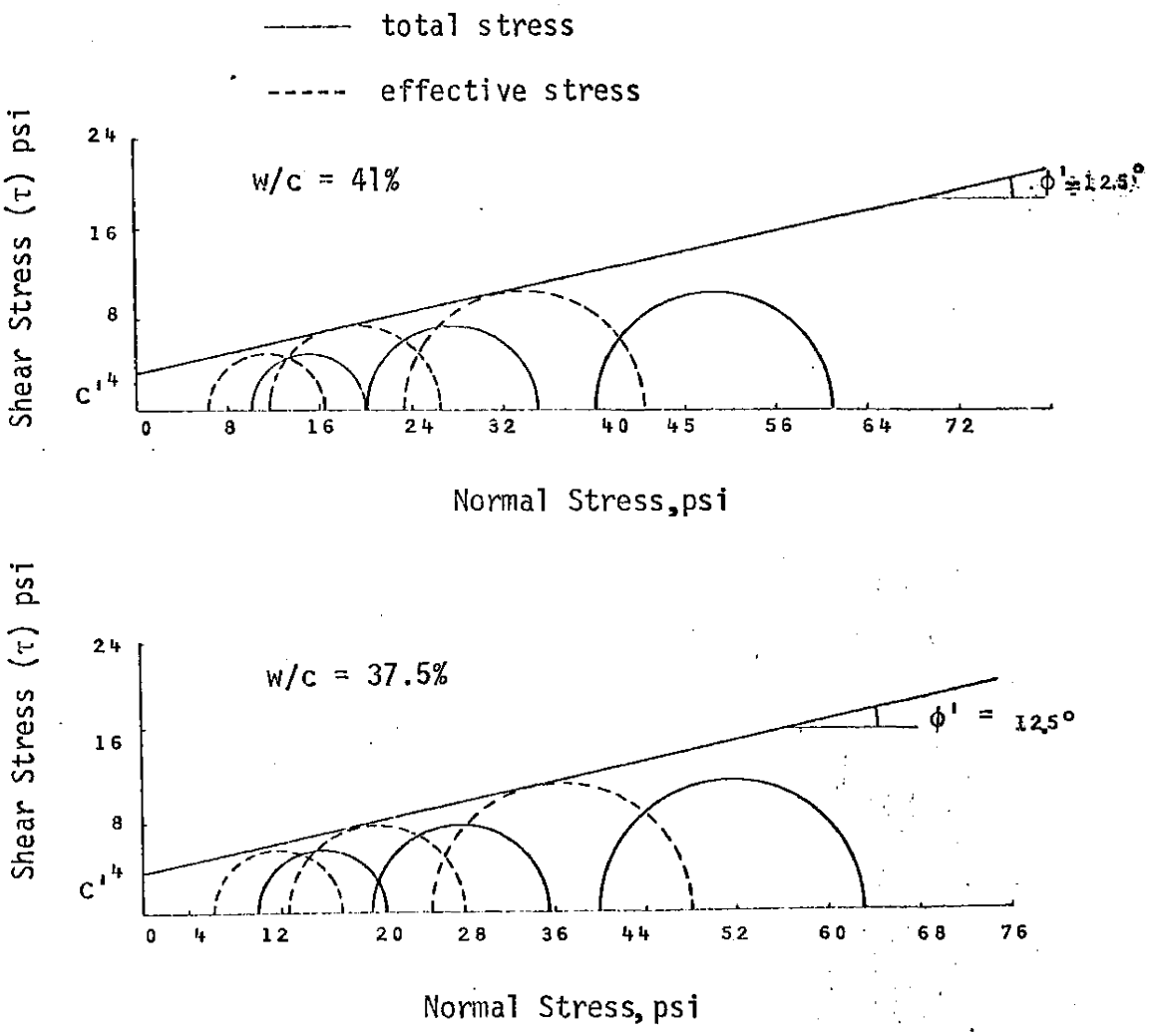

FIG. 27. -- STRENGTH PROPERTIES OF REMOLDED SPECIMENS

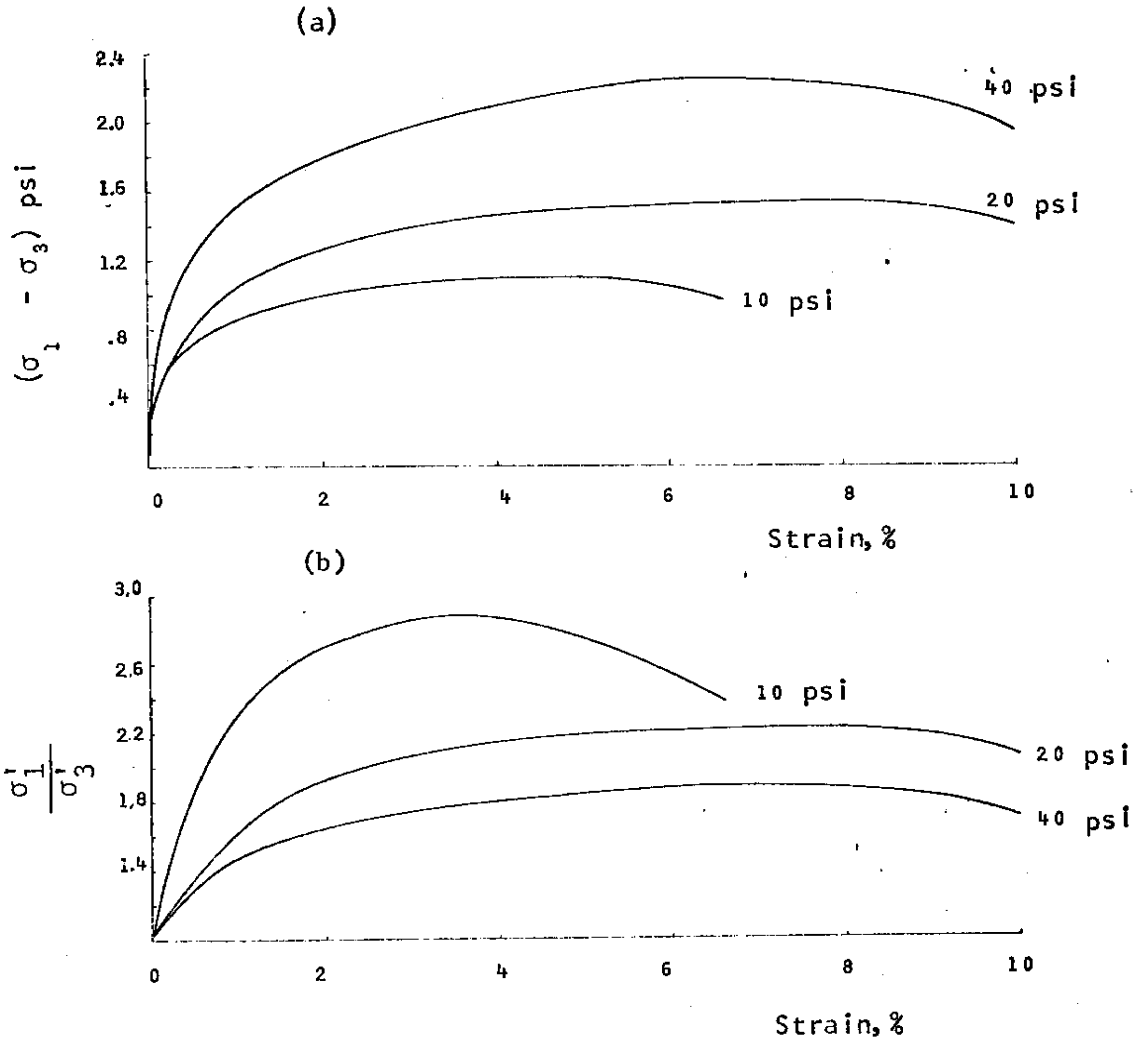

FIG. 28.-- (a) STRESS-STRAIN RELATIONSHIPS OF REMOLDED BEAUMONT CLAY WITH w/c = 37.5%

(b) EFFECTIVE PRINCIPAL STRESS RATIO - STRAIN RELATIONSHIPS

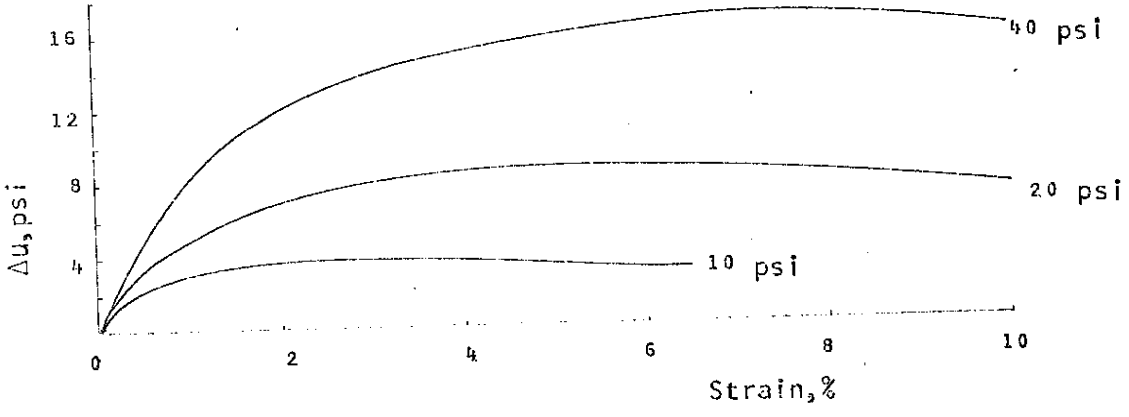

FIG. 29.— RELATIONSHIPS BETWEEN EXCESS PORE WATER PRESSURE AND STRAIN FOR REMOLDED CLAY WITH w/c = 37.5%

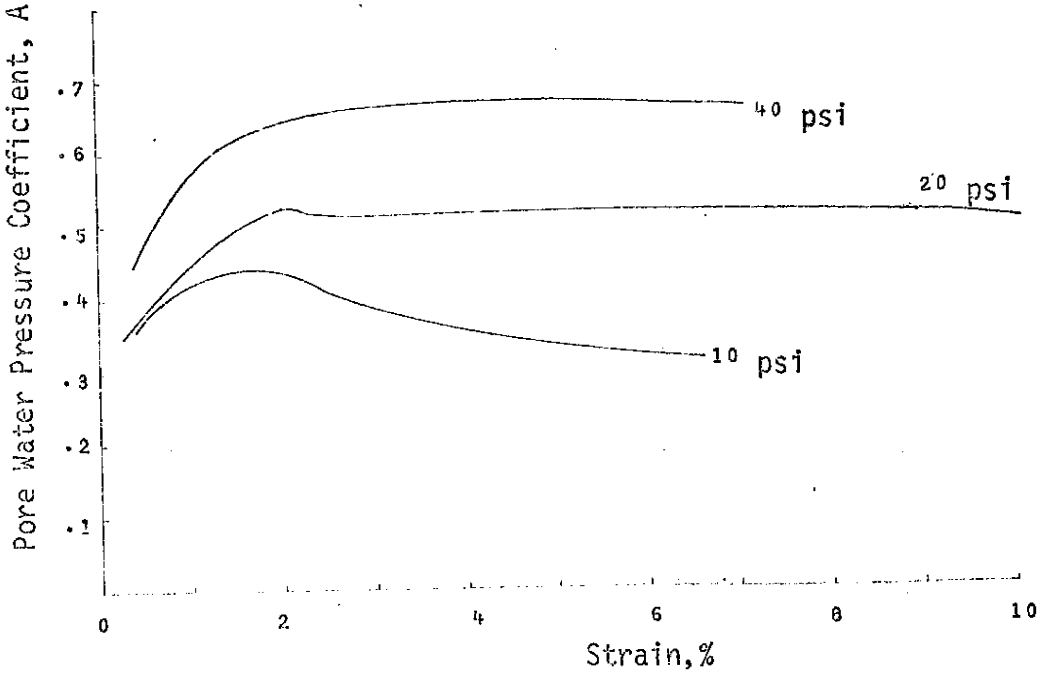

FIG. 30.--RELATIONSHIPS BETWEEN PORE WATER PRESSURE COEFFICIENTS, A, AND STRAIN FOR REMOLDED CLAY WITH w/c = 37.5%

Drained Tests

The results of the drained triaxial tests are presented in Figs. 31-33. The strength of the material obtained from these tests is:

$$\phi_d = 13.0^o$$

$$c_d = 3.6 \text{ psi}$$

It appears that the drained angle of shearing resistance, ϕ_d, is about 4^o less than the value of ϕ' found from consolidated undrained tests. This difference can be attributed to several factors: first, there is the ever present possibility of variation in specimens, primarily in the clay composition; second, the effect of the rate of strain which is slower in drained tests than in consolidated undrained tests; and third, all drained test specimens contained pre-existing failure planes with smooth shiny surfaces which were oriented in the direction most liable for failure. The cohesion found from drained tests is higher than in the consolidated undrained tests, possibly as a result of the lower moisture content of the drained test specimens.

The volume change--strain relationship is shown in Fig. 33. As mentioned previously, these curves confirm the results of the pore water pressure measured in consolidated undrained tests. The volume of the specimens decreased with the strain during the application of the deviator stress. This behavior is similar to the behavior of the pore water pressure in the consolidated undrained tests, where the change in pore water pressure, Δu, was positive. The same reasoning used before to explain the behavior of the pore water pressure in the

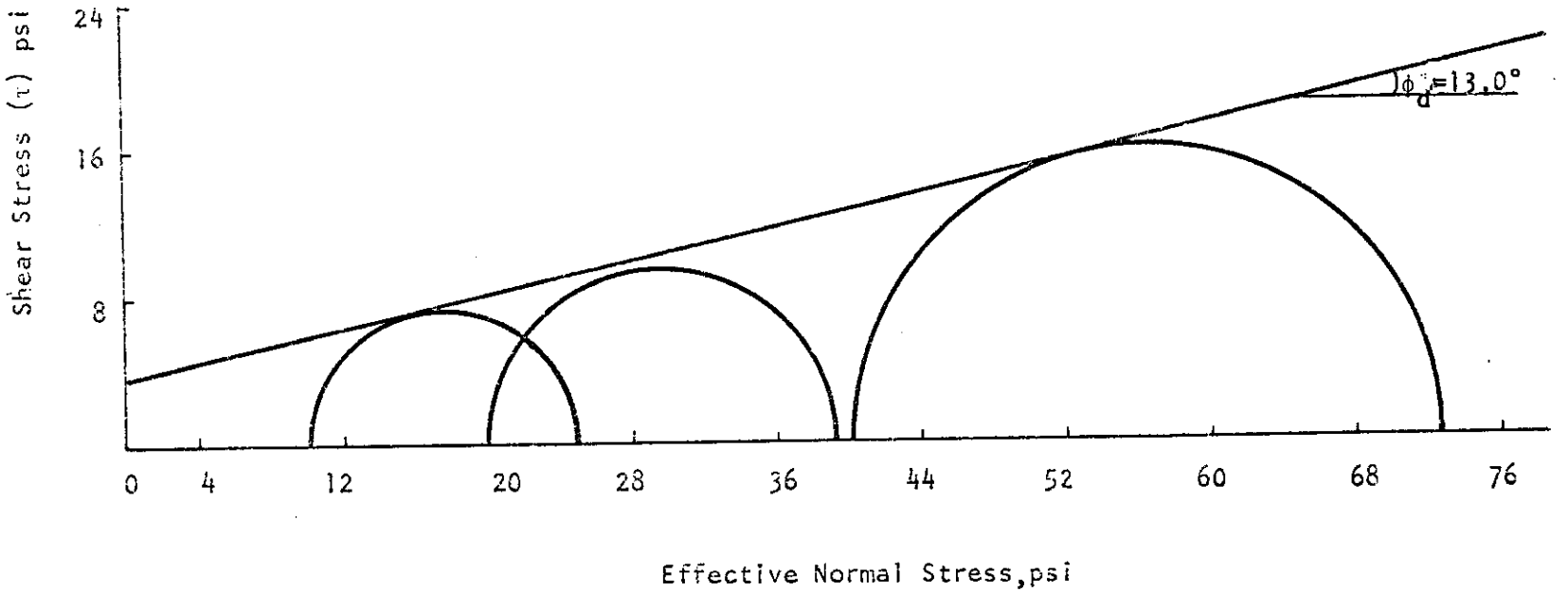

FIG. 31.-- FAILURE ENVELOPE FOR DRAINED TESTS

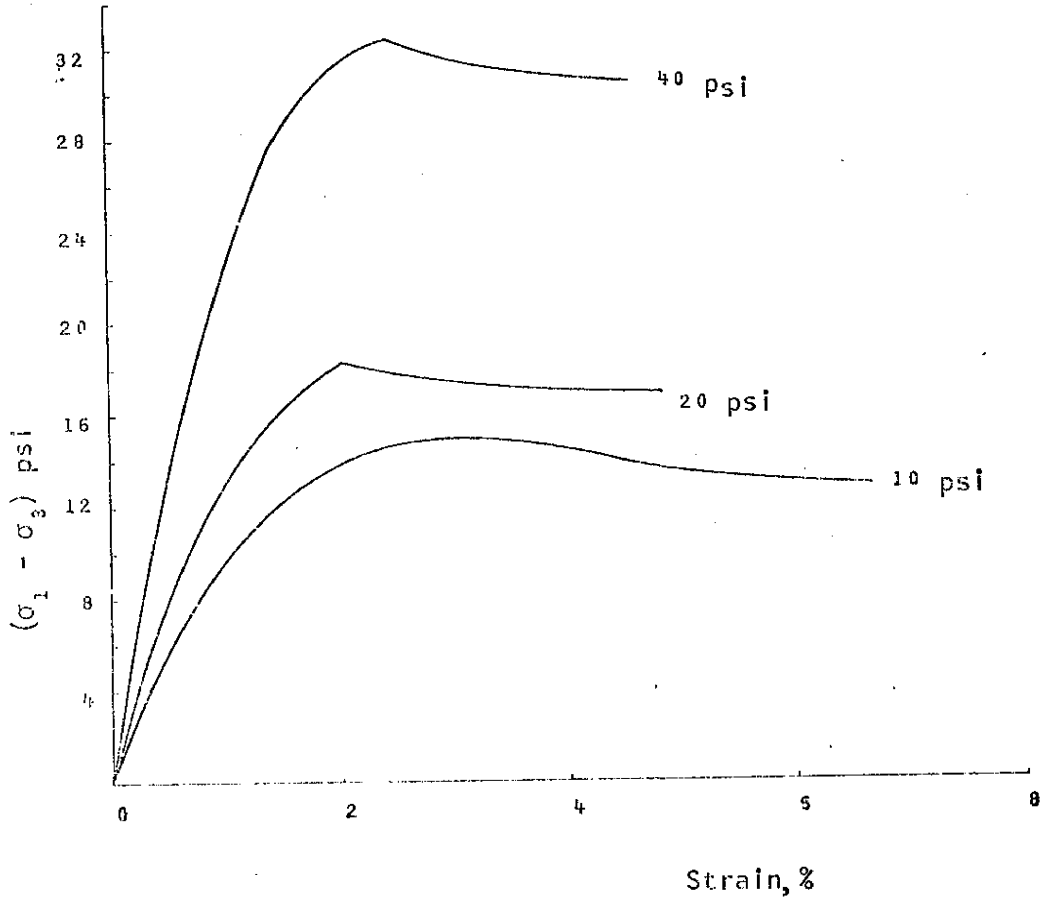

FIG. 32.-- STRESS - STRAIN RELATIONSHIPS FOR DRAINED TESTS

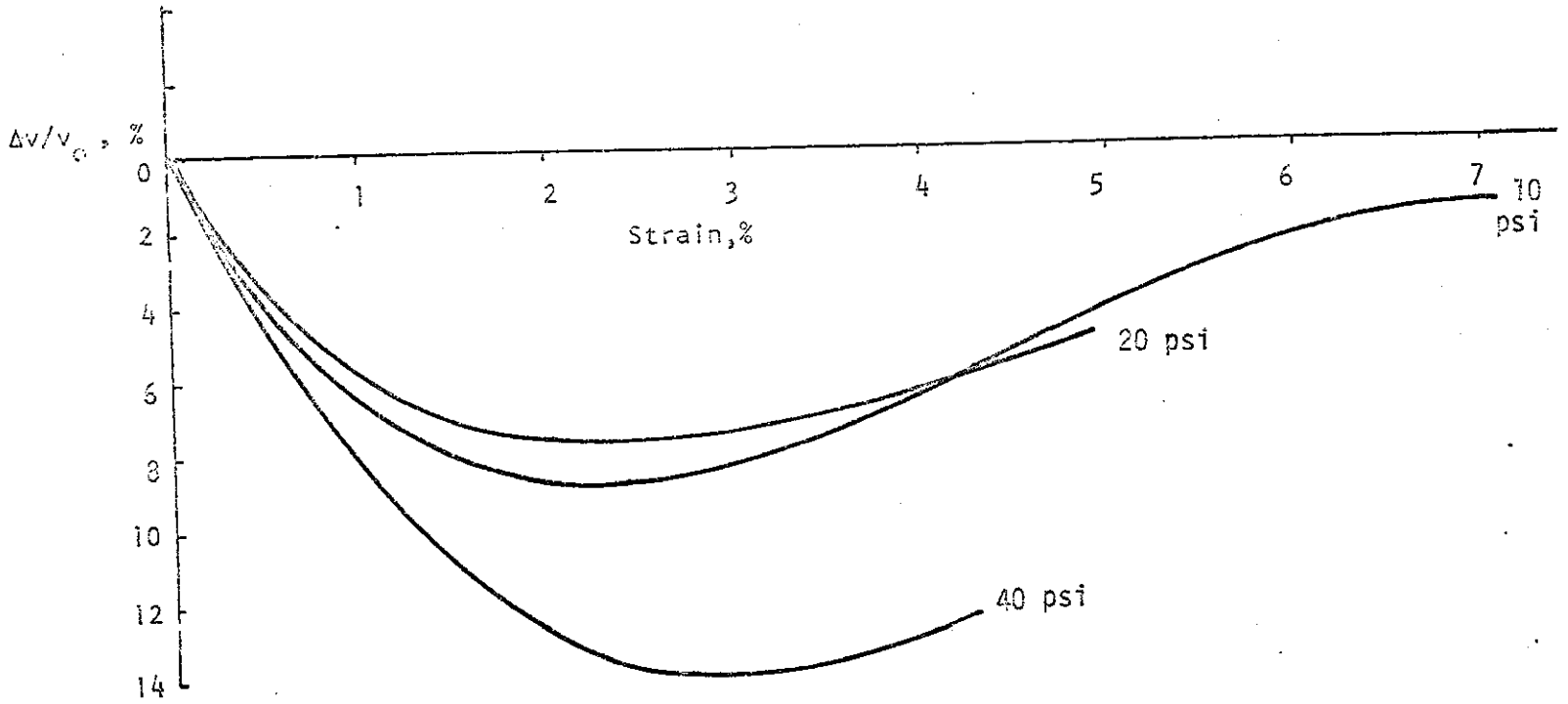

FIG. 33.--RELATIONSHIPS BETWEEN VALUE CHANGE AND STRAIN OF DRAINED TESTS

consolidated undrained tests can be applied here to explain the volume change behavior of drained tests.

Unconsolidated Undrained Tests

The results of the unconsolidated undrained tests on undisturbed specimens oriented in both vertical and horizontal directions are given in Table 7. These tests were carried out at a constant rate of strain of 0.02 inches/minute, which is slower than routine practice, in order to determine more accurately the deviator stress. These tests were performed confined (the majority of them) and unconfined. Owing to the scatter of results, it is difficult to say whether the confining pressure had an effect on the shear strength, c_u, of the specimens. This is a result of the existing joints and their orientations in each individual specimen. These joints are a major factor in controlling the shear strength. However, Bishop and Henkel (9) have reported that the shear strength of fissured clay decreased when the clay was tested under a confining pressure less than the one existing in the field. This reduction in strength is attributed to the opening of fissures under low confining pressure.

There were considerable variations in the undrained strengths, c_u, of all specimens. Again, these variations are more likely to be associated with the degree of fissuring and with the pre-existing failure planes. The undrained strength was relatively low when the pre-existing failure plane was oriented in a direction more liable for failure. It was observed in the tests that most of the specimens

TABLE 7.--SUMMARY OF RESULTS OF UNCONSOLIDATED UNDRAINED TESTS ON UNDISTURBED SPECIMENS

Depth ft.	Boring No.	Specimen Orientation	Confining Pressure, σ_3 psi	Water Content, %	cu = $1/2(\sigma_1-\sigma_3)_f$, psi	Failure Strain, %
20-21.5	CB-1A	Vertical	20	33.8	14.19	3.63
20-21.5	CB-1A	Horizontal	40	33.6	18.16	3.10
22-23.5	CB-1A	Horizontal	10	28.9	12.85	1.38
22-23.5	CB-1A	Horizontal	20	29.1	6.99	1.33
24-25	CB-1A	Vertical	5	30.0	13.77	4.64
24-25	CB-1A	Vertical	10	30.0	13.34	5.33
24-25	CB-1A	Vertical	20	30.0	8.35	3.92
24-25	CB-1A	Vertical	40	30.1	9.25	3.87
24-25	CB-1A	Vertical	20	29.7	6.98	0.66
24-25	CB-1A	Vertical	0	29.3	10.62	1.81
24-25	CB-1A	Horizontal	20	30.0	17.57	2.47
24-25	CB-1A	Horizontal	10	29.7	12.29	1.40
24-25	CB-1A	Horizontal	30	30.0	14.40	2.96
25-26.5	CB-1A	Vertical	20	34.7	5.77	0.40
25-26.5	CB-1A	Vertical	20	33.0	12.73	8.67
25-26.5	CB-1A	Vertical	40	34.1	10.74	11.42
25-26.5	CB-1A	Vertical	0	33.8	7.16	1.62
25-26.5	CB-1A	Horizontal	40	34.8	9.50	3.53
25-26.5	CB-1A	Horizontal	20	32.2	8.30	3.59
25-26.5	CB-1A	Horizontal	10	36.1	11.07	1.46
22-24	CB-1	Vertical	10	27.0	16.20	3.30
22-24	CB-8	Vertical	20	26.5	7.90	10.30
22-24*	CB-8	Vertical	20	27.0	9.02	2.56
20-22*	CB-8	Vertical	10	35.0	7.86	1.99
29-31*	CB-1	Vertical	10	27.8	11.10	2.38
29-31	CB-1	Vertical	10	27.8	12.49	2.39

*Soil Specimens 2.8 inches in diameter and 6.0 inches in height.

failed either entirely or partially on a pre-existing failure plane. It was noted, in general, that the weaker the specimen the smaller the failure strain. The variation in the percentage of clay minerals was probably another factor which affected the strength properties of the clay.

There is also a variation in the average values of shear strength in the vertical and horizontal directions as shown in Table 8. In one series, in which the water content was about 30 percent, the average undrained strength in the horizontal direction was about 42 percent higher than the average shear strength in the vertical direction. The overall average strength of all specimens tested in a horizontal direction was 26 percent higher than the vertical specimens. In general, the horizontal specimens failed at a smaller strain than the vertical specimens.

TABLE 8.--UNDRAINED TESTS ON UNDISTURBED SPECIMENS

Depth ft.	Horizontal Strength / Vertical Strength
20 - 21.5	1.28
24 - 25	1.42
25 - 26.5	1.05

It is well known that the undrained strengths of fissured clays are influenced by the size of the specimens tested (10, 40, 48). Therefore, a few tests were carried out on specimens 2.8 inches in diameter

and 6 inches in length. The average shear strength from these tests was about 10 percent less than the average shear strength of 1.5 by 3.0 inch specimens. The effect of specimen size on the shear strength is very significant with respect to present routine tests in the laboratory. Therefore, more tests are needed to investigate this point thoroughly.

The stress-strain curves of the unconsolidated undrained specimens exhibit all degrees of variation, depending on the degree of fissuring and on the natural orientation of the pre-existing failure planes. Fig. 34 shows the stress-strain curves of two specimens; one of them failed along the fissures, the other on a pre-existing failure plane. The specimen that failed along the fissured surfaces has a higher strength and has a slight peak, while the specimen that failed on the pre-existing plane does not show any peak.

The results of undrained tests on remolded specimens are given in Table 9. The undrained strength (c_u) varies with the moisture content as well as with the percent and type of clay minerals. Fig. 35 shows the variation of the undrained strength with water content for two different samples of Beaumont Clay.

The sensitivity of Beaumont Clay (the ratio of undisturbed to remolded undrained strength) ranged from 0.98 to 1.33 for these tests; the results are presented in Table 10. Thus, it showed little sensitivity and can be classified as insensitive (49). Actually, the elimination of fissures and pre-existing failure planes, by remolding, led in several cases to a somewhat greater strength than the clay

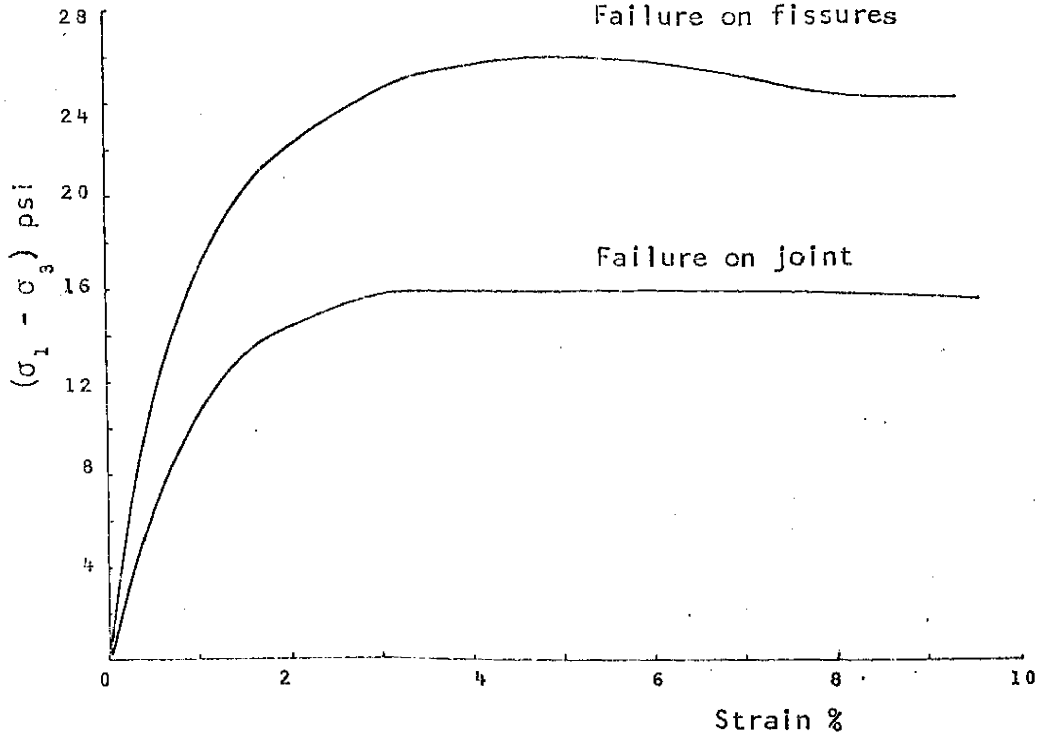

FIG. 34. -- EFFECT OF JOINT AND FISSURES ON STRESS-STRAIN CURVES

TABLE 9.--SUMMARY OF RESULTS OF UNCONSOLIDATED UNDRAINED TESTS ON REMOLDED SPECIMENS

Depth ft.	Boring No.	Rate of Strain in./min.	Confining Pressure, %	Water Content, %	cu = 1/2 $(\sigma_1 - \sigma_3)_f$ psi	Failure Strain, %
20-21.5	CB-1A	.020	20	32.80	13.35	8.63
20-21.5	CB-1A	.020	20	32.70	12.60	8.67
20-21.5	CB-1A	.020	20	34.70	9.72	7.49
20-21.5	CB-1A	.020	20	34.10	11.11	8.75
20-21.5	CB-1A	.020	40	36.40	8.67	7.55
20-21.5	CB-1A	.020	10	34.30	9.19	7.53
20-21.5	CB-1A	.020	10	33.00	10.22	8.14
24-25	CB-1A	.020	20	32.40	10.20	9.46
24-25	CB-1A	.020	20	32.40	10.72	10.09
24-25	CB-1A	.020	20	31.50	8.76	10.86
24-25	CB-1A	.020	20	30.30	11.76	8.71
25-26.5	CB-1A	.020	20	33.20	9.06	8.86
25-26.5	CB-1A	.020	40	29.60	10.15	9.64
25-26.5	CB-1A	.020	10	32.90	8.62	8.88
22-23.5	CB-1A	.020	20	35.20	7.55	8.94
22-23.5	CB-1A	.045	20	35.20	7.34	11.60
22-23.5	CB-1A	.045	20	35.80	7.01	11.60
22-23.5	CB-1A	.009	20	36.00	7.05	10.13
22-23.5	CB-1A	.060	20	34.60	7.48	11.60
22-23.5	CB-1A	.0024	20	34.70	7.14	8.03
22-23.5	CB-1A	.00024	20	32.20	7.11	6.67

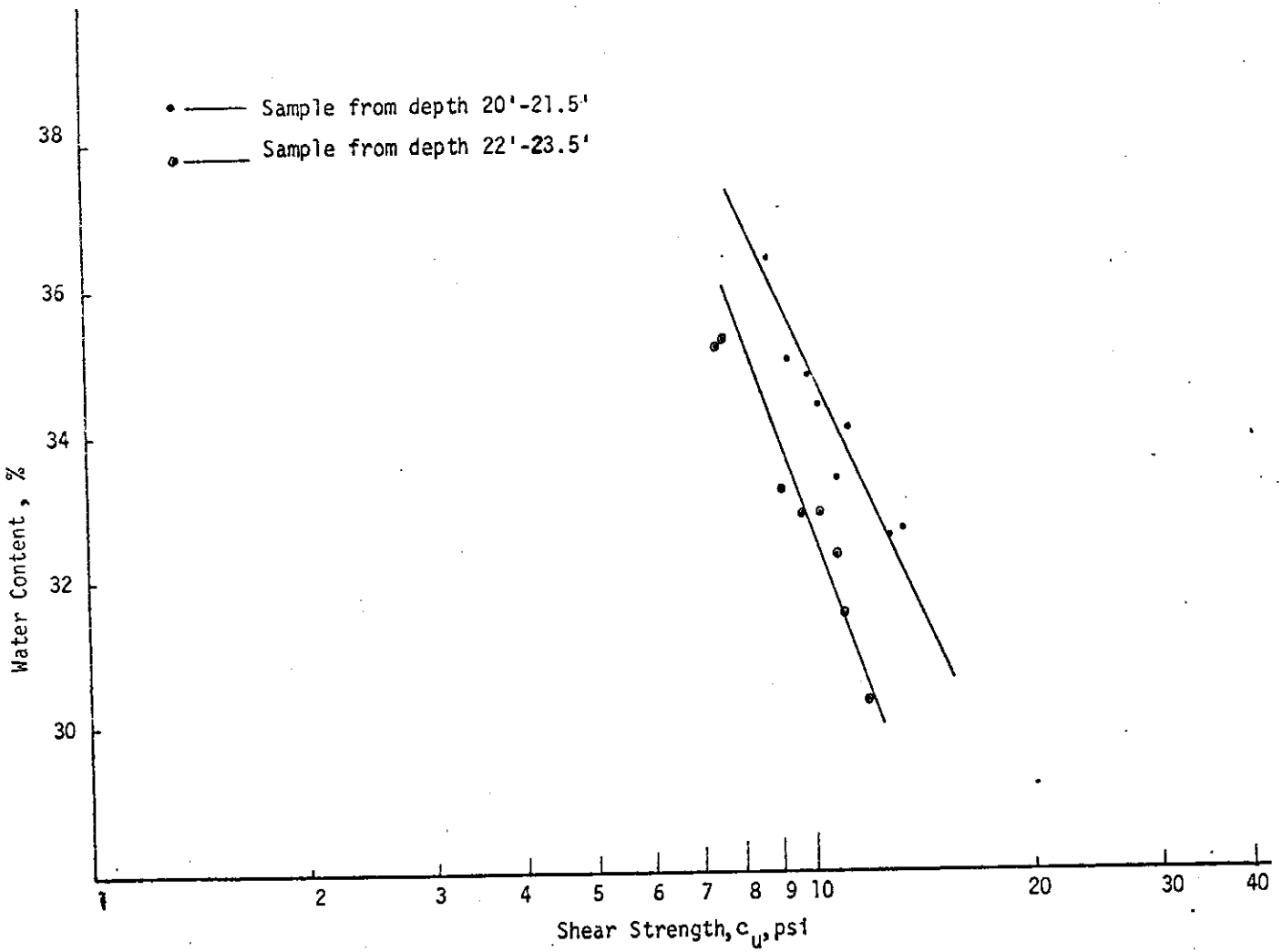

FIG. 35.-- RELATIONSHIP BETWEEN WATER CONTENT AND UNDRAINED SHEAR STENGTH FOR REMOLDED CLAY

possessed in its natural state.

TABLE 10.--UNDRAINED TESTS, REMOLDED VERSUS UNDISTURBED STRENGTHS

Depth ft.	c_u, psi		Sensitivity
	Undisturbed	Remolded	
20 - 21.5	14.19	10.69	1.33
22 - 23.5	-----	7.24	----
24 - 25	10.39	10.37	1.00
25 - 26.5	9.10	9.28	0.98

In the field, the rate of load application is usually much slower than the rate used in the laboratory. The effect of the rate of strain on the undrained shear strength of remolded specimens was checked by conducting a limited number of tests, and the results are presented in Fig. 36.

It is clear that the slower the rate of strain the lower the shear strength. However, the effect is small. The strength decreased slightly when the time to failure increased from 100 to 900 minutes as shown in Fig. 36. The rate of strain probably affects the value of pore water pressure, and it would be worthwhile investigating this point in Beaumont Clay.

Direct Shear Tests

Consolidated drained tests were conducted on three sets of Beaumont Clay specimens. The index properties of these sets were

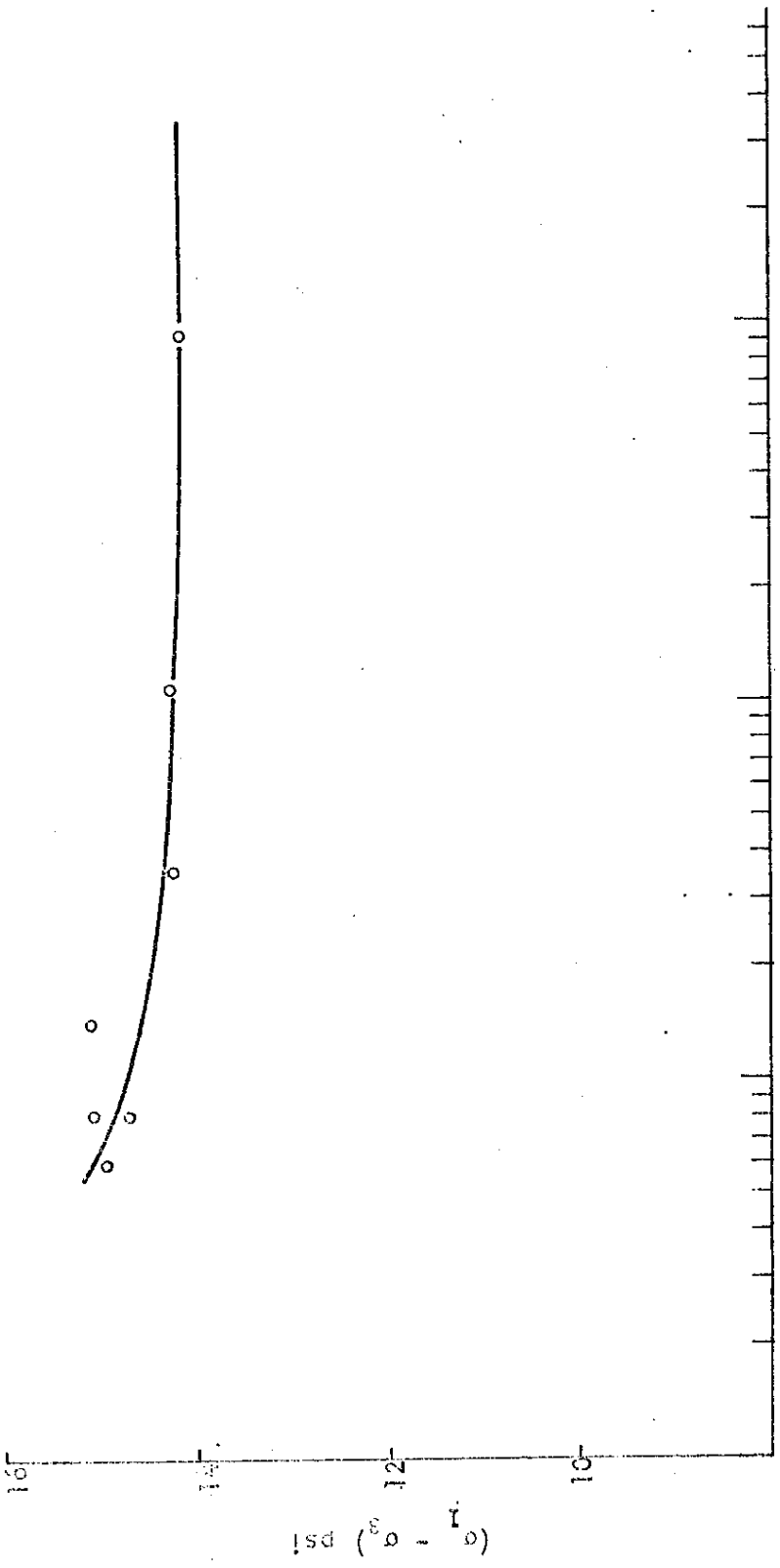

FIG. 36.-- TIME EFFECT ON SHEAR STRENGTH

different. However, the X-ray diffraction analyses showed that they had the same clay minerals, except that the proportion of the clay minerals varied from one set to another.

The strength properties of the first set, which is from a depth of 20-21.5 feet, are shown in Table 11 and in Fig. 37. The peak strength can be represented by the parameters:

$$c_d = 5.35 \text{ psi}$$

$$\phi_d = 15.5^{o}$$

The residual strength parameters are:

$$c'_r = 1.00 \text{ psi}$$

$$\phi'_r = 8.0^{o}$$

Fig. 38 shows typical stress-displacement curves for different consolidation pressures. As the clay is strained, the shearing resistance increases until it reaches a maximum, which is called the peak strength. With further displacement, the resistance to shear, or the strength of the clay, gradually falls to a constant, or nearly constant, value called the residual strength. The displacement needed to reach the residual strength was about 2.5 inches for the specimens tested in this research.

In moving from the peak to the residual, the angle of shearing resistance for specimens at a depth of 20-21.5 feet decreased from 15.5^{o} to 8.0^{o}. At the same time, the cohesion intercept fell from 5.35 psi to 1.0 psi. Skempton (45) related the decrease in the angle of shearing resistance to the development of a thin band of oriented clay particles in the direction of shearing. Morgenstern and Tchalenko

TABLE 11.--SUMMARY OF DIRECT SHEAR TESTS

Group No.	Depth ft.	Boring No.	Water Content %	L.L., %	P.L., %	P.I., %	L.I., %	CF <2u %	PI/CF	Peak Strength		Residual Strength		ϕ'_r if $c'_r = 0$
										c_d, psi	ϕ_d	c'_r, psi	ϕ'_r	
1	20-21.5	CB-1A	32.90	94	29	65	.06	76	.85	5.35	15.5°	1.00	8.0°	10.5°
2	23-25	CB-1	30.00	84	27	57	.05	77	.74	4.51	16.4°	1.08	9.0°	11.7°
3	29-31	CB-1	27.50	62	22	40	.14	56	.72	3.60	24.0°	1.88	10.7°	14.5°

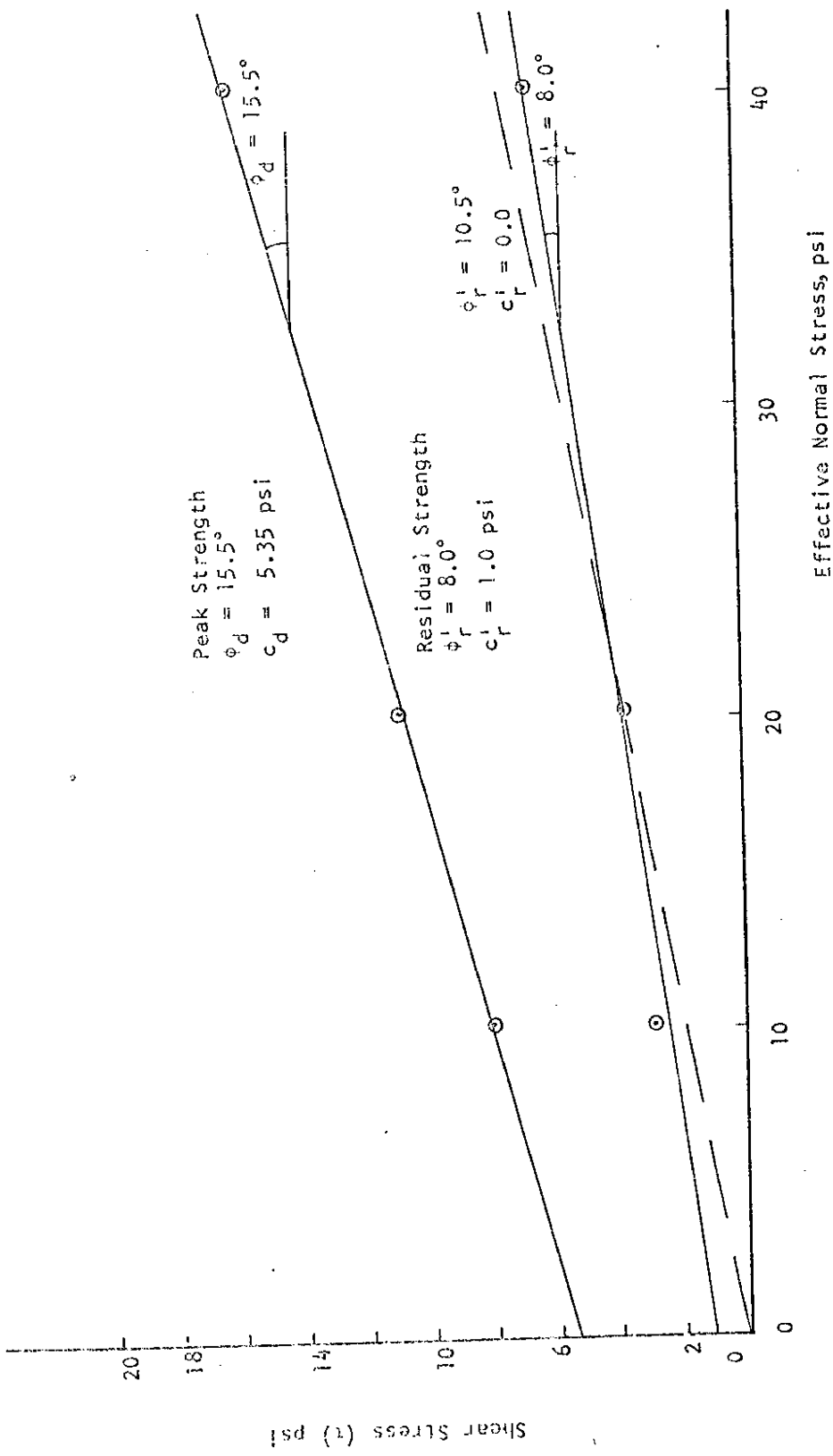

FIG. 37. --PEAK AND RESIDUAL STRENGTH PROPERTIES OF BEAUMONT CLAY FROM DEPTH 20 - 21.5 FEET

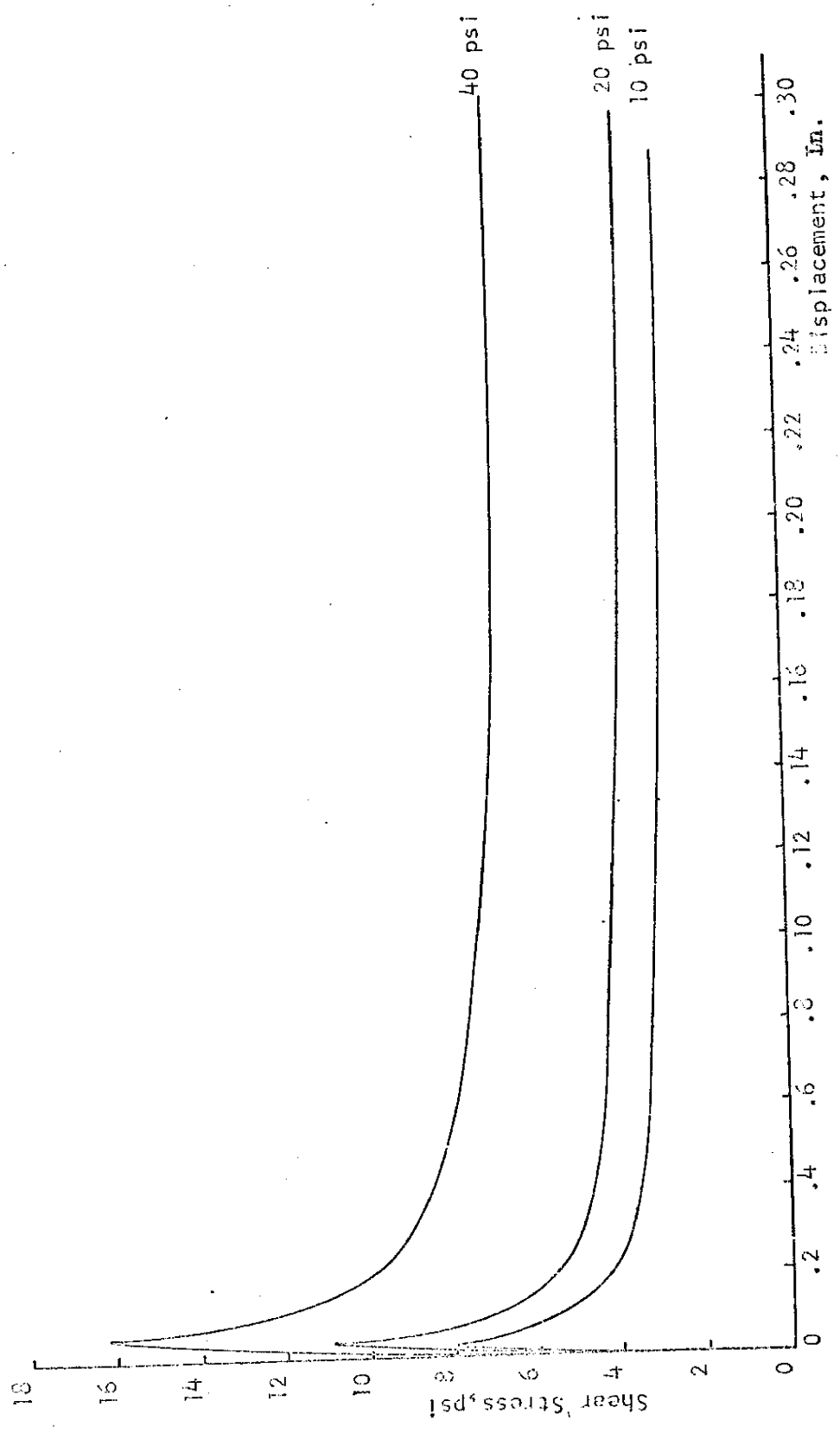

FIG. 38.--STRESS - DISPLACEMENT CURVES FOR SPECIMENS FROM DEPTH 20-21.5 FEET.

(35) found that the thickness of the oriented band of clay particles in the London Clay was about 50μ thick. The oriented clay particles form a continuous shiny shear surface. Fig. 39 is a photograph of this surface for the Beaumont Clay.

It is known that internal friction is caused mainly by an interlocking effect of the particles and by the friction between these particles (30). As the position and orientation of the particles changed during repeated shearing, the interlocking effect and, consequently, the angle of internal friction decreased to a limiting value. Indeed, the re-orientation of the particles eliminated the interlocking effect in the shear plane.

The cohesion component decreased a considerable amount when the shear strength dropped from the peak to the residual, but never became zero. In all the residual tests of this study, a small value of cohesion was measured. Skempton and Petley (50) also measured a small value of cohesion in the residual shear tests. In the field the cohesion component disappears completely as reported by Terzaghi (52) and Skempton (45). The cohesion obtained in the laboratory from the residual shear tests can be related to the nature of the direct shear tests, which probably caused some experimental errors, and to the higher strain rate as compared with the field rate.

If the cohesion intercept is considered to be zero, and a best-fitting line is drawn through the origin, the angle of residual strength becomes 10.5^{o} for the first set (see Fig. 37).

FIG. 39.--SURFACE OF SHEAR PLANES AT THE END OF RESIDUAL TESTS

Fig. 40 shows a typical stress-displacement curve for each individual shearing of one specimen until the residual strength was obtained. It appears that the largest reduction in shear strength occurred with the first shearing; subsequent shearing curves do not show a peak. The strength decreased slightly with each additional shearing process until it reached a constant or nearly constant value. This value was reached at the fifth shearing reversal for the Beaumont Clay.

Fig. 41 illustrates the relationship between the volume change, $\Delta V/V_o$, and the displacement for each subsequent shearing. The specimen which was consolidated under 10 psi showed an increase in the volume with displacement; whereas, under 40 psi normal pressure, the specimen reduced in volume with displacement. When the volume of the specimen increased, consequently, the water content increased, too. This increase in water content probably contributed to the shear strength reduction from peak to residual. It also explains why the reduction in the percentage of shear strength from peak to residual is higher under low pressure than it is under high pressure.

The strength properties of the second and third sets of specimens are presented in Figs. 42 and 43, respectively.

From the test results, it can be seen that the residual angles of shearing resistance can be correlated with the liquid limit. This relationship is drawn in Fig. 44. It is also valid for the new values of ϕ'_r where c'_r is taken to be zero.

More data on Beaumont Clay is needed to verify the validity of the relationship between the liquid limit and the residual angle of

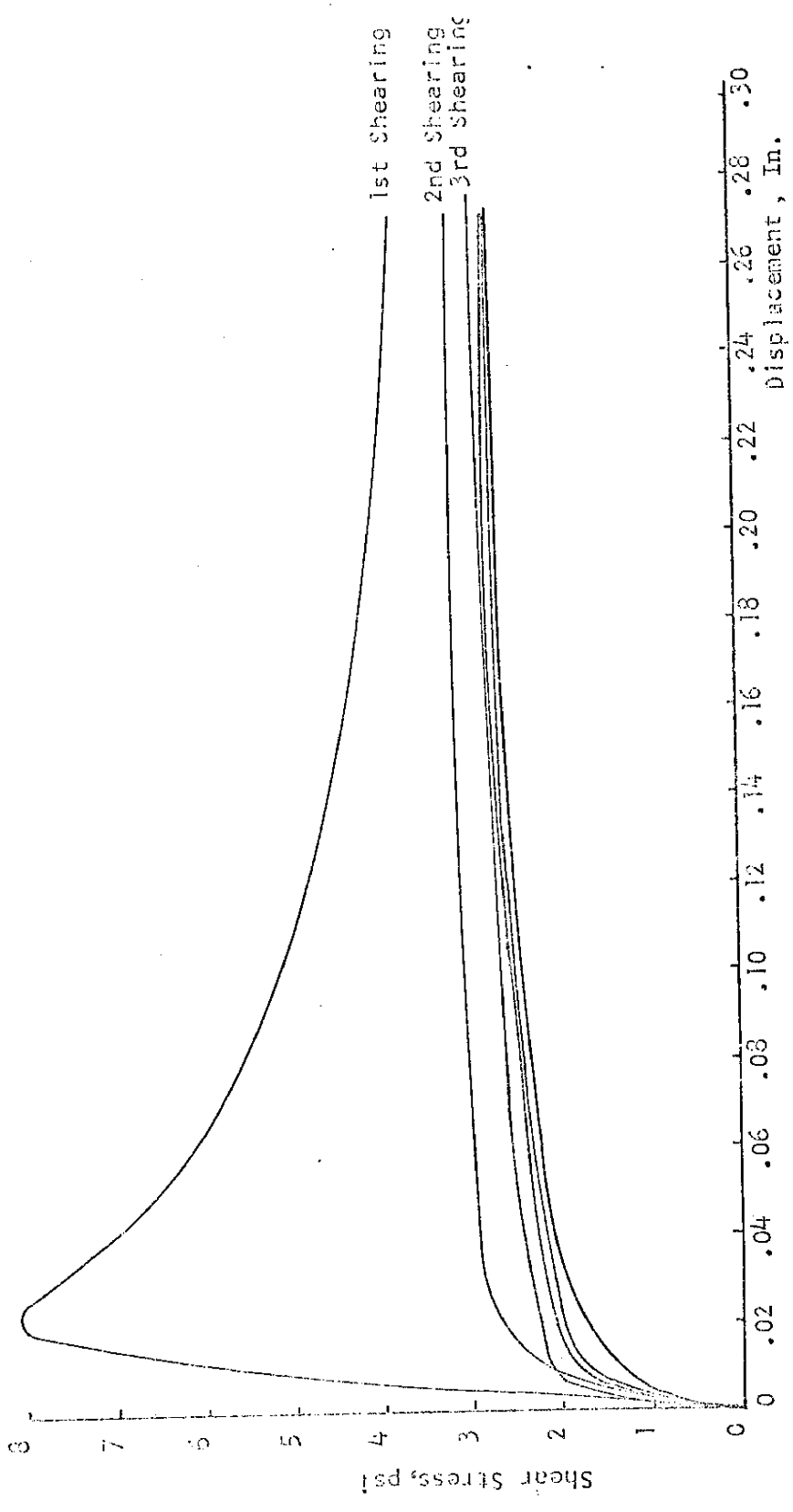

FIG. 40.—STRESS – DISPLACEMENT CURVES FOR SPECIMEN FROM DEPTH 20–21.5 FEET

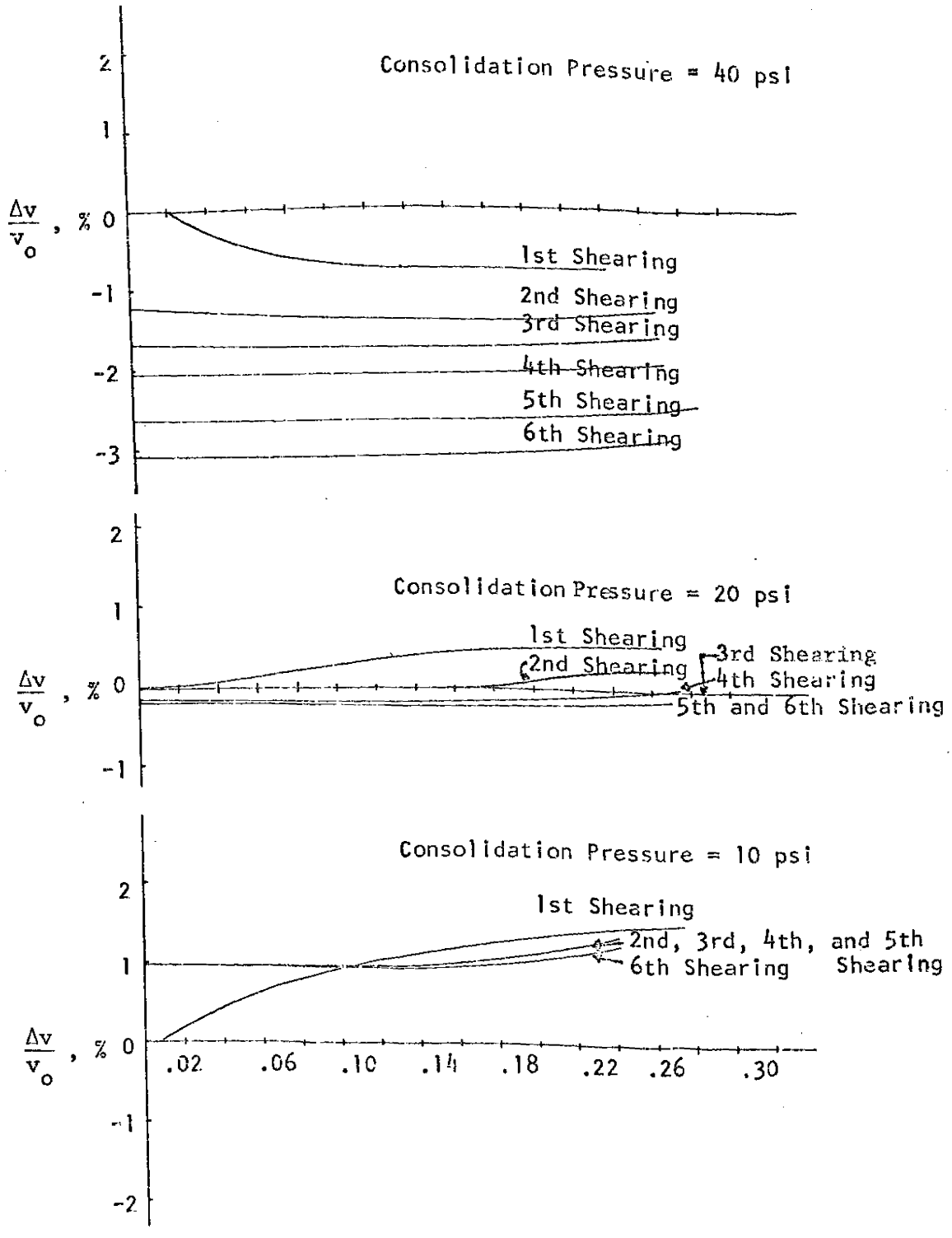

FIG. 41.--RELATIONSHIPS BETWEEN VOLUME CHANGE AND DISPLACEMENT, DIRECT SHEAR TESTS

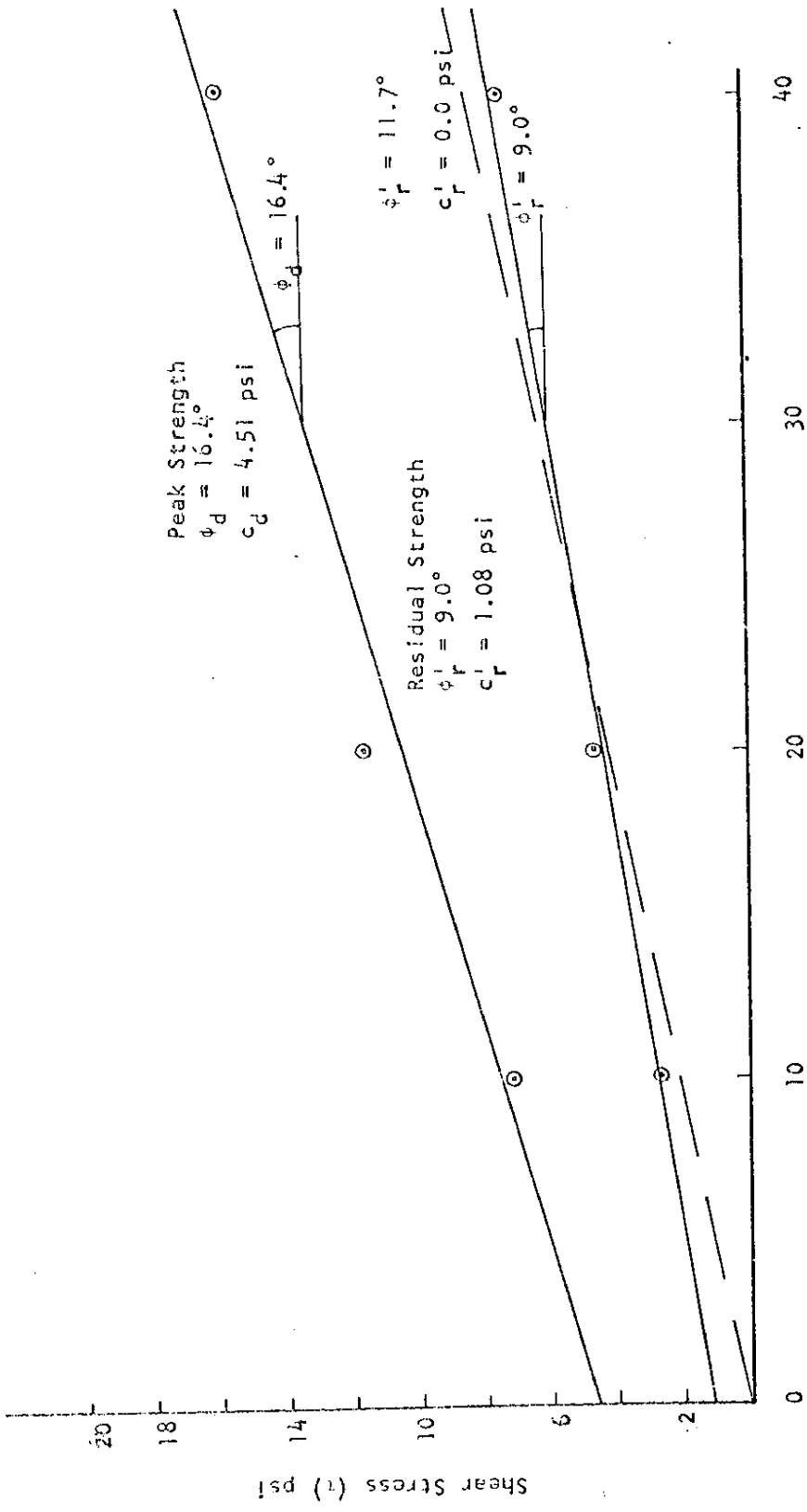

FIG. 42.-- PEAK AND RESIDUAL STRENGTH PROPERTIES OF BEAUMONT CLAY FROM DEPTH 23 - 25 FEET

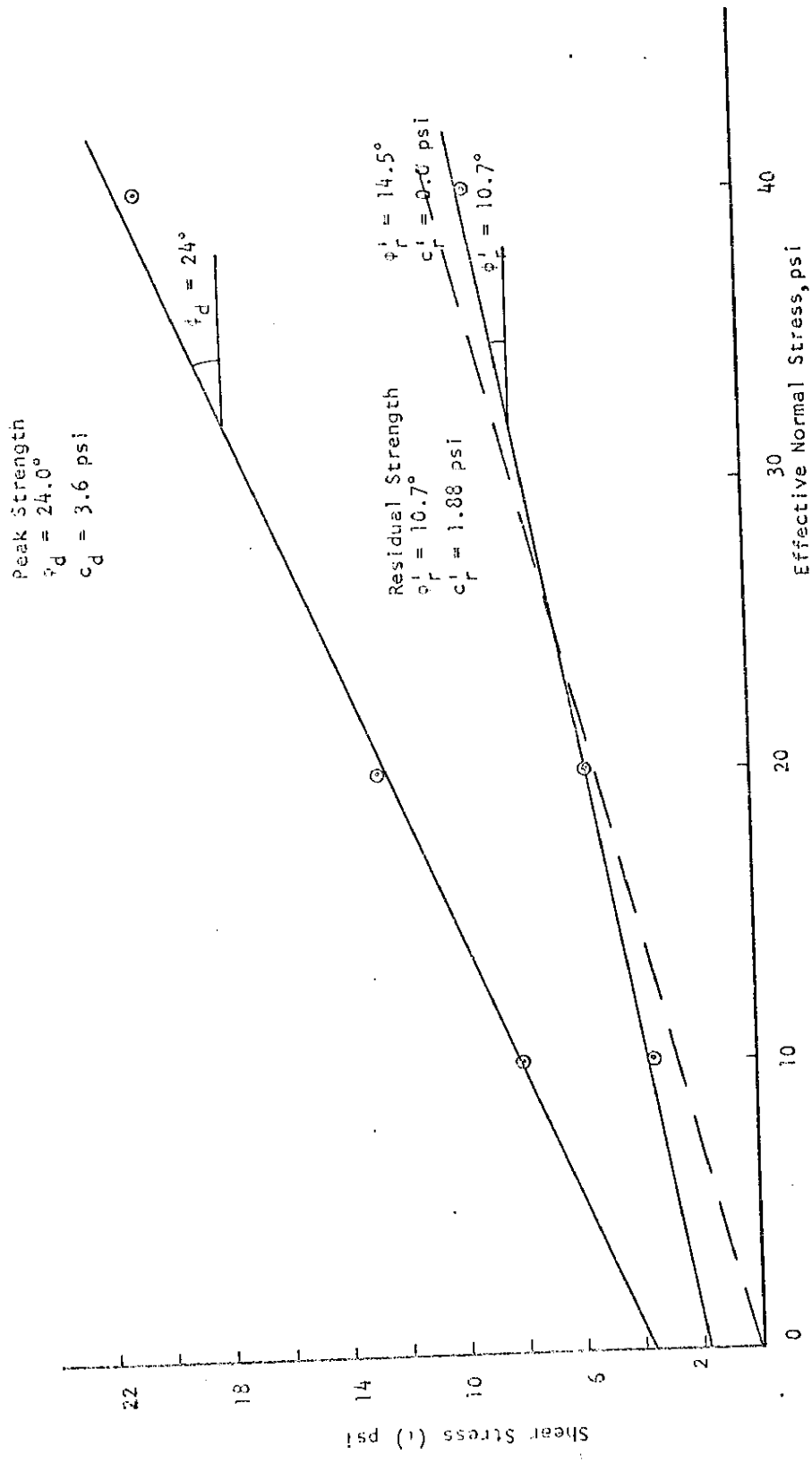

FIG. 43. --PEAK AND RESIDUAL STRENGTH PROPERTIES OF BEAUMONT CLAY FROM DEPTH 29 - 31 FEET

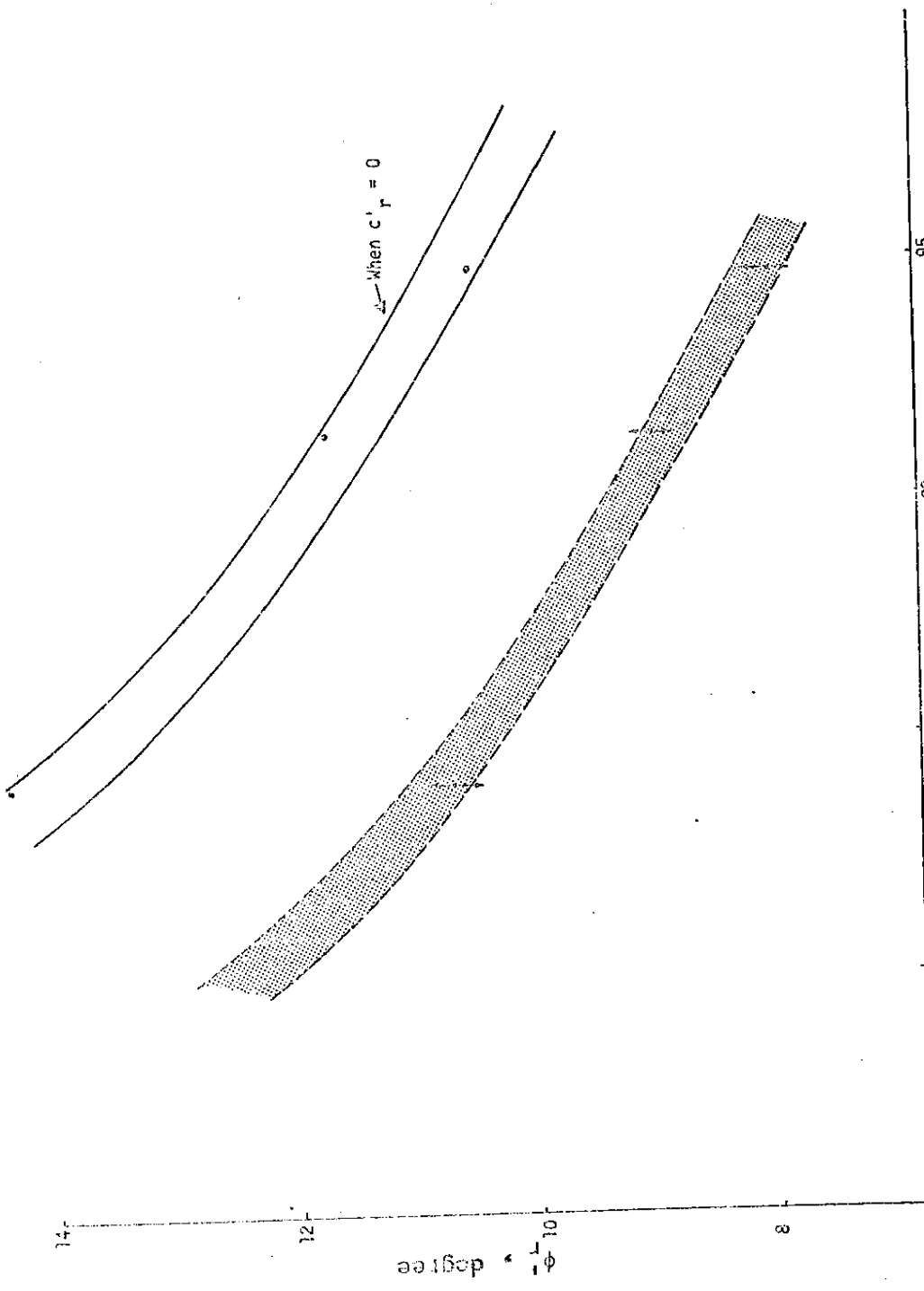

FIG. 44.— RELATIONSHIP BETWEEN LIQUID LIMIT AND ϕ'_r

shearing resistance. If there is a definite relationship, this will be a powerful tool for estimating the residual strengths of the soil.

In connection with problems of slope stability, bearing capacity, and earth pressures, Taylor (51), Bjerrum (13), Bishop (5) and many others have concluded that the state of limiting equilibrium in these problems is associated with non-homogeneous mobilization of shearing resistance and thus with progressive failure. This may lead to major difficulties in relating the soil shearing resistance which is found in the laboratory with the average shearing resistance in the field. The difference between these two results can be investigated by considering, first, the difference between the peak and the residual strength; and secondly, the strain which is required for this difference to be established.

Considering the Beaumont Clay, it can be seen from Fig. 38 that the loss in strength in passing from peak to residual was proportional to the normal effective stress, and to establish the residual strength, about 2.5 inches of displacement was required. The strength loss can be expressed quantitatively in terms of the brittleness index (I_B) from the following expression (5):

$$I_B = \frac{\tau_f - \tau_r}{\tau_f} \%$$

The brittleness index increases with a decrease of the effective normal stress, as presented in Fig. 45. At a low normal effective stress, 10 psi, the reduction in strength was about 66 percent. The reduction in the strength for a normal effective stress of 40 psi was 57 percent.

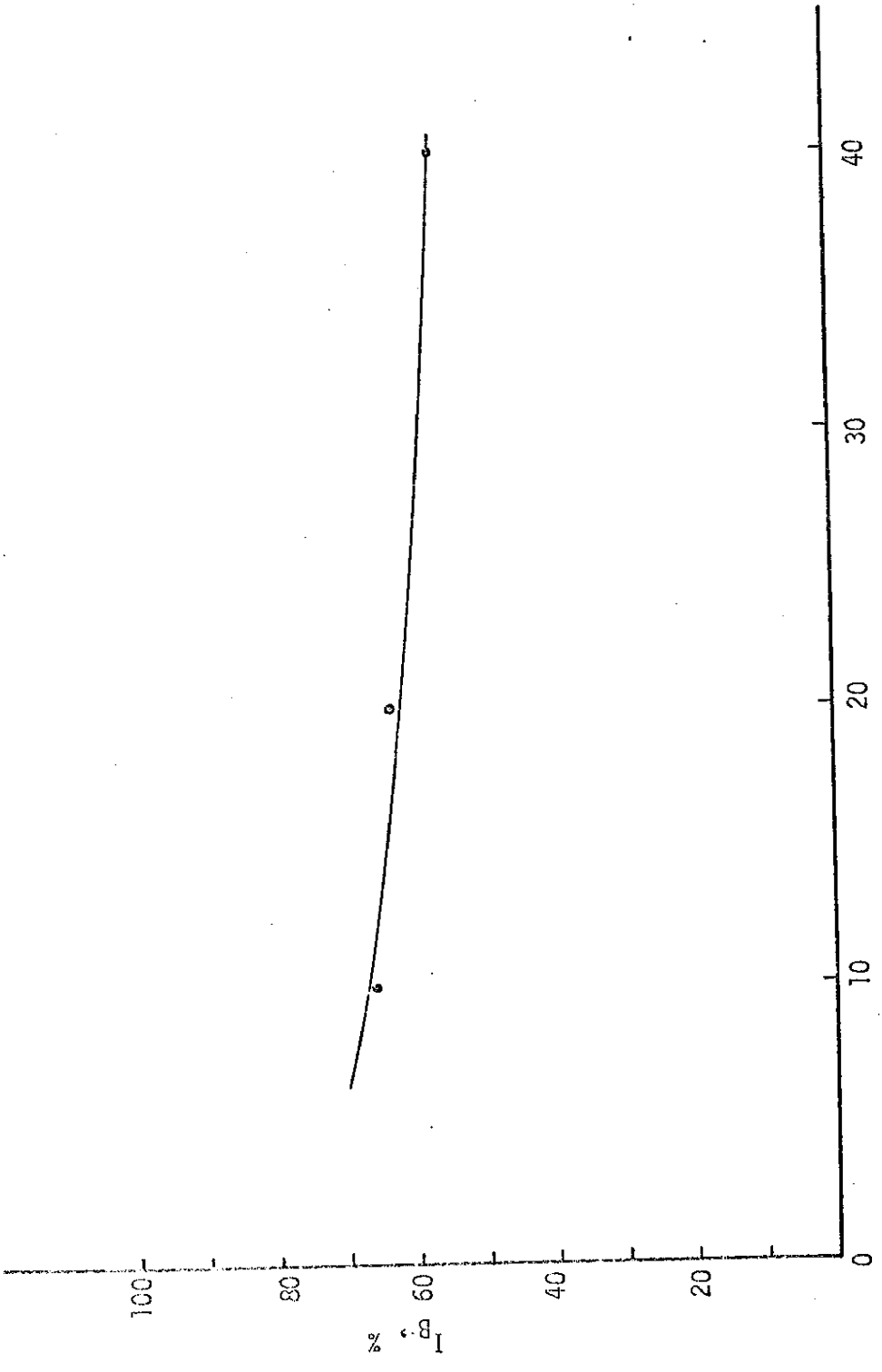

FIG. 45.--BRITTLENESS PARAMETER AND ITS VARIATION WITH STRESS

In the case of slope stability problems, the dangerous point is the toe of the slope, where the reduction in strength is more than at any other point due to a small normal effective stress. So it is more probable that progressive failure starts from the toe of the slope and extends further up the slope. In the case of Beaumont Clay, this can be an important factor in long term slope stability. Bjerrum (13) reached the same conclusion in treating the progressive failure of natural slopes in other soils.

Comparison Between the Results of the Triaxial and the Direct Shear Tests

The comparison between the results of the triaxial and the direct shear tests is presented in Table 12. The effective angle of shearing resistance from the consolidated undrained triaxial tests and the direct shear tests can be considered equal without significant error. However, there is a considerable difference in the cohesion value.

TABLE 12.--TRIAXIAL VERSUS DIRECT SHEAR TESTS

Depth ft.	Specimen Orientation	Triaxial		Direct Shear	
		c', psi	ϕ'	c_d, psi	ϕ_d
20 - 21.5	Vertical	2.90	15.5^o	5.35	15.5^o
	Horizontal	3.50	15.5^o		
22 - 23.5	Vertical	1.40	17.3^o	4.51	16.4^o
	Horizontal	4.60	17.0^o		

The cohesion from the direct shear tests is higher than the cohesion from the triaxial tests for specimens oriented in the vertical direction (Table 12). In the case of the specimens oriented in the horizontal direction, the difference between the cohesion obtained in the triaxial tests and the direct shear tests is small. In fact, in one test series they are equal. This similarity in the cohesion value is probably due to the fact that the specimens in the direct shear tests were sheared along a horizontal plane.

It is obvious that the shear strength in the horizontal direction is higher than in the vertical direction due to the higher value of cohesion in the horizontal direction. If the mode of failure takes place along a horizontal direction in Beaumont Clay, one should expect a higher strength than if the failure happens along a vertical direction. Usually, failure planes in the field have all degrees of orientation ranging from vertical to horizontal, and it would be a worthwhile endeavor to develop a complete relationship between shear strength and orientation.

CHAPTER VI

SUMMARY AND CONCLUSIONS

This investigation is the first effort known to the author to rather completely define certain geotechnical properties of the Beaumont Clay, particularly the shear strength of the soil in terms of effective stress parameters. A detailed study of this formation is warranted because of the extensive construction activity in the Beaumont Clay area, and because of the unusual nature of the material.

The Beaumont Clay formation was formed during the Pleistocene epoch. As a result of cyclic drying and wetting during and after deposition, the clay is fissured, jointed, and desiccated. The fissures are randomly oriented and vary in intensity throughout the depth tested. In general, the degree of fissuring appears to increase as the amount of montmorillonite clay increases. However, the layer which contains the lowest percent of montmorillonite is very badly fissured. All indications are that this layer was subjected to weathering longer than the adjoining layers.

The in situ water content and the liquid limit vary considerably with relatively small changes in depth. More than likely this is the result of a variation in the percentage of montmorillonite clay. X-ray diffraction data confirmed this point and showed that the montmorillonite content varied from 23-47 percent. More illite appears when the montmorillonite content decreases.

Consolidation tests indicate that Beaumont Clay is over-consolidated. The preconsolidation pressure is roughly 4.7 tsf; however, this value is not constant but varies with depth. Geological history does not indicate a significant overburden pressure in the past; thus, it must be assumed that the preconsolidation pressures are the result of desiccation. The rebound portion of the consolidation curves shows that the bond between the clay particles is not strong; consequently, the stored strain energy is not too high. The swell pressure, as averaged from conventional consolidation tests and from consolidated undrained triaxial tests, is 1.25 tsf. From this information, the ratio of horizontal to vertical effective stress (K_o) was estimated to be 1.5.

The shear strength behavior of the soil is mainly controlled by the polished weak planes (joints) and to a lesser extent by the fissures. When the weak planes are inclined in a direction close to that expected for shear failure, the shear plane takes this path and the shear strength is significantly reduced.

The results of consolidated undrained triaxial tests (with pore pressure measurements) show that the effective angle of shearing resistance, ϕ', varies from 16-20^o. Similar results were obtained from drained direct shear tests using peak strength values. However, consolidated drained triaxial tests gave angles approximately 4^o lower than obtained from consolidated undrained triaxial or drained direct shear tests.

The pore water pressure developed under the application of the deviator stress is rather unique for a material known to be over-consolidated. It reaches a maximum value, and with further strain, it shows a slight decrease. With low consolidation pressures, it decreases somewhat but never becomes negative as expected in over-consolidated soils. The pore pressures are controlled to a great extent by the weak planes and fissures, which, under shear, tend to open slightly and increase the mass permeability of the soil.

Tests on specimens cut at varying orientations in the mass showed that the effective angle of shearing resistance is almost the same in the vertical and horizontal direction. However, the effective cohesion is higher in the horizontal direction than in the vertical. This was borne out by the direct shear tests (where failure is induced in the horizontal direction). The higher cohesion in the horizontal direction is the result of the higher horizontal stresses to which the soil has been subjected in its geologic history.

There was no major difference in the pore water pressure behavior in the horizontal and vertical oriented specimens. However, at relatively high strains the horizontal specimens had lower pore water pressures than the vertical specimens.

In general, most of the triaxial specimens did not show the characteristics of brittle failure, although the stress-strain curves of some specimens did show a slight peak. Undisturbed specimens in the consolidated undrained tests failed at rather small strains (1-4 percent).

Both the peak and residual strengths were obtained from the direct shear tests. The cohesion, as well as the angle of shearing resistance, decreased in passing from the peak to the residual state. The decrease in the angle of shearing resistance ranged from 7-13°. This decrease in strength is associated with the elimination of the interlocking component of shearing resistance and reorientation of clay particles along the shearing surface. It was found that the residual angles of shearing resistance were related to the liquid limit.

There was considerable variation in the unconsolidated undrained shear strength (c_u) in both vertical and horizontal directions. The lower values corresponded to failure along polished joints which had inclinations more liable to the direction of failure. The higher values were obtained when the specimens were free from joints and the fissures had strong cohesion. The overall average value of c_u in the horizontal direction was about 26 percent higher than the average value in the vertical direction. Again, this was the result of the higher stress which the material was subjected to during its geological history.

The structure of the clay has a pronounced effect on the strength properties. For remolded specimens, the effective angle of shearing resistance decreased 4.5°. It is believed that the sampling process affected the strength properties due to the fact that it introduced some disturbance to the clay structure. It would be very important and interesting to investigate the geotechnical properties on samples

taken by hand from the field so the effect of mechanical disturbance could be evaluated.

In many civil engineering works, and especially in slope stability, bearing capacity, and retaining wall problems, the properties of Beaumont Clay which are presented in this report are useful and applicable. The study reveals that the discontinuities, which include fissures and joints, are the dominant features in Beaumont Clay structure. The strength along these discontinuities, which is nearly equal to the residual strength, is a major factor to be considered in long term stability problems.

CHAPTER VII

RECOMMENDATIONS FOR FUTURE RESEARCH

The structural nature of Beaumont Clay and itscomplicated stress history indicate that more study is needed. In order to get a clearer picture about the behavior of Beaumont Clay, the following topics are suggested for future research:

1. Investigation of the geotechnical properties of Beaumont Clay in different areas is needed.
2. Further research is needed to study the orientation of joints and fissures in the field and, if possible, to correlate the shear strength with the orientation of these discontinuities. Also, it is necessary to investigate the shear strength in the vicinity and on the surface of faults.
3. It is desirable to check the shear strength in the field by performing a field test on a large specimen. Also, to establish a clear correlation, in the laboratory, between the shear strength and the size of specimens is very important.
4. It is felt that the sampling technique has a big effect on the the shear strength and probably on the characteristics of the stress-strain curves,too. So it is necessary to investigate this point.
5. Information on the time dependency of shear parameters is essential in Beaumont Clay.

6. A correlation between the shear parameters found in the laboratory and the active parameters in the field should be established.
7. It is worthwhile to investigate the effect of strain rate on the variation of pore water pressure in Beaumont Clay.

REFERENCES

1. Aas, G., "Vane Test for Investigation of Anisotropy of Undrained Shear Strength of Clay," Proc. of the Geotechnical Conference on Shear Strength Properties of Natural Soils and Rocks, Oslo, 1967, Vol. 1, pp. 3-8.

2. Bernard, H. A., Le Blanc, R. J., and Major, C. F., "Recent and Pleistocene Geology of Southeast Texas," Geology of the Gulf Coast and Central Texas and Guide Book of Excursions, Houston Geological Society, 1962, pp. 175-224.

3. Bishop, A. W., "The Use of Pore-Pressure Coefficients in Practice," Geotechnique, 1953, Vol. 3, No. 3, pp. 148-152.

4. Bishop, A. W., "The Strength of Soil as Engineering Material," Geotechnique, 1966, Vol. 16, No. 2, pp. 91-130.

5. Bishop, A. W., Discussion on "Progressive Failure--with Special Reference to the Mechanism Causing It." Proc. of the Geotechnical Conference on Shear Strength Properties of Natural Soil and Rock, Oslo, 1967, Vol. 2, pp. 142-150.

6. Bishop, A. W. and Bjerrum, L., "The Relevance of the Triaxial Test to the Solution of Stability Problem," ASCE Research Conference on Shear Strength of Cohesive Soils, Boulder, Colorado, 1960, pp. 437-501.

7. Bishop, A. W. and Blight, G. E., "Some Aspects of Effective Stress in Saturated and Partly Saturated Soils," Geotechnique, 1963, Vol. 13, No. 3, pp. 177-197.

8. Bishop, A. W., and Eldin, A. K. G., "Undrained Triaxial Tests on Saturated Sands and Their Significance in the General Theory of Shear Strength," Geotechnique, 1950, Vol. 2, No. 1, pp. 13-22.

9. Bishop, A. W., and Henkel, D. J., "The Measurement of Soil Properties in the Triaxial Test," Edward Arnold, London, 2nd ed., 1962.

10. Bishop, A. W., and Little, A. L., "The Influence of the Size and Orientation of the Sample on the Apparent Strength of the London Clay at Maldon Essex," Proc. of the Geotechnical Conference on Shear Strength Properties of Natural Soil and Rock, Oslo, 1967, Vol. 1, pp. 89-96.

11. Bishop, A. W., Webb, D., and Lewin, P., "Undisturbed Samples of London Clay from the Ashford Common Shaft: Strength-Effective Stress Relationship," Geotechnique, 1965, Vol. 15, No. 1, pp. 1-31.

12. Bjerrum, L., "Fundamental Considerations on the Shear Strength of Soil," Geotechnique, 1954, Vol. 5, No. 2, pp. 209-218.

13. Bjerrum, L., "Progressive Failure in Slopes of Over Consolidated Plastic Clay and Clay Shales," Proceedings, Journal of the Soil Mechanics and Foundations Division, ASCE, Vol. 93, No. SM5, Proc. Paper 5456, Sept. 1967, pp. 1-49.

14. Blight, G. E., "Strength Characteristics of Desiccated Clay," Proceedings, Journal of the Soil Mechanics and Foundations Division, ASCE, Vol. 92, No. SM6, Nov. 1966, pp. 19-37.

15. Brown, G., Editor, "X-ray Identification and Crystal Structures of Clay Minerals," The Mineralogical Society of London, London, 2nd ed., 1961.

16. Casagrande, A., "The Determination of the Preconsolidation Load and Its Practical Significance," Proc. 1st International Conference on Soil Mechanics and Foundation Engineering, Cambridge, Mass., 1936, Vol. 1, p. 60.

17. Cassel, F. L., "Slips in Fissured Clay," Proc. 2nd International Conference on Soil Mechanics and Foundation Engineering, Rotterdam, 1948, Vol. 2, pp. 46-50.

18. Dawson, R. F., "Settlement Studies on the San Jacinto Monument," Second Texas Conference on Soil Mechanics and Foundation Engineering, Austin, Texas, 1947,

19. Doeriny, J., "Review of Quaternary Surface Formation of Gulf Coast Region," American Association of Petroleum Geologist Bull., 1956, Vol. 40, No. 8, pp. 1816-1862.

20. Focht, J. A., and Sullivan, R. A., "Two Slides in Over Consolidated Pleistocene Clays," Proc. 7th International Conference on Soil Mechanics and Foundation Engineering, Mexico, 1969, Vol. 1, pp. 571-576.

21. Gibson, R. E., and Henkel, D. J., "Influence of Duration of Tests and Constant Rate of Strain on Measured 'Drained' Strength," Geotechnique, 1954, Vol. 4, No. 1, pp. 6-15.

22. Gray, E. W., "The Geology, Ground Water, and Surface Subsidence of the Baytown-La Porte Area, and Harris County, Texas," Unpublished thesis, Texas A&M University, College Station, Texas, August, 1958.

23. Henkel, D. J., "Investigation of Two Long-term Failures in London Clay Slopes at Wood Green and Northolt," Proc. 4th International Conference on Soil Mechanics and Foundation Engineering, London, 1957, Vol. 2, pp. 315-320.

24. Henkel, D. J., "The Shear Strength of Saturated Remolded Clays," ASCE Research Conference on Shear Strength of Cohesive Soils, Boulder, Colorado, 1960, pp. 533-554.

25. Henkel, D. J., and Skempton, A. W., "A Landslide at Jackfield, Shropshire, in a Heavily Over-consolidated Clay," Geotechnique, 1955, Vol. 5, No. 2, pp. 131-142.

26. Hvorslev, M. J., "Physical Components of the Shear Strength of Saturated Clays," ASCE Research Conference on Shear Strength of Cohesive Soils, Boulder, Colorado, 1960, pp. 169-273.

27. Kenney, T. D., "The Influence of Mineral Composition on the Residual Strength of Natural Soils," Proc. of the Geotechnical Conference on Shear Strength Properties of Natural Soil and Rock, Oslo, 1967, Vol. 1, pp. 123-129.

28. Kunze, G. W., and Rich, C. I., "Mineralogical Methods" IN C. J. Rich, L. F. Seatz, and G. W. Kunze, ed. Certain Properties of Selected Southeastern United States Soils and Mineralogical Procedures for their Study. Southern Cooperative Series, 1959, Bull. No. 61:135-140.

29. Lambe, T. W., "Soil Testing for Engineers," John Wiley & Sons, Inc., New York, 1951.

30. Lambe, T. W., "A Mechanistic Picture of Shear Strength in Clay," ASCE Research Conference on Shear Strength of Cohesive Soils, Boulder, Colorado, 1960, pp. 555-580.

31. Lo, K. Y., "Stability of Slopes in Anisotropic Soils," Journal of the Soil Mechanics and Foundation Division ASCE, Vol. 91, No. 5 Proc. paper 4405, July, 1965, pp. 85-106.

32. Marsland, A., and Butler, M. E., "Strength Measurement of Stiff Fissured Barton Clay from Famley (Hampshire)," Proc. of the Geotechnical Conference on Shear Strength Properties of Natural Soil and Rock, Oslo, 1967, Vol. 1, pp. 139-145.

33. Mishtak, J., "Soil Mechanics Aspects of the Red River Floodway," Canadian Geotechnical Journal, 1964, Vol. 1, No. 3, pp. 133-146.

34. Morgenstern, N. R., "Shear Strength of Stiff Clay," Proc. of the Geotechnical Conference on Shear Strength Properties of Natural Soil and Rock, Oslo, 1967, Vol. 2, pp. 59-69.

35. Morgenstern, N. R. and Tchalenko, J. S., "Microstructural Observations on Shear Zones from Slips in Natural Clays," Proc. of the Geotechnical Conference on Shear Strength Properties of Natural Soil and Rock, Oslo, 1967, Vol. 1, pp. 147-152.

36. Peterson, R., Jaspar, J. L., Rivard, P. J., and Iverson, N. L., "Limitation of Laboratory Shear Strength in Evaluating Stability of Highly Plastic Clays," Proc., ASCE Research Conference on the Shear Strength of Cohesive Soils, Boulder, Colorado, 1960, pp. 765-791.

37. Rosenquist, T., "Physico-Chemical Properties of Soils and Soil Water Systems," Journal of the Soil Mechanics and Foundation Division, ASCE, Vol. 85, No. SM2, Proc. paper 2000, April 1959, pp. 31-53.

38. Scafe, D. W., "A Clay Mineral Investigation of Six Cores from the Gulf of Mexico," Unpublished dissertation, Texas A&M University, College Station, Texas, January 1968.

39. Sellards, E. H., Adkins, W. S., and Plummer, R. B., "The Geology of Texas," The University of Texas, Bulletin No. 3232, Austin, 3rd Printing, 1954.

40. Simons, N. E., "Discussion on the Shear Strength of Stiff Clay," Proc. of the Geotechnical Conference on Shear Strength Properties of Natural Soil and Rock, Oslo, 1967, Vol. 2, pp. 159-160.

41. Skempton, A. W., "The Colloidal Activity of Clays," Proc. 3rd International Conference on Soil Mechanics and Foundation Engineering, Switzerland, 1953, Vol. 1, pp. 57.

42. Skempton, A. W., "The Pore Pressure Coefficients A and B," Geotechnique, 1954, Vol. 3. No. 3, pp. 143-147.

43. Skempton, A. W., "Effective Stress in Soils, Concrete and Rocks," Conference on Pore Pressure and Suction in Soils, London, 1960, pp. 4-16.

44. Skempton, A. W., "Horizontal Stress in an Over-Consolidated Eocene Clay," Proc. 5th International Conference on Soil Mechanics and Foundation Engineering, Paris, 1961, Vol. 1, pp. 351-357.

45. Skempton, A. W., "Long-term Stability of Clay Slopes," Rankine Lecture, Geotechnique, 1964, Vol. 14, No. 2, pp. 75-102.

46. Skempton, A. W., and Brown, J. D., "A Landslide in Boulder Clay at Selset, Yorkshire," Geotechnique, 1961, Vol. 11, No. 4, pp. 280-293.

47. Skempton, A. W. and Golder, H. Q. "Practical Examples of the $\phi = 0$ Analysis of Stability of Clays," Proc. 2nd International Conference on Soil Mechanics and Foundation Engineering, Rotterdam, 1948, Vol. 2, pp. 63-70.

48. Skempton, A. W., and La Rochelle, P., "The Bradwell Slip: A Short-term Failure in London Clay," Geotechnique, 1965, Vol. 15, No. 3, pp. 221-242.

49. Skempton, A. W., and Northey, R. D., "The Sensitivity of Clays," Geotechnique, 1952, Vol. 3, No. 1, pp. 30-51.

50. Skempton, A. W., and Petley, D. J., "The Strength Along Structural Discontinuity in Stiff Clays," Proc. of the Geotechnical Conference on Shear Strength Properties of Natural Soil and Rock, Oslo, 1967, Vol. 2, pp. 29-46.

51. Taylor, D. W., "Fundamentals of Soil Mechanics," John Wiley & Sons, Inc., New York, 1948.

52. Terzaghi, K., "Stability of Slopes of Natural Clay," Proc. 1st International Conference on Soil Mechanics and Foundation Engineering, Cambridge, Massachusetts, 1936, Vol. 1, pp. 161-165.

53. Terzaghi, K., "The Shearing Resistance of Saturated Soils and the Angle Between the Planes of Shear," Proc. 1st International Conference on Soil Mechanics and Foundation Engineering, Cambridge, Massachusetts, 1936, Vol. 1, pp. 54-56.

54. Terzaghi, K., "Theoretical Soil Mechanics," John Wiley, New York, 1943.

55. Ward, W. H., Marsland, A., and Samuels, S. G., "Properties of the London Clay at the Ashford Common Shaft: In-Situ and Undrained Strength Tests," Geotechnique, 1965, Vol. 15, No. 4, pp. 321-342.

56. Whitman, R. V., "Some Considerations and Data Regarding the Shear Strength of Clay," ASCE Research Conference on Shear Strength of Cohesive Soils, Boulder, Colorado, 1960, pp. 581-614.

APPENDIX A

X-RAY DIFFRACTION PATTERNS OF BEAUMONT CLAY

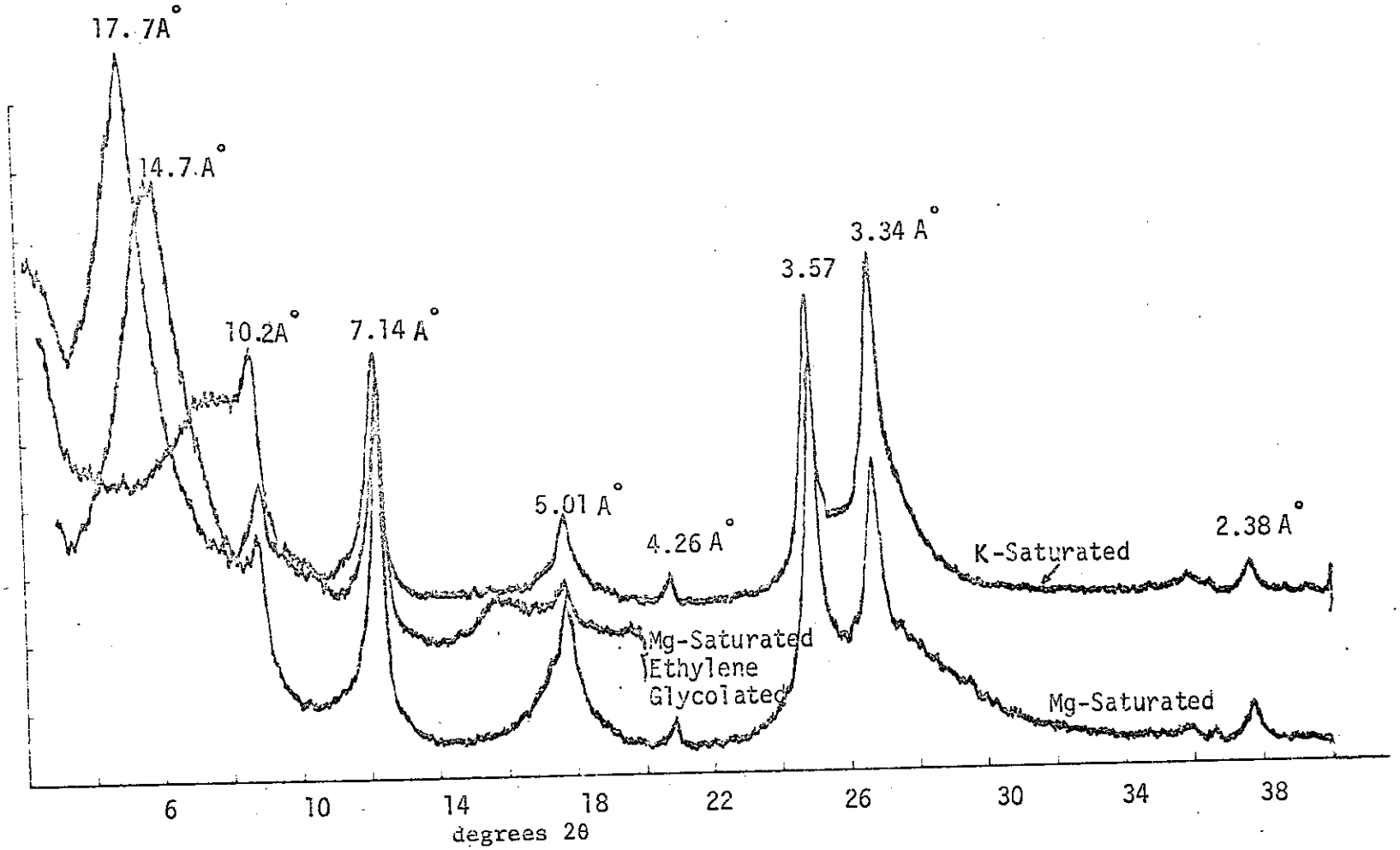

FIG. A-1.-- X-RAY DIFFRACTION PATTERNS OF K^{+} and Mg^{++} SATURATED SAMPLES OF THE <2μ FRACTION FROM DEPTH 20 - 22 FEET

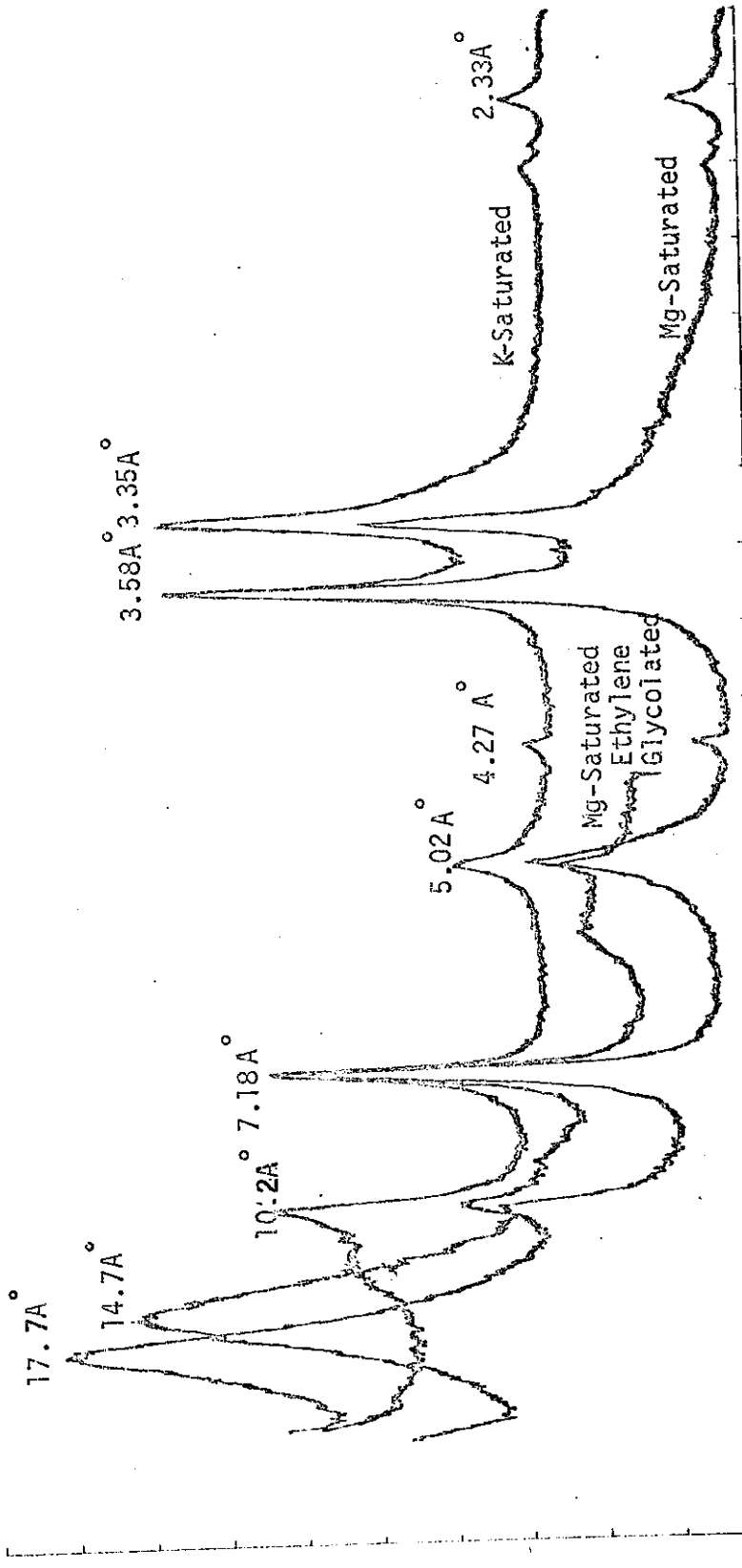

FIG. A-2. - X-RAY DIFFRACTION PATTERNS OF K^{+} and Mg^{++} SATURATED SAMPLES OF THE <2μ FRACTION FROM DEPTH 24 - 25 FEET

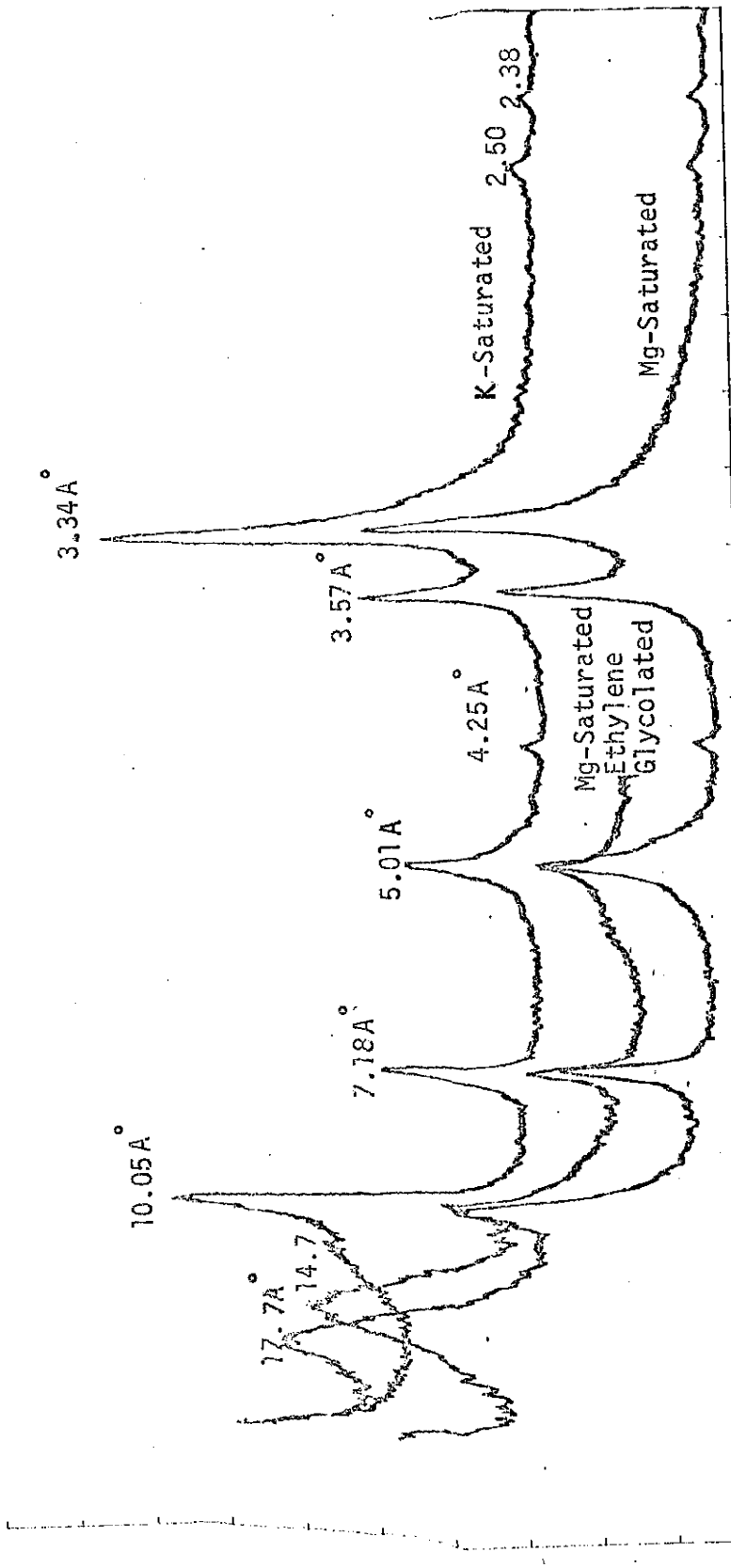

FIG. A-3.-- X-RAY DIFFRACTION PATTERNS OF K^{+} and Mg^{++} SATURATED SAMPLES OF THE <2μ FRACTION FROM DEPTH 29 - 31 FEET

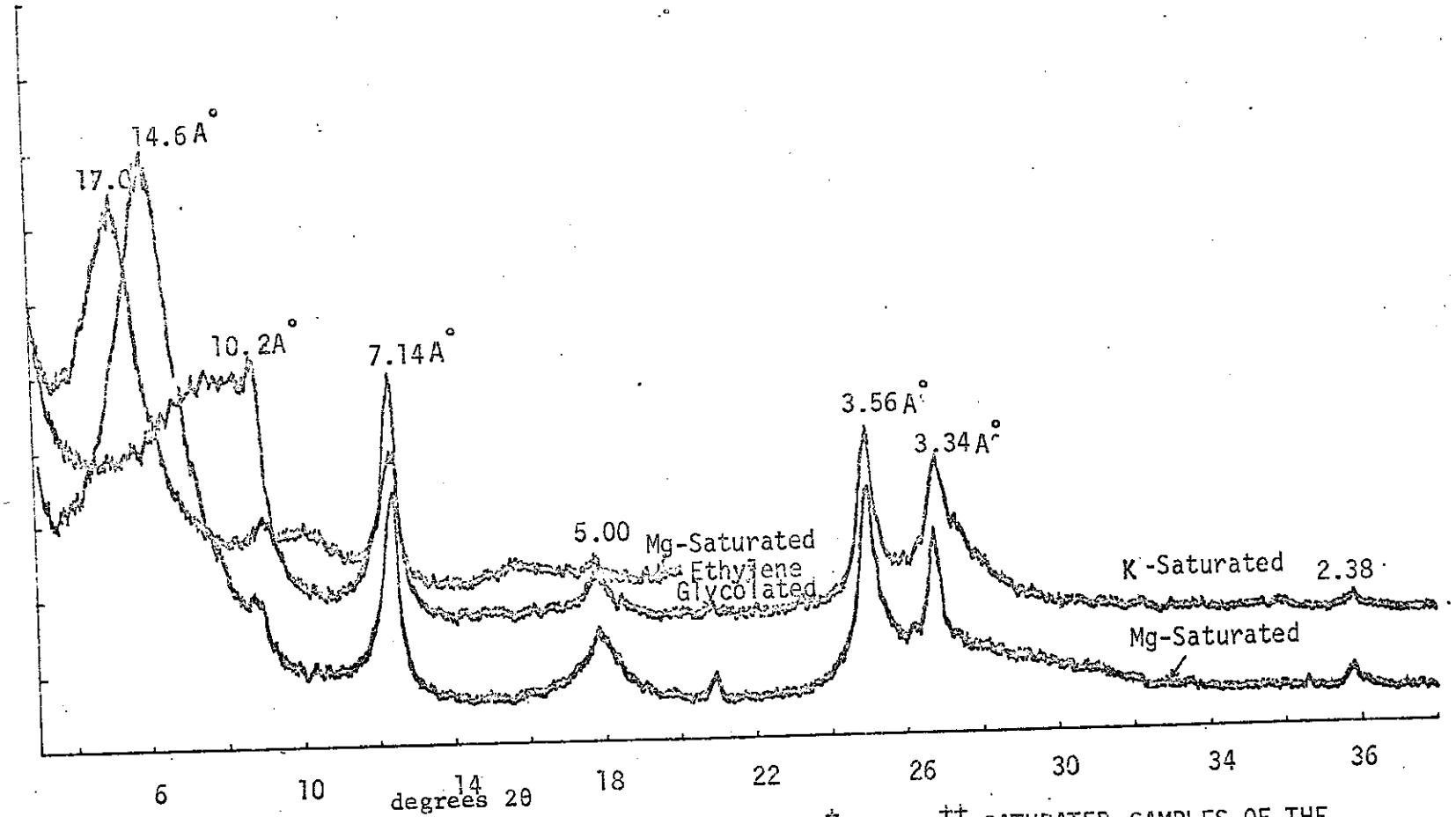

FIG. A-4. -- X-RAY DIFFRACTION PATTERNS OF K^{+} and Mg^{++} SATURATED SAMPLES OF THE <2μ FROM JOINT SURFACE MATERIAL

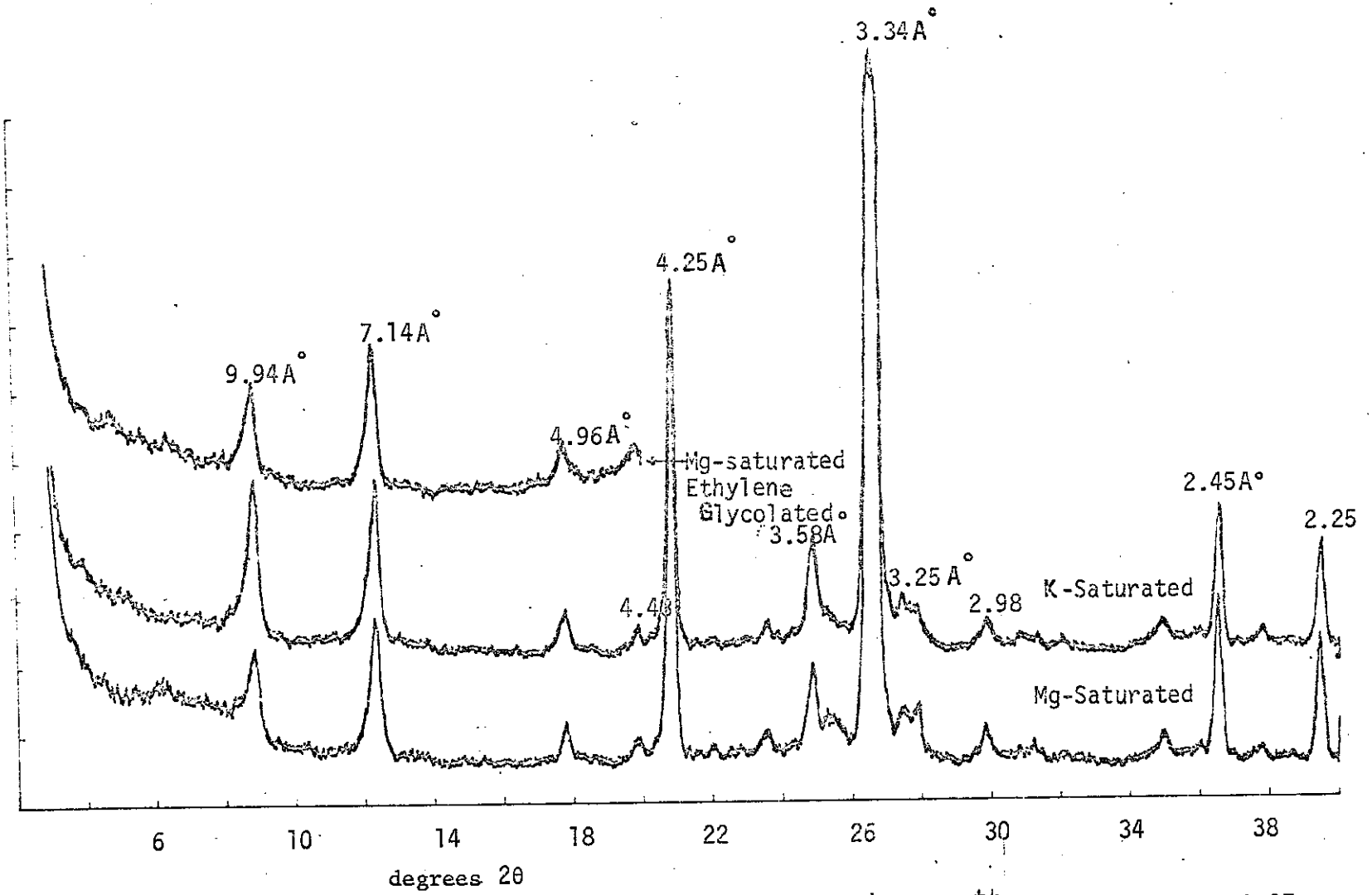

FIG. A-5. - X-RAY DIFFRACTION PATTERNS OF K^+ AND Mg^{++} SATURATED SAMPLES OF THE 50 - 2μ FRACTION FROM DEPTH 20 - 22 FEET

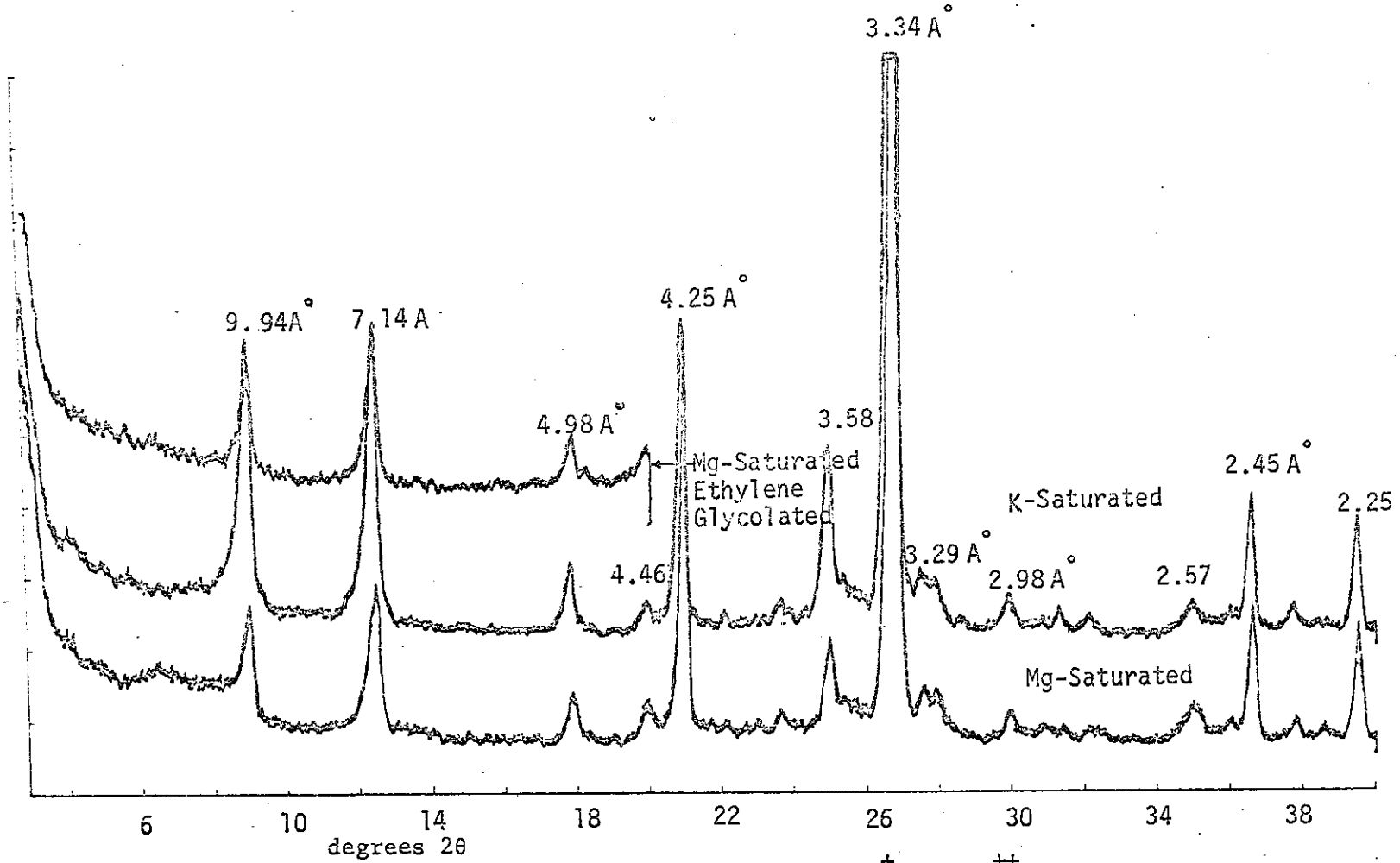

FIG. A-6.-- X-RAY DIFFRACTION PATTERNS OF K^{+} AND Mg^{++} SATURATED SAMPLES OF THE 50 - 2μ FRACTION FROM DEPTH 24 - 25 FEET

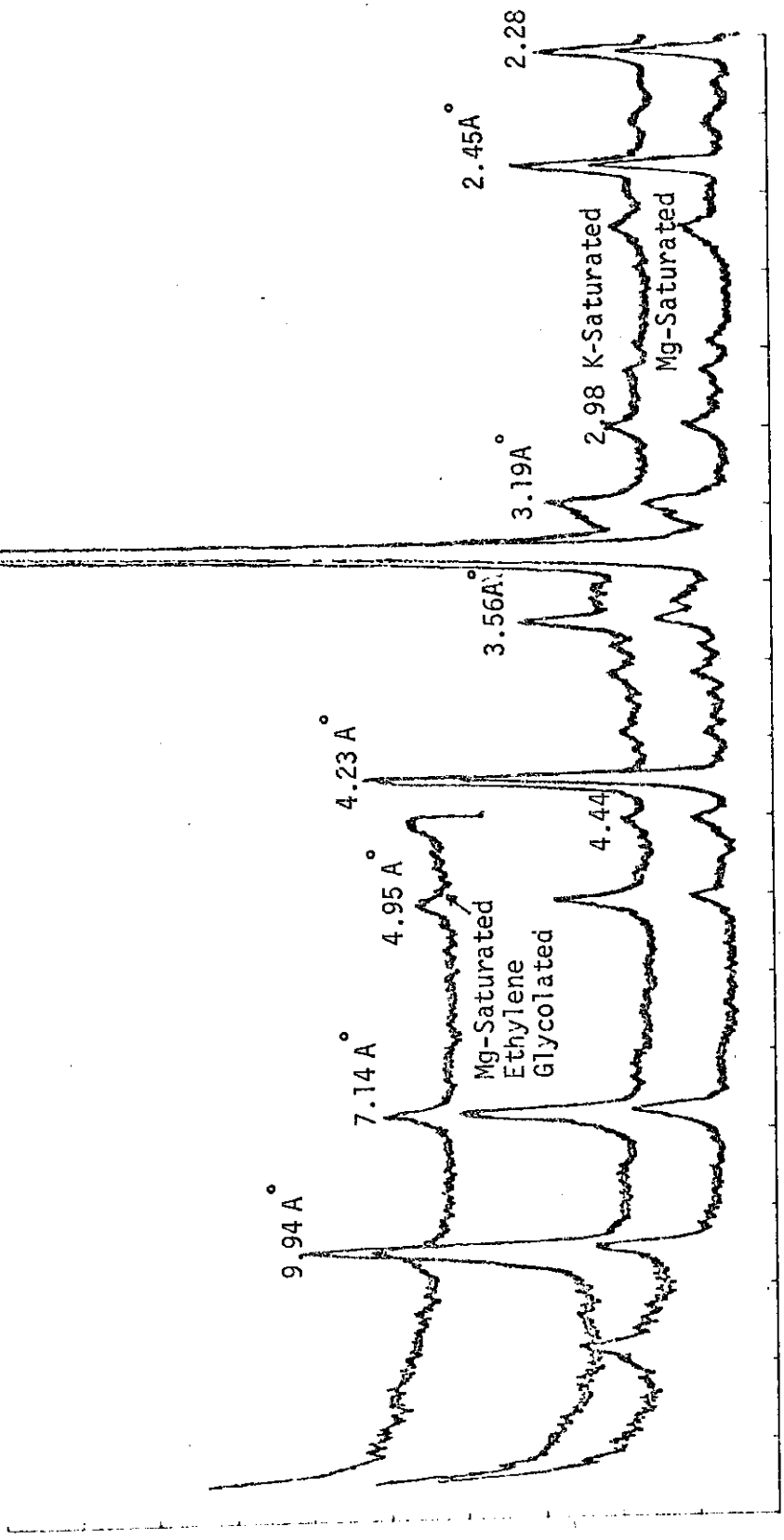

FIG. A-7.--X-RAY DIFFRACTION PATTERNS OF K^{+} and Mg^{++} SATURATED SAMPLES OF THE 50 - 2μ FRACTION FROM DEPTH 29 - 31 FEET

APPENDIX B

DATA OF TRIAXIAL COMPRESSION TESTS

Boring No. CB-1 Weight of Sample (gm) 173

Depth (ft.) 20-22 Moisture Content (%) 30.2

Size of Sample (In.) 1.5 X 3 Consolidation Pressure (Psi) 10

Rate of test (in./min.) .00024 Back Pressure (kg/cm^2) 2.00

Strain E%	Load ΔP lb.	Excess Pore Pressure ΔU Psi	$\sigma_1 - \sigma_3$ Psi	$\frac{\sigma_1 - \sigma_3}{\bar{\sigma}_3}$	Pore Press. Coeff. A
.087	2.7	--	1.530	.153	--
.183	4.3	.569	2.430	.257	.234
.257	7.5	1.138	4.235	.478	.269
.320	12.8	1.706	7.220	.870	.234
.413	13.8	2.417	7.780	1.030	.311
.510	14.9	2.702	8.390	1.149	.322
.933	19.3	2.840	10.830	1.514	.263
1.530	22.7	2.630	12.660	1.718	.208
1.837	23.3	2.630	12.950	1.757	.203
2.100	23.8	2.275	13.190	1.706	.173
2.267	24.2	1.990	13.390	1.672	.149
2.420	24.6	1.849	13.590	1.667	.136
2.533	24.8	1.683	13.690	1.645	.123
2.580	25.2	1.635	13.900	1.661	.118
2.767	25.5	1.564	14.040	1.664	.111
2.883	25.8	1.422	14.190	1.656	.100
3.000	26.1	1.351	14.330	1.659	.094
3.237	26.4	1.280	14.470	1.659	.088
3.470	26.7	1.208	14.590	1.667	.083
3.783	27.1	1.138	14.770	1.640	.080
3.943	27.2	.995	14.790	1.570	.070
4.150	27.3	.569	14.810	1.540	.040
4.653	27.8	.284	15.010	1.520	.020
4.893	27.8	.142	14.970	1.510	.010
5.370	28.1	.000	15.060	1.450	.000
5.847	28.4	- .427	15.140	1.440	-.030

Boring No. CB-1 Weight of Sample (gm) 169.5

Depth (ft.) 20-22 Moisture Content (%) 33.5

Size of Sample (In.) 1.5 X 3 Consolidation Pressure (Psi) 20

Rate of test (in./min.) .00024 Back Pressure (kg/cm^2) 2.10

Strain E%	Load ΔP lb.	Excess Pore Pressure ΔU Psi	$\sigma_1 - \sigma_3$ Psi	$\frac{\sigma_1 - \sigma_3}{\sigma_3}$	Pore Press. Coeff. A
.054	2.0	--	1.132	--	--
.114	3.6	.213	2.036	.103	.105
.177	4.7	1.070	2.660	.141	.402
.247	8.7	1.420	4.920	.265	.290
.267	10.2	2.130	5.760	.322	.370
.307	12.7	2.840	7.170	.418	.396
.350	15.7	3.130	8.860	.525	.353
.397	16.7	3.840	9.420	.583	.408
.510	21.1	4.550	11.890	.770	.383
.637	23.3	5.400	13.110	.898	.411
.733	25.2	5.550	14.170	.981	.392
1.370	31.2	6.110	17.420	1.254	.350
1.487	31.7	5.970	17.680	1.260	.338
1.640	32.2	5.830	17.890	1.263	.326
1.790	32.7	5.830	18.170	1.282	.321
2.100	33.4	5.970	18.530	1.321	.322
2.330	34.2	5.670	18.900	1.319	.300
2.490	34.4	5.600	19.000	1.319	.295
2.600	35.2	5.120	19.450	1.307	.263
3.150	35.6	4.980	19.560	1.302	.255
3.500	36.7	4.550	20.060	1.296	.226
4.130	37.3	4.270	20.270	1.289	.211
5.070	38.2	3.840	20.540	1.271	.187
6.030	38.3	3.700	20.370	1.250	.182
7.040	38.2	3.560	20.111	1.223	.177
7.440	38.0	3.130	19.900	1.180	.157
8.360	36.7	2.840	19.020	1.108	.149

Boring No. CB-1 Weight of Sample (gm) 167.5

Depth (ft.) 20-22 Moisture Content (%) 33.2

Size of Sample (In.) 1.5 X 3 Consolidation Pressure (psi) 40

Rate of test (in./min.) .00024 Back Pressure (kg/cm^2) 2.20

Strain E%	Load ΔP lb.	Excess Pore Pressure ΔU Psi	$\sigma_1 - \sigma_3$ Psi	$\frac{\sigma_1 - \sigma_3}{\bar{\sigma}_3}$	Pore Press. Coeff. A
.047	2.5	.1420	1.42	.036	.1000
.113	3.5	.2280	1.98	.050	.1150
.187	4.0	.5690	2.26	.057	.2520
.277	6.0	1.280	3.39	.088	.3780
.370	8.0	1.991	4.51	.119	.4410
.453	13.2	2.990	7.44	.201	.4020
.630	24.0	5.260	13.51	.389	.3890
.840	32.0	6.540	17.97	.538	.3640
1.070	38.5	8.960	21.57	.696	.4150
1.353	44.5	10.380	24.86	.840	.4160
1.813	48.8	11.520	27.13	.954	.4250
1.960	50.0	11.660	27.76	.981	.4200
2.870	53.5	11.520	29.43	1.035	.3910
3.340	54.5	11.520	29.83	1.049	.3860
3.810	54.9	11.520	29.90	1.051	.3850
4.320	55.5	11.376	30.07	1.052	.3780
4.910	55.9	11.234	30.10	1.048	.3730
5.390	56.0	10.807	29.99	1.029	.3600
5.870	56.3	10.096	30.01	1.005	.3360
6.830	56.3	9.812	29.69	.985	.3304
9.400	55.7	9.527	28.58	.939	.3330
9.480	55.7	9.527	28.55	.938	.3360

Boring No. CB-1A
Depth (ft.) 20-21.5
Size of Sample (In,) 1.5 X 3
Rate of Test (in./min.) .00024
Weight of Sample (gm) 167.9
Moisture Content (%) 34.7
Consolidation Pressure (psi) 10
Back Pressure (kg/cm^2) 2.30

Strain E%	Load ΔP lb.	Excess Pore Pressure ΔU Psi	$\sigma_1 - \sigma_3$ Psi	$\frac{\sigma_1 - \sigma_3}{\sigma_3}$	Pore Press. Coeff. A
.020	.3	---	.17	----	---
.060	.9	.071	.508	.050	.140
.100	2.5	.142	1.410	.143	.100
.367	8.3	1.280	4.680	.540	.273
.507	10.0	1.850	5.630	.691	.328
.623	13.0	2.560	7.315	.983	.350
.750	14.9	2.770	8.373	1.158	.331
.827	16.0	2.840	8.985	1.255	.316
1.330	11.9	2.990	11.120	1.590	.269
1.480	20.5	2.990	11.440	1.630	.261
1.710	21.5	2.990	11.970	1.710	.249
2.013	22.9	2.840	12.710	1.760	.224
2.240	23.5	2.840	13.010	1.820	.219
2.473	24.2	2.700	13.360	1.830	.202
2.710	24.7	2.670	13.610	1.860	.196
2.940	25.1	2.490	13.800	1.840	.180
3.330	25.7	1.920	14.070	1.740	.136
3.970	26.0	1.351	14.140	1.630	.096
4.440	26.4	1.140	14.280	1.610	.080
4.920	26.4	0.640	14.210	1.520	.045
5.560	26.4	0.142	14.120	1.430	.010
5.720	26.4	0.142	14.090	1.420	.010

Boring No. CB-1A
Depth (ft.) 20-21.5
Size of Sample (In.) 1.5 X 3
Rate of test (in./min.) .00024

Weight of Sample (gm) 169.97
Moisture Content (%) 33.80
Consolidation Pressure (psi) 20
Back Pressure (kg/cm^2) 2.00

Strain E%	Load ΔP lb.	Excess Pore Pressure ΔU Psi	$\sigma_1 - \sigma_3$ Psi	$\frac{\sigma_1 - \sigma_3}{\sigma_3}$	Pore Press. Coeff. A
.073	.5	----	.283	-----	---
.040	1.0	.284	.565	.029	.503
.120	4.1	1.137	2.320	.123	.490
.260	10.5	2.560	5.925	.340	.432
.430	15.7	3.130	8.850	.524	.353
.540	19.2	4.410	10.810	.690	.407
.600	20.7	4.700	11.650	.760	.403
1.010	25.7	5.690	14.410	1.012	.394
1.150	27.1	5.830	15.170	1.071	.380
1.410	28.6	6.110	15.970	1.150	.380
1.520	29.2	6.260	16.280	1.185	.380
1.670	30.0	6.330	16.700	1.222	.380
1.903	30.7	6.540	17.050	1.650	.383
2.130	31.6	6.680	17.510	1.330	.380
2.360	32.6	6.540	18.020	1.353	.362
2.593	33.0	6.620	18.201	1.352	.367
2.903	33.7	6.620	18.530	1.380	.363
3.060	34.2	6.680	18.770	1.410	.356
3.290	35.0	6.540	19.170	1.430	.341
3.830	35.7	6.400	19.440	1.440	.330
4.540	37.1	6.110	20.050	1.440	.305
4.930	37.8	5.830	20.350	1.430	.286
4.400	38.5	5.546	20.620	1.420	.269
5.720	38.5	5.404	20.550	1.410	.262
5.800	38.5	5.404	20.530	1.400	.262

Boring No. CB-1A
Depth (ft.) 20-21.5
Size of Sample (In.) 1.5 X 3
Rate of test (in./min.) .00024

Weight of Samples (gm) 167.9
Moisture Content (%) 34.18
Consolidation Pressure (psi) 40
Back Pressure (kg/cm^2) 2.60

Strain E%	Load ΔP lb.	Excess Pore Pressure ΔU Psi	$\sigma_1 - \sigma_3$ Psi	$\frac{\sigma_1 - \sigma_3}{\bar{\sigma}_3}$	Pore Press. Coeff. A
.050	1.80	.284	1.019	.026	.279
.107	4.00	1.137	2.260	.058	.503
.170	11.20	2.130	6.330	.167	.337
.200	14.80	4.050	8.360	.233	.485
.243	17.20	4.240	9.715	.272	.436
.287	20.00	4.410	11.293	.317	.390
.387	24.50	6.400	13.820	.412	.463
.530	28.80	7.390	16.220	.497	.456
.620	31.00	8.240	17.450	.549	.472
.703	33.00	8.970	18.550	.595	.484
.883	35.00	9.950	19.640	.654	.507
1.127	37.40	10.520	20.940	.710	.502
1.230	38.50	10.950	21.530	.741	.508
1.380	39.50	10.950	22.060	.759	.496
1.520	40.90	11.376	22.800	.797	.499
1.670	41.90	11.518	23.330	.819	.494
2.120	44.00	11.660	24.390	.861	.478
2.280	44.40	11.518	24.570	.863	.469
2.430	45.00	11.660	24.860	.874	.468
2.890	45.90	11.660	25.240	.891	.462
3.130	46.10	11.800	25.290	.896	.466
3.610	46.30	11.660	25.270	.892	.461
4.290	46.30	11.589	25.090	.883	.462
4.970	45.70	11.400	24.590	.861	.464
5.470	45.00	11.100	24.090	.837	.461
5.950	44.70	10.81	23.810	.816	.454

Boring No. CB-1A
Depth (ft.) 20-21.5
Size of Sample (In.) 1.5 X 3
Rate of test (in./min.) .00024

Weight of Sample (gm) 16-.0
Moisture Content (%) 34.65
Consolidation Pressure (psi) 60
Back Pressure (kg/cm^2) 1.6

Strain E%	Load ΔP lb.	Excess Pore Pressure ΔU Psi	$\sigma_1 - \sigma_3$ Psi	$\frac{\sigma_1 - \sigma_3}{\bar{\sigma}_3}$	Pore Press. Coeff. A
.080	9.3	3.410	5.23	.093	.652
.220	15.3	5.688	8.61	.159	.660
.380	25.1	8.532	14.10	.275	.605
.550	33.0	11.090	18.51	.381	.599
.650	36.3	11.660	20.34	.423	.582
1.120	47.7	15.640	26.60	.603	.588
1.300	50.7	16.630	28.22	.655	.589
1.520	53.3	17.200	29.61	.696	.586
1.920	57.8	18.910	31.97	.783	.591
2.260	60.3	19.910	33.24	.834	.599
2.580	62.0	20.050	34.08	.859	.588
2.800	63.3	20.900	34.72	.894	.598
3.020	64.5	20.900	35.29	.909	.592
3.730	66.4	20.900	36.05	.929	.580
4.100	66.4	20.760	35.89	.921	.578
4.450	66.4	20.330	35.77	.908	.568
4.770	66.3	20.190	35.60	.900	.567
5.100	65.5	19.766	35.04	.877	.564
5.600	64.3	19.620	34.23	.854	.573

Boring No. CB-1A | Weight of Sample (gm) 171.88

Depth (ft.) 20-21.5 | Moisture Content (%) 31.95

Size of Sample (In.) 1.5 X 3 | Consolidation Pressure (psi) 10

Rate of test (in./min.) .00024 | Back Pressure (kg/cm^2) 2.30

HORIZONTAL SAMPLE

Strain E%	Load ΔP lb.	Excess Pore Pressure ΔU Psi	$\sigma_1 - \sigma_3$ Psi	$\frac{\sigma_1 - \sigma_3}{\sigma_3}$	Pore Press. Coeff. A
.02	3.9	.280	2.210	.227	.130
.08	5.3	.711	2.998	.323	.240
.18	3.9	.280	2.204	.227	.130
.24	5.3	.710	2.994	.322	.237
.27	9.2	1.420	5.195	.605	.274
.31	12.2	1.850	6.887	.845	.268
.41	11.2	1.635	6.320	.755	.259
.45	13.8	2.420	7.779	1.030	.311
.50	15.8	2.700	8.900	1.231	.304
.56	17.6	2.920	9.910	1.400	.294
.68	20.2	2.990	11.360	1.621	.263
.81	22.6	3.270	12.690	1.923	.258
1.02	25.2	3.400	14.124	2.140	.241
1.16	26.1	3.400	14.610	2.210	.233
1.36	26.4	3.100	14.740	2.130	.212
1.85	26.7	2.560	14.840	1.990	.172
2.23	26.7	2.130	14.780	1.880	.144
2.84	26.1	1.500	14.360	1.690	.109
3.41	25.3	1.280	13.840	1.590	.092
3.90	24.9	1.140	13.550	1.530	.084
5.11	24.2	.280	13.000	1.340	.022
5.52	23.6	.140	12.630	1.280	.011
6.68	23.6	00	12.470	1.250	00
6.80	23.6	00	12.450	1.240	00

Boring No. CB-1A
Depth (ft.) 20-21.5
Size of Sample (In.) 1.5 X 3
Rate of test (in/min.) .00024

Weight of Sample (gm) 171.60
Moisture Content (%) 34.65
Consolidation Pressure (psi) 20
Back Pressure (kg/cm^2) 1.6

HORIZONTAL SAMPLE

Strain E%	Load ΔP lb.	Excess Pore Pressure ΔU Psi	$\sigma_1 - \sigma_3$ Psi	$\frac{\sigma_1 - \sigma_3}{\bar{\sigma}_3}$	Pore Press. Coeff. A
.04	2.3	.213	1.302	.065	.164
.06	3.2	.284	1.810	.091	.157
.14	10.8	1.706	6.105	.330	.280
.20	14.2	2.133	8.024	.444	.270
.24	16.2	2.986	9.150	.532	.330
.33	22.9	3.980	12.920	.790	.308
.43	26.9	4.550	15.170	.970	.300
.64	32.0	5.550	18.000	1.230	.300
1.09	37.0	5.830	20.720	1.440	.280
1.24	37.9	5.688	21.190	1.461	.268
1.55	38.5	5.546	21.460	1.455	.258
2.15	39.1	4.480	21.660	1.384	.210
2.59	38.9	3.270	21.460	1.270	.150
3.00	38.1	3.130	20.930	1.230	.149
3.85	37.6	2.560	20.470	1.161	.125
4.91	37.0	1.706	19.920	1.078	.086
5.14	36.2	1.564	19.440	1.044	.080
5.63	36.0	.995	19.240	1.002	.052
5.91	35.9	.853	19.127	.989	.045

Boring No. CB-1A
Depth (ft.) 20-21.5
Size of Sample (In.) 1.5 X 3
Rate of test (in./min.) .00024
Weight of Sample (gm) 167.71
Moisture Content (%) 34.5
Consolidation Pressure (psi) 40
Back Pressure (kg/cm^2) 2.8

HORIZONTAL SAMPLE

Strain E%	Load ΔP lb.	Excess Pore Pressure ΔU Psi	$\sigma_1 - \sigma_3$ Psi	$\frac{\sigma_1 - \sigma_3}{\sigma_3}$	Pore Press. Coeff. A
.080	3.3	.711	1.865	.047	.380
.120	4.0	.853	2.260	.058	.377
.150	7.3	1.560	4.160	.108	.376
.190	12.0	2.840	6.770	.182	.420
.220	19.0	4.260	10.720	.299	.397
.280	25.4	5.400	14.320	.412	.375
.390	31.1	6.680	17.520	.526	.380
.470	38.9	8.110	21.870	.686	.371
.617	45.6	9.280	25.610	.833	.366
.693	47.7	10.090	26.770	.895	.372
1.123	57.5	11.660	32.140	1.134	.363
1.227	59.5	11.800	33.210	1.178	.355
1.370	60.7	12.370	33.830	1.224	.365
1.520	61.5	12.300	34.230	1.236	.359
1.670	62.1	12.500	34.510	1.255	.363
2.000	62.7	12.500	34.760	1.264	.360
2.340	63.0	12.500	34.840	1.267	.360
2.580	63.0	12.370	34.750	1.258	.356
2.740	62.7	12.220	34.530	1.237	.354
2.990	62.1	11.800	34.110	1.198	.346
3.500	60.1	11.380	32.840	1.147	.346
4.280	55.9	10.380	30.300	1.023	.343
5.050	52.0	9.530	27.960	.918	.341
5.800	50.0	8.810	26.670	.855	.331
5.960	49.9	8.603	26.570	.846	.324

Boring No. CB-1A | Weight of Sample (gm) 168.42

Depth (ft.) 20-21.5 | Moisture Content (%) 32.66

Size of Sample (in.) 1.5 X 3 | Consolidation Pressure (psi) 60

Rate of test (in./min.) .00024 | Back Pressure (kg/cm^2) 2.10

HORIZONTAL SAMPLE

Strain E%	Load ΔP lb.	Excess Pore Pressure ΔU Psi	$\sigma_1 - \sigma_3$ Psi	$\frac{\sigma_1 - \sigma_3}{\bar{\sigma}_3}$	Pore Press. Coeff. A
.06	10.5	2.49	5.930	.102	.420
.10	17.0	4.19	9.600	.173	.437
.15	23.0	5.69	12.480	.240	.438
.24	31.3	7.11	17.660	.335	.403
.48	46.0	10.38	25.900	.525	.401
.62	51.0	11.39	28.690	.592	.397
.77	55.0	12.23	30.900	.651	.396
1.29	63.2	14.36	35.320	.779	.407
1.40	64.5	14.50	36.010	.796	.403
1.84	67.1	15.64	37.300	.846	.419
2.19	68.4	16.07	37.880	.868	.424
2.42	69.0	16.35	38.130	.879	.429
2.65	69.1	16.21	38.090	.875	.425
2.97	69.3	16.26	38.076	.876	.426
3.13	69.6	16.38	38.180	.877	.430
3.25	69.6	16.78	38.130	.888	.440
4.15	70.6	18.06	38.318	.919	.470
5.19	71.0	18.20	38.117	.918	.477
5.74	71.5	19.05	38.163	.938	.499

Boring No. CB-1A
Depth (ft.) 22-23.5
Size of Sample (In.) 1.5 X 3
Rate of test (in./min.) .00024

Weight of Sample (gm) 166.9
Moisture Content (%) 34.65
Consolidation Pressure (psi) 10
Back Pressure ($kg.cm^2$) 2.80

Strain E%	Load ΔP lb.	Excess Pore Pressure ΔU Psi	$\sigma_1 - \sigma_3$ Psi	$\frac{\sigma_1 - \sigma_3}{\bar{\sigma}_3}$	Pore Press. Coeff. A
.073	.5	.14	.283	.029	.503
.223	1.3	.43	.734	.077	.580
.343	4.4	1.14	2.483	.280	.458
.383	7.4	1.45	4.170	.488	.348
.507	9.9	1.85	5.577	.684	.330
.647	11.5	2.40	6.470	.851	.370
.797	12.2	2.40	6.850	.901	.353
.947	12.9	2.56	7.235	.972	.354
1.180	13.4	2.70	7.500	1.030	.360
1.410	13.7	2.70	7.650	1.048	.350
1.650	14.3	2.56	7.960	1.070	.320
2.360	14.5	2.40	8.017	1.055	.299
3.077	15.2	2.13	8.340	1.060	.256
3.550	15.5	1.85	8.460	1.040	.220
4.020	16.1	1.71	8.750	1.055	.195
4.260	16.5	1.60	8.940	1.060	.180
5.810	17.0	1.40	9.070	1.055	.157
6.640	17.5	1.35	9.250	1.070	.146
7.360	17.7	1.28	9.280	1.064	.138

Boring No. CB-1A
Depth (ft.) 22-23.5
Size of Sample (In.) 1.5 X 3
Rate of test (in./min.) .00024

Weight of Sample (gm) 166.50
Moisture Content (%) 34.38
Consolidation Pressure (psi) 20
Back Pressure (kg/cm^2) 2.30

Strain E%	Load ΔP lb.	Excess Pore Pressure ΔU Psi	$\sigma_1 - \sigma_3$ Psi	$\frac{\sigma_1 - \sigma_3}{\sigma_3}$	Pore Press. Coeff. A
.067	1.0	.028	.566	.028	.050
.140	1.6	.199	.905	.046	.220
.210	2.2	.284	1.240	.063	.230
.303	7.1	1.280	4.010	.214	.320
.393	12.3	2.840	6.940	.404	.410
.507	15.6	3.980	8.790	.549	.453
.653	16.7	4.270	9.390	.597	.454
.800	17.8	4.340	9.998	.638	.434
1.410	20.0	5.400	11.160	.764	.484
1.560	20.5	5.400	11.430	.783	.473
1.790	21.0	5.400	11.670	.799	.463
2.280	20.5	5.600	11.340	.788	.494
2.900	21.7	5.600	11.930	.828	.471
3.300	21.8	5.400	11.930	.817	.453
4.260	22.0	5.260	11.920	.809	.441
5.217	22.3	5.120	11.960	.803	.428
5.770	22.5	4.980	12.000	.799	.415
6.250	22.9	4.830	12.150	.801	.409

Boring No. CB-1A
Depth (ft.) 22-23.5
Size of Sample (In.) 1.5 X 3
Rate of test (in./min.) .00024

Weight of Sample (gm) 166.51
Moisture Content (%) 33.92
Consolidation Pressure (psi) 40
Back Pressure (kg/cm^2) 2.80

Strain E%	Load ΔP lb.	Excess Pore Pressure ΔU Psi	$\sigma_1 - \sigma_3$ Psi	$\frac{\sigma_1 - \sigma_3}{\sigma_3}$	Pore Press. Coeff. A
.053	1.70	.711	.962	.024	.740
.120	2.60	.995	1.470	.038	.677
.190	3.10	1.137	1.750	.045	.650
.280	2.30	1.280	1.300	.034	.980
.360	2.30	1.280	1.297	.033	.987
.440	2.70	1.350	1.520	.039	.889
.590	3.10	1.560	1.740	.045	.899
.720	5.10	2.270	2.870	.076	.793
.860	7.00	2.770	3.930	.106	.706
1.010	13.50	4.550	7.570	.213	.601
1.090	19.10	5.830	10.700	.313	.545
1.200	23.20	7.250	12.980	.396	.559
1.370	28.60	8.530	15.970	.507	.534
1.490	31.30	9.670	17.460	.576	.554
1.670	35.40	10.810	19.710	.675	.548
2.010	39.90	12.370	22.140	.801	.558
2.217	42.40	13.010	23.480	.870	.554
2.700	47.10	14.220	25.900	1.010	.549
3.040	49.10	14.500	26.960	1.060	.538
3.377	51.20	15.360	28.010	1.140	.548
3.600	52.10	15.360	28.440	1.150	.540
3.830	53.10	15.640	28.910	1.187	.540
3.950	53.40	15.780	29.040	1.199	.543
7.910	41.10	12.510	21.430	.779	.584
8.080	40.80	11.660	21.240	.749	.549
8.330	40.10	11.660	20.810	.734	.560
8.570	39.60	11.880	20.500	.727	.576

Boring No. CB-1A
Depth (ft.) 22-23.5
Size of Sample (In.) 1.5 X 3
Rate of test (in./min.) .00024

Weight of Sample (gm) 165.78
Moisture Content (%) 35.45
Consolidation Pressure (psi) 60
Back Pressure (kg/cm^2) 2.10

Strain E%	Load ΔP lb.	Excess Pore Pressure ΔU Psi	$\sigma_1 - \sigma_3$ Psi	$\frac{\sigma_1 - \sigma_3}{\sigma_3}$	Pore Press. Coeff. A
.063	1.40	.142	.792	.0132	.179
.081	2.20	1.140	1.240	.0210	.917
.105	2.70	1.140	1.530	.0260	.743
.125	4.40	1.490	2.480	.0430	.602
.151	4.80	1.850	2.700	.0470	.684
.170	6.60	2.700	3.710	.0650	.728
1.120	25.70	8.390	14.950	.2910	.560
1.270	32.80	10.380	18.330	.3710	.566
1.580	42.60	13.940	23.740	.5190	.587
1.897	48.80	15.640	27.100	.6150	.577
2.060	51.10	16.640	28.340	.6580	.587
2.300	54.70	17.350	30.260	.7140	.573
2.570	57.60	18.770	31.770	.7760	.591
2.720	58.80	19.340	32.390	.8020	.597
3.150	62.20	20.620	34.110	.8720	.604
3.600	64.70	21.300	35.300	.9190	.603
4.290	66.80	21.470	36.200	.9460	.593
4.760	67.70	21.470	36.500	.9540	.588
5.410	66.80	21.330	35.780	.9320	.596
9.180	57.60	18.630	29.620	.7210	.629

Boring No. CB-1A
Depth (ft.) 22-23.5
Size of Sample (In.) 1.5 X 3
Rate of test (in./min.) .00024

Weight of Sample (gm) 168.72
Moisture Content (%) ---
Consolidation Pressure (psi) 10
Back Pressure (kg/cm^2) 1.90

HORIZONTAL SAMPLE

Strain E%	Load ΔP lb.	Excess Pore Pressure ΔU Psi	$\sigma_1 - \sigma_3$ Psi	$\frac{\sigma_1 - \sigma_3}{\bar{\sigma}_3}$	Pore Press. Coeff. A
.047	2.2	.284	1.240	.128	.230
.107	3.9	.569	2.206	.234	.258
.153	6.3	.995	3.560	.396	.279
.260	7.3	1.351	4.123	.477	.328
.327	11.2	1.850	6.320	.775	.292
.420	16.0	2.840	9.020	1.260	.315
.537	19.2	3.130	10.810	1.570	.289
.597	21.0	3.270	11.820	1.760	.277
.790	24.2	3.840	13.590	2.210	.280
.997	26.6	3.840	14.910	2.420	.258
1.200	29.1	3.550	16.280	2.520	.218
1.350	30.0	3.470	16.760	2.570	.207
1.570	31.1	3.270	17.330	2.570	.189
1.960	32.7	2.910	18.150	2.560	.160
3.150	33.1	1.420	18.150	2.115	.078
3.630	33.2	1.140	18.120	2.050	.063
3.980	33.6	.710	18.270	1.970	.039
9.700	28.1	-1.420	14.370	1.260	-.099
9.940	28.0	-1.420	14.280	1.250	-.100

Boring No. CB-1A | Weight of Sample (gm) 168.60

Depth (ft.) 22-23.5 | Moisture Content (%) 32.4

Size of Sample (In.) 1.5 X 3 | Consolidation Pressure (psi) 20

Rate of test (in./min.) .00024 | Back Pressure (kg/cm^2) 2.80

HORIZONTAL SAMPLE

Strain E%	Load ΔP lb.	Excess Pore Pressure ΔU Psi	$\sigma_1 - \sigma_3$ Psi	$\frac{\sigma_1 - \sigma_3}{\sigma_3}$	Pore Press. Coeff. A
.030	3.20	.427	1.81	.092	.236
.060	7.15	1.420	4.04	.217	.352
.097	10.50	1.706	5.94	.325	.287
.140	18.00	3.130	10.17	.603	.307
.320	23.80	4.690	13.43	.877	.349
.430	27.10	5.120	15.28	1.030	.335
.540	30.60	5.970	17.23	1.230	.347
.670	33.10	6.680	18.62	1.393	.359
.870	35.90	7.390	20.15	1.600	.367
1.020	36.90	7.390	20.68	1.640	.357
1.330	37.30	6.000	20.84	1.490	.288
1.490	37.30	5.970	20.81	1.480	.287
1.730	37.30	5.900	20.75	1.470	.284
1.980	37.10	5.690	20.59	1.440	.276
2.220	36.60	5.400	20.26	1.390	.267
2.530	36.10	5.120	19.90	1.340	.257
2.960	35.10	4.690	19.28	1.260	.243
3.210	34.60	4.690	18.96	1.240	.248
3.460	34.10	4.550	18.64	1.210	.244
3.780	33.80	4.340	18.41	1.175	.235
4.900	33.20	4.270	17.88	1.140	.213
5.800	32.50	3.690	17.33	1.060	.200
6.280	32.20	3.410	17.09	1.030	.193
6.760	32.10	3.270	16.95	1.010	.193

Boring No. CB-1A
Depth (ft.) 22-23.5
Size of Sample (In.) 1.5 X 3
Rate of test (in./min.) .00024

Weight of Sample (gm) 171.4
Moisture Content (%) 30.60
Consolidation Pressure (psi) 40
Back Pressure (kg/cm^2) 1.70

HORIZONTAL SAMPLE

Strain E%	Load ΔP lb.	Excess Pore Pressure ΔU Psi	$\sigma_1 - \sigma_3$ Psi	$\frac{\sigma_1 - \sigma_3}{\sigma_3}$	Pore Press. Coeff. A
.063	1.2	.142	.68	.0171	.210
.120	2.3	.213	1.30	.0330	.164
.217	6.1	1.280	3.45	.0890	.371
.330	16.4	3.130	9.25	.2520	.338
.400	23.2	5.400	13.08	.3800	.413
.490	29.0	6.680	16.34	.4930	.410
.570	34.2	7.390	19.25	.5930	.384
.670	38.7	8.670	21.77	.6980	.398
.777	42.5	9.670	23.88	.7910	.405
.880	46.5	10.380	26.10	.8860	.398
1.240	55.3	12.500	30.90	1.1300	.405
1.440	58.1	12.900	32.40	1.2000	.399
1.660	60.0	13.510	33.41	1.2690	.404
1.880	61.5	14.010	34.17	1.3230	.410
2.190	62.2	14.080	34.45	1.3370	.409
2.510	62.5	14.080	34.50	1.3390	.408
2.920	61.5	13.510	33.81	1.2840	.400
3.270	59.4	13.150	32.54	1.2190	.404
4.050	54.9	12.660	29.83	1.097	.424
5.080	49.7	11.450	26.71	.941	.429
5.700	48.1	11.300	25.68	.900	.440
6.070	47.2	11.090	25.10	.873	.442
6.570	46.2	10.950	24.40	.844	.449

Boring No. CB-1A | Weight of Sample (gm) 167.80

Depth (ft.) 22-23.5 | Moisture Content (%) 31.70

Size of Sample (In.) 1.5 X 3 | Consolidation Pressure (psi) 60

Rate of test (in./min.) .00024 | Back Pressure (kg/cm^2) 2.20

HORIZONTAL SAMPLE

Strain E%	Load ΔP lb.	Excess Pore Pressure ΔU Psi	$\sigma_1 - \sigma_3$ Psi	$\frac{\sigma_1 - \sigma_3}{\bar{\sigma}_3}$	Pore Press. Coeff. A
.047	2.3	.711	1.302	.022	.546
.110	3.6	1.280	2.040	.035	.627
.183	4.0	1.420	2.260	.039	.630
.313	6.1	2.420	3.440	.060	.703
.460	7.2	2.700	4.060	.071	.665
.610	8.0	2.840	4.500	.079	.632
.757	9.0	3.130	5.060	.089	.618
.850	14.0	4.410	7.860	.142	.561
.903	21.8	6.680	12.230	.231	.546
.977	28.0	8.250	15.700	.305	.525
1.037	32.5	8.820	18.210	.358	.484
1.273	47.2	12.510	26.390	.559	.474
1.430	53.2	14.220	29.690	.652	.479
1.597	58.8	15.500	32.760	.741	.473
1.870	65.0	17.210	36.120	.814	.476
2.300	71.2	18.910	39.280	.962	.481
2.850	75.2	20.330	41.370	1.050	.491
3.400	76.0	20.410	41.570	1.057	.491
4.260	75.0	20.330	40.660	1.032	.500
4.760	73.2	19.840	39.480	.989	.502
6.070	71.0	19.340	37.760	.935	.512

Boring No. CB-8 Weight of Sample (gm) 166.85

Depth (ft.) 33-35 Moisture Content (%) 34.3

Size of Sample (In.) 1.5 X 3 Consolidation Pressure (psi) 10

Rate of test (in./min.) .00024 Back Pressure (kg/cm^2) 1.50

Strain E%	Load ΔP lb.	Excess Pore Pressure ΔU Psi	$\sigma_1 - \sigma_3$ Psi	$\frac{\sigma_1 - \sigma_3}{\bar{\sigma}_3}$	Pore Press. Coeff. A
.070	.5	.0280	.283	.028	.099
.140	1.0	.0711	.565	.057	.126
.217	1.5	.1140	.848	.086	.135
.280	2.8	.4270	1.580	.165	.270
.323	5.5	1.1380	3.104	.350	.366
.367	8.2	1.7780	4.626	.563	.384
.743	16.0	2.8440	8.992	1.260	.316
.950	17.9	2.9860	10.038	1.431	.297
1.297	19.2	2.8440	10.731	1.500	.265
1.410	19.9	2.8300	11.108	1.550	.255
1.643	20.1	2.7300	11.194	1.540	.244
1.877	20.9	2.7020	11.612	1.590	.233
2.190	21.1	2.2750	11.685	1.510	.195
2.430	21.5	2.0620	11.879	1.500	.174
3.453	22.5	1.5640	12.301	1.460	.127
3.937	22.2	1.1380	12.075	1.360	.094
4.403	23.1	.8530	12.500	1.360	.068
4.960	23.3	.5690	12.540	1.330	.045
5.513	24.0	.5690	12.840	1.360	.044
5.597	23.8	.4270	12.720	1.330	.033

Boring No. CB-8 | Weight of Sample (gm) 167.9

Depth (ft.) 33-35 | Moisture Content (%) 33.2

Size of Sample (In.) 1.5 X 3 | Consolidation Pressure (psi) 20

Rate of test (in./min.) .00024 | Back Pressure (kg/cm^2) 1.70

Strain E%	Load ΔP lb.	Excess Pore Pressure ΔU Psi	$\sigma_1 - \sigma_3$ Psi	$\frac{\sigma_1 - \sigma_3}{\bar{\sigma}_3}$	Pore Press. Coeff. A
.083	2.6	.142	1.471	.074	.097
.190	3.4	.569	1.921	.099	.296
.300	4.1	.711	2.314	.120	.307
.407	5.1	1.210	2.876	.153	.420
.487	11.1	2.560	6.255	.359	.410
.570	16.9	3.410	9.515	.574	.359
.743	21.7	4.410	12.195	.782	.360
.887	23.1	4.830	12.964	.855	.373
1.333	25.4	5.400	14.191	.972	.381
1.567	25.9	5.400	14.440	.989	.374
1.883	26.1	5.120	14.500	.974	.353
2.283	26.2	4.830	14.490	.955	.334
2.443	26.2	4.760	14.470	.949	.329
2.760	26.6	4.550	14.650	.948	.311
2.920	26.6	4.550	14.620	.946	.311
3.160	26.6	4.480	14.580	.939	.307
3.400	26.9	4.266	14.710	.935	.290
4.830	27.1	4.120	14.600	.919	.282
5.300	27.4	3.930	14.690	.917	.267
6.097	28.1	3.555	14.940	.908	.238
6.180	27.9	3.555	14.820	.901	.239

Boring No. CB-8 Weight of Sample (gm) 173.2

Depth (ft.) 28-30 Moisture Content (%) 29.50

Size of Sample (In.) 1.5 X 3 Consolidation Pressure (psi) 20

Rate of test (in./min.) .00024 Back Pressure (kg/cm^2) 1.70

Strain E%	Load ΔP lb.	Excess Pore Pressure ΔU Psi	$\sigma_1 - \sigma_3$ Psi	$\frac{\sigma_1 - \sigma_3}{\bar{\sigma}_3}$	Pore Press. Coeff. A
.067	.80	.1422	.453	.023	.310
.140	1.20	.2840	.679	.034	.420
.213	2.00	.4260	1.130	.058	.378
.287	2.30	.4980	1.299	.067	.383
.357	3.00	.5690	1.693	.087	.336
.387	6.90	1.4220	3.890	.210	.366
.670	21.00	4.4100	11.810	.760	.373
.800	23.40	4.6900	13.140	.850	.357
.930	25.30	5.4040	14.190	.970	.381
1.070	27.00	5.6900	15.125	1.060	.376
1.210	28.30	5.9700	15.830	1.120	.377
1.360	29.50	6.1900	16.480	1.190	.375
1.503	30.40	6.5400	16.950	1.260	.386
1.650	31.50	6.6800	17.540	1.316	.380
1.800	32.50	6.7500	18.070	1.364	.373
1.947	33.10	6.6800	18.380	1.380	.363
2.097	34.00	6.6800	18.850	1.415	.354
2.240	35.00	6.5400	19.370	1.430	.345
2.320	35.20	6.4000	19.470	1.430	.329
2.630	36.10	6.5400	19.910	1.510	.328
3.090	37.80	6.6800	20.740	1.550	.322
3.710	38.50	6.5400	20.990	1.560	.308
4.380	39.20	5.9700	21.224	1.510	.281
5.340	39.50	5.5500	21.170	1.460	.262

Boring No. CB-8 Weight of Sample (gm) 170.7

Depth (ft.) 33-35 Moisture Content (%) 32.60

Size of Sample (In.) 1.5 X 3 Consolidation Pressure (psi) 40

Rate of test (in./min.) .00024 Back Pressure (kg/cm^2) 2.00

Strain E%	Load ΔP lb.	Excess Pore Pressure ΔU Psi	$\sigma_1 - \sigma_3$ Psi	$\frac{\sigma_1 - \sigma_3}{\bar{\sigma}_3}$	Pore Press. Coeff. A
.006	1.3	.014	.735	.018	.019
.283	5.5	1.422	3.105	.081	.458
.337	10.4	2.560	5.830	.156	.439
.393	18.2	4.410	10.260	.288	.429
.460	25.0	5.900	14.090	.413	.420
.533	31.3	7.250	17.628	.538	.411
.817	45.5	11.090	25.550	.884	.434
.977	51.3	12.440	28.764	1.040	.433
1.090	54.8	12.800	30.690	1.128	.417
1.210	57.7	13.510	32.270	1.220	.418
1.320	60.3	13.790	33.700	1.286	.409
1.460	62.5	13.940	34.870	1.338	.400
1.627	65.3	14.220	36.370	1.411	.391
1.800	67.3	14.430	37.420	1.463	.386
1.950	68.3	14.650	37.920	1.496	.386
2.100	68.8	14.500	38.130	1.495	.380
2.230	69.3	14.360	38.360	1.496	.374
2.410	69.3	14.220	38.290	1.485	.371
2.620	66.1	14.220	36.450	1.414	.390
2.780	65.4	14.210	36.002	1.396	.395
3.830	59.3	12.660	32.290	1.181	.392
4.360	55.5	11.234	30.050	1.045	.374
5.700	51.3	10.665	27.390	.934	.389
5.860	51.1	10.665	27.240	.929	.392

Boring No. C3-8 | Weight of Sample (gm) 168.2

Depth (ft.) 33-35 | Moisture Content (%) 32.0

Size of Sample (In.) 1.5 X 3 | Consolidation Pressure (psi) 40

Rate of test (in./min.) .00024 | Back Pressure (kg/cm^2) 2.35

Strain E%	Load ΔP lb.	Excess Pore Pressure ΔU Psi	$\sigma_1 - \sigma_3$ Psi	$\frac{\sigma_1 - \sigma_3}{\bar{\sigma}_3}$	Pore Press. Coeff. A
.070	.60	.284	.339	.0086	.838
.100	4.60	1.850	2.600	.0690	.711
.120	8.90	2.990	5.030	.1370	.594
.150	12.10	3.840	6.840	.1910	.561
.230	18.00	5.546	10.168	.2940	.545
.360	26.20	7.963	14.780	.4680	.538
.520	32.50	9.530	18.310	.6070	.520
.680	37.70	-----	21.200	---	----
.860	42.40	-----	23.800	---	----
1.050	46.30	-----	25.940	---	----
1.240	49.50	-----	27.680	---	----
1.440	52.80	-----	29.460	---	----
1.640	55.70	-----	31.020	---	----
1.700	56.90	15.930	31.670	1.3300	.503
1.840	58.60	16.070	32.570	1.3800	.490
1.980	59.70	16.350	33.130	1.4300	.493
2.120	61.20	16.640	33.920	1.4800	.490
2.270	61.70	16.780	34.140	1.5000	.490
2.460	62.70	16.920	34.630	1.5130	.488
2.560	62.50	16.350	34.480	1.4700	.474
2.750	61.80	15.930	34.030	1.4300	.468
2.930	60.70	15.640	33.360	1.3880	.469
3.100	59.90	15.360	32.860	1.3500	.467
3.280	58.70	15.070	32.140	1.3060	.469
3.590	56.20	14.360	30.680	1.2120	.468
4.450	51.70	13.790	27.970	1.0930	.493
5.240	50.00	12.800	26.830	.9980	.477

Boring No. CB-1A
Depth (ft.) 22-23.5
Size of Sample (In.) 1.5 X 3
Rate of test (in./min.) .00024

Weight of Sample (gm) 159.50
Moisture Content (%) 37.35
Consolidation Pressure (psi) 10
Back Pressure (kg/cm^2) 2.70

REMOLDED SAMPLE

Strain E%	Load ΔP lb.	Excess Pore Pressure ΔU Psi	$\sigma_1 - \sigma_3$ Psi	$\frac{\sigma_1 - \sigma_3}{\sigma_3}$	Pore Press. Coeff. A
.053	2.10	.284	1.189	.122	.240
.080	4.90	.854	2.772	.313	.308
.197	9.30	1.920	5.256	.651	.365
.327	11.50	2.700	6.491	.889	.383
.467	12.90	2.840	7.271	1.016	.390
.617	13.50	2.990	7.597	1.083	.394
.843	14.50	3.200	8.141	1.197	.394
1.070	15.50	3.630	8.683	1.347	.418
1.530	16.70	3.980	9.311	1.547	.443
2.000	17.60	4.200	9.770	1.683	.436
2.470	18.50	4.200	10.217	1.760	.410
2.940	19.40	4.270	10.662	1.860	.402
3.730	19.90	4.130	10.848	1.847	.380
4.360	20.50	3.980	11.102	1.857	.358
4.843	20.50	3.910	11.046	1.820	.354
5.810	19.90	3.270	10.614	1.577	.307
6.633	18.30	2.990	9.675	1.379	.308

Boring No. CB-1A | Weight of Sample (gm) 160.76

Depth (ft.) 22-23.5 | Moisture Content (%) 37.40

Size of Sample (In.) 1.5 X 3 | Consolidation Pressure (psi) 20

Rate of test (in./min.) .00024 | Back Pressure (kg/cm^2) 2.90

REMOLDED SAMPLE

Strain E%	Load ΔP lb.	Excess Pore Pressure ΔU Psi	$\sigma_1 - \sigma_3$ Psi	$\frac{\sigma_1 - \sigma_3}{\sigma_3}$	Pore Press. Coeff. A
.070	.60	.142	.340	.0170	.417
.140	1.50	.356	.848	.0432	.420
.207	2.40	.711	1.356	.0703	.525
.243	5.70	1.109	3.220	.1710	.344
.290	7.29	1.280	4.116	.2200	.311
.337	10.50	1.991	5.926	.3290	.336
.453	13.60	2.702	7.670	.4430	.352
.587	15.80	3.626	8.894	.5430	.408
.733	16.70	3.910	9.387	.5830	.416
.873	18.10	4.270	10.160	.6460	.420
1.323	20.30	5.420	11.343	.7780	.478
1.550	21.20	5.830	11.818	.8340	.492
2.010	22.60	6.612	12.540	.9370	.527
2.470	24.00	6.826	13.254	1.0060	.515
2.940	25.00	7.110	13.740	1.0660	.518
3.410	25.60	7.252	14.002	1.0980	.518
3.880	26.4	7.470	14.370	1.1460	.520
4.903	27.7	7.820	14.916	1.2390	.524
5.460	28.2	7.963	15.097	1.2540	.529
5.930	28.7	7.892	15.288	1.2630	.516
6.490	29.0	7.764	15.356	1.2550	.506
7.040	29.2	7.537	15.370	1.2330	.490
10.990	27.0	6.683	13.608	1.0220	.490
11.660	25.2	6.540	12.606	.9370	.519

Boring No. CB-1A
Depth (ft.) 22-23.5
Size of Sample (In.) 1.5 X 3
Rate of test (in./min.) .00024
Weight of Sample (gm) 161.40
Moisture Content (%) 37.30
Consolidation Pressure (psi) 40
Back Pressure (kg/cm^2) 2.30

REMOLDED SAMPLE

Strain E%	Load ΔP lb.	Excess Pore Pressure ΔU Psi	$\sigma_1 - \sigma_3$ Psi	$\frac{\sigma_1 - \sigma_3}{\sigma_3}$	Pore Press. Coeff. A
.037	3.20	.995	1.811	.0460	.540
.077	6.10	1.706	3.450	.0901	.495
.113	9.40	2.560	5.317	.1420	.482
.157	12.00	3.270	6.784	.1850	.483
.200	14.80	3.982	8.364	.2320	.478
.257	16.60	4.238	9.376	.2620	.452
.373	19.70	4.977	11.114	.3170	.446
.503	21.80	5.830	12.282	.3590	.474
.640	23.70	6.540	13.334	.3990	.489
.853	25.60	7.252	14.370	.4390	.505
1.070	27.30	8.674	15.293	.4880	.568
1.290	28.70	9.670	16.042	.5290	.602
1.737	31.10	10.949	17.305	.5960	.632
2.270	33.40	11.803	18.480	.6550	.640
2.880	35.50	12.940	19.524	.7220	.663
3.337	36.80	13.220	20.143	.7520	.660
3.643	37.80	13.650	20.624	.7740	.661
4.310	40.40	14.500	21.776	.8540	.667
5.430	41.70	14.790	22.330	.8860	.664
5.983	42.30	15.070	22.519	.9030	.670
6.460	42.80	15.360	22.671	.9250	.677
6.930	34.10	14.930	22.713	.9060	.659
11.400	32.30	13.082	16.200	.6040	.809

Boring No. CB-1A
Depth (ft.) 22-23.5
Size of Sample (In.) 1.5 X 3
Rate of test (in./min.) .00024

Weight of Sample (gm) 156.7
Moisture Content(%) 41.1
Consolidation Pressure (psi) 10
Back Pressure (kg/cm^2) 2.10

REMOLDED SAMPLE

Strain E%	Load ΔP lb.	Excess Pore Pressure ΔU Psi	$\sigma_1 - \sigma_3$ Psi	$\frac{\sigma_1 - \sigma_3}{\sigma_3}$	Pore Press. Coeff. A
.040	3.0	.284	1.70	.175	.167
.087	5.4	.569	3.06	.324	.186
.140	7.3	1.209	4.13	.470	.292
.203	8.8	1.536	4.97	.587	.310
.270	9.9	1.635	5.59	.668	.293
.340	10.6	1.850	5.98	.734	.310
.480	11.9	2.560	6.71	.902	.381
.630	12.5	2.960	7.03	.999	.421
.780	13.1	2.990	7.36	1.050	.406
.900	13.7	3.020	7.69	1.102	.394
1.090	14.2	3.060	7.95	1.146	.385
1.240	14.8	3.200	8.28	1.205	.385
1.390	15.1	3.270	8.43	1.253	.388
1.940	16.2	3.410	8.99	1.364	.380
2.170	16.8	3.550	9.31	1.428	.382
2.490	17.1	3.630	9.44	1.498	.386
2.720	17.4	3.700	9.58	1.521	.386
3.120	17.7	3.700	9.71	1.541	.380
3.510	18.2	3.700	9.94	1.578	.372
3.910	18.3	3.700	9.96	1.581	.371
5.030	18.2	3.560	9.79	1.520	.364
5.520	17.4	3.200	9.31	1.369	.343
6.010	16.8	3.060	8.94	1.288	.342
6.500	16.0	3.000	8.47	1.210	.354

Boring No. CB-1A | Weight of Sample (gm) 155.1
Depth (ft.) 22-23.5 | Moisture Content (%) 40.85
Size of Sample (In.) 1.5 X 3 | Consolidation Pressure (psi) 20
Rate of test (in./min.) .00024 | Back Pressure (kg/cm^2) 1.30

REMOLDED SAMPLE

Strain E%	Load ΔP lb.	Excess Pore Pressure ΔU Psi	$\sigma_1 - \sigma_3$ Psi	$\frac{\sigma_1 - \sigma_3}{\sigma_3}$	Pore Press. Coeff. A
.060	1.50	.280	.85	.043	.330
.130	2.30	.498	1.30	.067	.383
.177	4.80	1.020	2.70	.142	.378
.220	7.20	1.560	4.07	.221	.383
.277	9.20	1.990	5.20	.289	.383
.340	10.30	2.560	5.81	.333	.416
.470	12.70	2.990	7.16	.421	.427
.610	14.10	3.700	7.94	.487	.466
.753	15.30	4.130	8.60	.542	.480
.900	16.30	4.690	9.15	.598	.512
1.200	17.80	5.620	9.96	.693	.564
1.500	19.00	5.950	10.80	.761	.551
1.960	20.50	6.830	11.38	.873	.600
2.420	21.80	7.250	12.05	.940	.595
2.890	23.20	7.540	12.76	1.024	.602
3.350	24.20	8.250	13.25	1.131	.623
3.740	24.70	8.250	13.46	1.146	.613
5.080	26.80	8.460	14.41	1.249	.587
5.560	27.30	8.520	14.60	1.272	.584
6.020	27.90	8.530	14.85	1.295	.574
6.500	28.20	8.530	14.93	1.302	.570
6.980	28.30	8.530	14.91	1.300	.572
10.900	22.30	7.110	11.25	.873	.632
11.380	22.30	7.110	11.19	.868	.636

Boring No. CB-1A | Weight of Sample (gm) 157.46

Depth (ft.) 22-23.5 | Moisture Content (%) 41.2

Size of Sample (In.) 1.5 X 3 | Consolidation Pressure (psi) 40

Rate of test (in./min.) .00024 | Back Pressure (kg/cm^2) 2.80

REMOLDED SAMPLE

Strain E%	Load ΔP lb.	Excess Pore Pressure ΔU Psi	$\sigma_1 - \sigma_3$ Psi	$\frac{\sigma_1 - \sigma_3}{\bar{\sigma}_3}$	Pore Press. Coeff. A
.053	1.80	.855	1.020	.026	.836
.127	2.50	1.140	1.410	.036	.808
.187	3.80	1.560	2.150	.056	.725
.230	6.60	2.420	3.730	.099	.645
.273	9.50	2.820	5.360	.145	.526
.323	11.60	3.410	6.550	.180	.521
.373	13.65	4.270	7.700	.216	.526
.437	14.90	4.410	8.400	.236	.526
.563	17.40	5.550	9.797	.284	.568
.697	19.50	6.540	10.960	.328	.597
.837	20.80	7.140	11.680	.355	.611
1.270	24.60	9.530	13.750	.451	.692
1.490	25.90	10.090	14.450	.483	.697
1.790	27.60	11.380	15.350	.536	.740
2.090	28.70	12.090	15.910	.570	.758
2.460	30.60	13.080	16.900	.628	.773
2.840	32.00	13.940	17.600	.675	.793
3.380	33.60	14.650	18.380	.725	.797
4.310	36.10	15.640	19.560	.803	.800
4.780	36.70	15.780	19.790	.817	.798
5.240	37.70	15.930	20.230	.840	.788
5.710	38.60	16.210	20.610	.866	.787
6.190	38.90	16.630	20.660	.884	.805
6.660	39.50	16.780	20.880	.899	.803
6.900	39.60	16.780	20.880	.899	.803
10.500	39.40	16.070	19.970	.834	.805
11.070	33.30	15.640	16.770	.688	.935

Boring No. CB-1A
Depth (ft.) 22-23.5
Size of Sample (In.) 1.5 X 3
Rate of test (in./min.) .000072
Weight of Sample (gm) 172.80
Moisture Content (%) 28.30
Consolidation Pressure (psi) 10
Back Pressure (kg/cm^2) 2.20

Strain E%	Load ΔP lb.	$\sigma_1 - \sigma_3$ Psi	Volume Change ΔV ML.	$\frac{\Delta V}{V_o}$
.067	4.1	2.320	- .08	- .0151
.143	7.3	4.134	- .13	- .0246
.290	5.4	3.050	- .13	- .0246
.387	10.1	5.710	- .18	- .0341
.513	12.6	7.120	- .24	- .0455
.680	14.9	8.410	- .28	- .0530
1.430	21.8	12.230	- .42	- .0795
1.610	22.9	12.830	- .47	- .0890
2.060	25.3	14.110	- .48	- .0910
2.760	27.0	14.940	- .43	- .0815
4.330	26.0	14.140	- .33	- .0625
4.570	25.9	14.040	- .28	- .0530
4.810	25.8	13.940	- .23	- .0435
5.060	25.6	13.790	- .20	- .0379
5.540	25.1	13.450	- .18	- .0341
5.780	25.0	13.360	- .16	- .0303
6.270	24.6	13.080	- .14	- .0265
7.110	24.4	12.850	- .08	- .0151

Boring No. CB-1A
Depth (ft.) 22-23.5
Size of Sample (In.) 1.5 X 3
Rate of test (in./min.) .000072
Weight of Sample (gm) 172.2
Moisture Content (%) 29.76
Consolidation Pressure (psi) 20
Back Pressure (kg/cm^2) 2.70

Strain E%	Load ΔP lb.	$\sigma_1 - \sigma_3$ Psi	Volume Change ΔV ML.	$\frac{\Delta V}{V_o}$
.032	3.0	1.699	- .030	- .0057
.064	6.1	3.450	- .045	- .0085
.140	6.6	3.730	- .05	- .0095
.273	10.3	5.820	- .07	- .0133
.391	8.2	4.630	- .10	- .0190
.725	13.7	7.710	- .15	- .0284
.889	19.6	11.030	- .24	- .0455
1.193	25.5	14.320	- .34	- .0645
1.441	28.5	15.970	- .35	- .0663
1.565	29.7	16.630	- .37	- .0700
1.813	32.7	18.400	- .38	- .0720
2.740	31.6	17.480	- .37	- .0700
2.980	31.6	17.430	- .37	- .0700
3.197	31.6	17.390	- .36	- .0680
3.630	31.6	17.310	- .35	- .0660
4.080	31.6	17.230	- .33	- .0625
4.690	31.6	17.114	- .30	- .0570
4.850	31.6	17.080	- .27	- .0510

Boring No. CB-1A
Depth (ft.) 22-23.5
Size of Sample (In.) 1.5 X 3
Rate of test (in./min.) .000072

Weight of Sample (gm) 170.2
Moisture Content (%) 30.35
Consolidation Pressure (psi) 40
Back Pressure (kg/cm^2) 2.80

Strain E%	Load ΔP lb.	$\sigma_1 - \sigma_3$ Psi	Volume Change ΔV ML.	$\frac{\Delta V}{V_o}$
.042	2.3	1.302	- .020	- .0038
.087	4.2	2.380	- .038	- .0070
.143	5.5	3.110	- .040	- .0076
.312	9.0	5.084	- .060	- .0114
.397	15.0	8.472	- .120	- .0230
.477	19.9	11.233	- .140	- .0270
.596	25.0	14.110	- .238	- .0450
.784	32.3	18.220	- .340	- .0640
.902	36.0	20.290	- .360	- .0680
1.034	40.3	22.700	- .440	- .0830
1.138	43.3	24.370	- .460	- .0870
1.263	46.4	26.096	- .510	- .0970
1.370	49.0	27.540	- .540	- .1020
1.480	51.6	28.973	- .560	- .1060
2.440	58.4	32.530	- .730	- .1380
2.760	58.0	32.200	- .720	- .1360
3.132	57.1	31.580	- .720	- .1360
3.427	56.8	31.321	- .720	- .1360
3.790	56.5	31.040	- .720	- .1350
4.010	56.2	30.800	- .710	- .1340
4.230	56.0	30.610	- .680	- .1290

APPENDIX C

DATA OF DIRECT SHEAR TESTS

Boring No. CB-1A
Depth (ft.) 20-21.5
Size of Sample (In.) 2.5 X .65
Rate of test (in./hr.) .007

Weight of Sample (gm) 101.1
Moisture Content (%) 32.60
Consolidation Pressure (psi) 10

Number of Shearing	Displacement Inch	Δh Inch	Load Lb.	Shearing Resistance psi	$\frac{\Delta V}{V_o}$ %
First Shearing	.0023	0	8.0	1.631	0
	.0060	0	19.3	3.934	0
	.0105	.0003	29.5	6.013	.046
	.0190	.0010	38.8	7.910	.153
	.0238	.0019	39.5	8.072	.292
	.0404	.0029	34.9	7.114	.446
	.0428	.0033	34.0	6.930	.508
	.0530	.0041	31.5	6.421	.631
	.0586	.0044	33.9	6.910	.677
	.0767	.0053	27.0	5.503	.815
	.0987	.0061	25.3	5.160	.938
	.1549	.0074	22.0	4.480	1.138
	.1800	.0082	21.0	4.280	1.261
	.2191	.0093	20.0	4.080	1.430
	.2652	.0099	19.0	3.873	1.523
Second Shearing	0	.0064	0	0	.985
	.0052	.0064	8.8	1.794	.985
	.0153	.0064	12.5	2.548	.985
	.0404	.0062	14.5	2.956	.954
	.1343	.0062	15.5	3.159	.954
	.1693	.0067	15.5	3.159	1.031
	.2165	.0072	15.7	3.200	1.110
	.2636	.0082	15.8	3.221	1.261
Third Shearing	0	.0065	0	0	1.000
	.0063	.0065	10.0	2.038	1.000
	.0215	.0065	11.1	2.263	1.000
	.0745	.0064	13.0	2.650	.984
	.1006	.0064	13.3	2.711	.984
	.1564	.0064	13.7	2.792	.984
	.2418	.0085	14.1	2.874	1.310
	.2661	.0090	14.6	2.976	1.380

(Cont'd.)

Number of Shearing	Displacement Inch	Δh Inch	Load Lb.	Shearing Resistance psi	$\frac{\Delta V}{V_o}$ %
Fourth Shearing	0	.0065	0	0	1.000
	.0629	.0065	12.0	2.446	1.000
	.1114	.0064	12.7	2.589	.984
	.1428	.0064	12.9	2.630	.984
	.2211	.0077	13.7	2.790	1.184
	.2436	.0083	14.1	2.870	1.280
Fifth Shearing	0	.0063	0	0	.969
	.0640	.0061	12.9	2.629	.938
	.0996	.0059	12.0	2.446	.907
	.1500	.0060	12.6	2.568	.923
	.2265	.0077	13.4	2.731	1.184
	.2438	.0077	13.7	2.792	1.184
	.2647	.0082	14.0	2.854	1.262
Sixth Shearing	0	.0061	0	0	.938
	.0277	.0061	9.3	1.896	.938
	.0635	.0061	11.0	2.242	.938
	.0946	.0061	11.8	2.405	.938
	.1728	.0060	12.5	2.548	.923
	.2058	.0065	13.0	2.650	1.000
	.2300	.0068	13.4	2.730	1.050
	.2647	.0078	14.0	2.854	1.200
	.2682	.0078	14.0	2.854	1.200

Boring No. CB-1A
Depth (ft.) 20-21.5
Size of Sample (In.) 2.5 X .65
Rate of test (in./hr.) .007

Weight of Sample (gm) 100.90
Moisture Content (%) 32.10
Consolidation Pressure (psi) 20

Number of Shearing	Displacement Inch	Δh Inch	Load Lb.	Shearing Resistance psi	$\frac{\Delta V}{V_o}$ %
First Shearing	.0034	0	12.0	2.450	0
	.0088	0	26.5	5.402	0
	.0162	0	40.6	8.276	0
	.0190	.0001	44.6	9.091	.015
	.0236	.0001	48.7	9.927	.015
	.0288	.0002	51.9	10.579	.031
	.0317	.0002	53.0	10.803	.031
	.0348	.0003	53.5	10.905	.046
	.0404	.0004	53.0	10.803	.062
	.0674	.0013	39.8	8.113	.200
	.0837	.0017	36.0	7.338	.262
	.1597	.0029	28.5	5.809	.446
	.1724	.0029	27.8	5.667	.446
	.2010	.0030	27.0	5.503	.462
	.2155	.0033	26.0	5.300	.508
	.2460	.0038	25.0	5.096	.585
	.2650	.0038	24.5	4.994	.585
Second Shearing	0	0	0	0	0
	.0125	0	17.2	3.506	0
	.0329	0	18.5	3.771	0
	.1038	0	19.7	4.015	0
	.1420	0	20.1	4.097	0
	.2015	.0008	20.3	4.138	.0123
	.2676	.0002	20.7	4.220	.0310
Third Shearing	0	-.0003	0	0	-.046
	.0112	-.0003	16.5	3.363	-.046
	.0275	-.0003	15.5	3.160	-.046
	.0480	-.0003	16.5	3.360	-.046
	.0755	-.0003	17.3	3.530	-.046
	.0964	-.0003	17.3	3.570	-.046
	.1609	-.0003	17.8	3.630	-.046
	.2027	-.0001	18.2	3.710	-.015
	.2201	-.0001	18.4	3.750	-.015
	.2600	.0002	19.0	3.870	.031
	.2670	.0002	19.4	3.950	.031

(Cont'd.)

Number of Shearing	Displacement Inch	Δh Inch	Load Lb.	Shearing Resistance psi	$\frac{\Delta V}{V}$ %
Fourth Shearing	0	-.0010	0	0	-.154
	.0484	-.0010	15.8	3.22	-.154
	.1038	-.0010	16.7	3.40	-.154
	.1264	-.0010	16.9	3.44	-.154
	.1700	-.0080	17.2	3.51	-.123
	.2603	-.0004	18.5	3.77	-.062
	.2706	+.0002	19.2	3.91	-.031
Fifth Shearing	0	-.0012	0	0	-.185
	.0067	-.0012	12.3	2.51	-.185
	.0197	-.0012	14.0	2.85	-.185
	.0434	-.0012	15.4	3.14	-.185
	.0536	-.0012	15.8	3.22	-.185
	.0709	-.0012	16.0	3.26	-.185
	.0918	-.0012	16.1	3.28	-.185
	.1668	-.0012	16.7	3.40	-.185
	.2015	-.0010	17.2	3.51	-.154
	.2430	-.0010	17.9	3.65	-.154
	.2639	-.0008	19.1	3.90	-.123
Sixth Shearing	0	-.0015	0	0	-.231
	.0051	-.0015	6.0	1.22	-.231
	.0235	-.0015	13.5	2.75	-.231
	.0454	-.0015	14.8	3.02	-.231
	.1112	-.0015	16.0	3.26	-.231
	.1616	-.0015	16.6	3.38	-.231
	.1965	-.0014	16.8	3.42	-.215
	.2691	-.0010	19.1	3.90	-.154

Boring No. CB-1A
Depth (ft.) 20-21.5
Size of Sample (In.) 2.5 X .65
Rate of test (in./hr.) .007

Weight of Sample (gm) 098.6
Moisture Content (%) 34.0
Consolidation Pressure (psi) 40

Number of Shearing	Displacement Inch	Δh Inch	Load Lb.	Shearing Resistance psi	$\frac{\Delta V}{V_o}$ %
First Shearing	.0027	0	7.3	1.488	0
	.0051	0	15.0	3.057	0
	.0075	0	22.5	4.586	0
	.0100	0	30.1	6.135	0
	.0142	0	41.0	8.357	0
	.0169	0	48.3	9.845	0
	.0201	0	54.7	11.150	0
	.0234	-.0004	61.0	12.434	-.062
	.0270	-.0008	66.7	13.600	-.123
	.0335	-.0011	73.5	14.982	-.169
	.0386	-.0016	76.5	15.593	-.246
	.0445	-.0021	78.5	16.000	-.323
	.0510	-.0025	79.3	16.164	-.385
	.0579	-.0030	79.5	16.200	-.461
	.0636	-.0035	78.8	16.062	-.538
	.1353	-.0038	55.2	11.252	-.585
	.1536	-.0047	53.7	10.946	-.723
	.1737	-.0048	52.5	10.701	-.738
	.1870	-.0048	50.5	10.294	-.738
	.1982	-.0050	49.5	10.090	-.769
	.2280	-.0050	46.8	9.539	-.769
	.2430	-.0050	45.5	9.274	-.769
	.2570	-.0050	44.5	9.071	-.769
	.2710	-.0050	43.5	8.870	-.769
Second Shearing	0	-.0079	0	0	-1.220
	.0176	-.0080	23.5	4.790	-1.231
	.0302	-.0083	25.6	5.218	-1.277
	.0987	-.0091	31.2	6.360	-1.400
	.1143	-.0091	31.5	6.421	-1.400
	.1616	-.0091	34.4	7.012	-1.400
	.1940	-.0089	35.8	7.297	-1.370
	.2573	-.0083	38.3	7.807	-1.277
	.2677	-.0083	38.3	7.807	-1.277

(Cont'd.)

Number of Shearing	Displacement Inch	Δh Inch	Load Lb.	Shearing Resistance psi	$\frac{\Delta V}{V_o}$ %
Third Shearing	0	-.0110	0	0	-1.69
	.0472	-.0111	26.5	5.400	-1.71
	.0779	-.0113	27.8	5.660	-1.71
	.09872	-.0113	28.2	5.740	-1.74
	.1503	-.0113	29.7	6.054	-1.74
	.2147	-.0109	33.3	6.780	-1.74
	.2419	-.0107	34.6	7.053	-1.68
	.2624	-.0104	35.9	7.300	-1.65
	.2659	-.0104	36.7	7.470	-1.60
Fourth Shearing	0	-.0133	0	0	-2.05
	.0075	-.0133	11.0	2.242	-2.05
	.0150	-.0133	21.8	4.444	-2.05
	.0284	-.0135	23.0	4.688	-2.08
	.0680	-.0139	26.8	5.463	-2.14
	.1469	-.0140	29.6	6.033	-2.15
	.1709	-.0139	30.5	6.217	-2.14
	.1880	-.0137	31.0	6.319	-2.11
	.2376	-.0130	33.0	6.726	-2.00
	.2672	-.0125	34.2	6.960	-1.92
Fifth Shearing	0	-.0170	0	0	-2.62
	.0584	-.0172	25.4	5.177	-2.65
	.0858	-.0175	26.3	5.361	-2.69
	.0991	-.0175	27.5	5.605	-2.69
	.1436	-.0175	29.3	5.972	-2.69
	.2138	-.0169	32.6	6.645	-2.60
	.2429	-.0166	33.1	6.747	-2.55
	.2863	-.0162	33.6	6.849	-2.49
	.2881	-.0162	33.9	6.910	-2.49
Sixth Shearing	0	-.0200	0	0	-3.08
	.0102	-.0200	18.2	3.710	-3.08
	.0285	-.0200	22.7	4.627	-3.08
	.0657	-.0203	24.9	5.075	-3.12
	.0843	-.0204	25.9	5.280	-3.14
	.1509	-.0203	28.7	5.850	-3.12
	.2091	-.0196	31.0	6.320	-3.02
	.2486	-.0192	32.2	6.561	-2.95
	.2680	-.0189	33.8	6.900	-2.91

Boring No. CB-1 Weight of Sample (gm) 102.7

Depth (ft.) 23-25 Moisture Content (%) 29.50

Size of Sample (In.) 0.65 X 2.5 Consolidation Pressure (psi) 10

Rate of test (in./hr.) .007

Number of Shearing	Displacement Inch	Δh Inch	Load Lb.	Shearing Resistance psi	$\frac{\Delta V}{V_o}$ %
First Shearing	.0068	.0002	15.1	3.08	.031
	.0182	.0009	28.4	5.79	.138
	.0323	.0021	33.9	6.91	.323
	.0372	.0026	34.6	7.05	.400
	.0476	.0034	34.7	7.07	.523
	.0588	.0043	34.7	7.08	.661
	.0738	.0055	31.8	6.48	.846
	.0837	.0064	29.9	6.10	.985
	.1521	.0098	23.8	4.85	1.510
	.1735	.0104	23.2	4.73	1.600
	.2093	.0117	21.6	4.40	1.800
	.2344	.0123	20.9	4.26	1.890
	.2398	.0124	20.5	4.18	1.910
	.2576	.0124	19.9	4.06	1.910
Second Shearing	0	.0090	0	0	1.380
	.0137	.0088	12.2	2.49	1.350
	.0235	.0086	13.4	2.73	1.320
	.0335	.0084	14.5	2.96	1.290
	.0403	.0083	14.7	3.00	1.280
	.1028	.0081	15.4	3.13	1.250
	.1203	.0083	15.5	3.15	1.280
	.1412	.0088	15.5	3.16	1.350
	.1832	.0099	15.6	3.18	1.520
	.2041	.0104	15.7	3.20	1.600
	.2705	.0112	15.9	3.24	1.720
Third Shearing	0	.0094	0	0	1.450
	.0047	.0094	3.7	.75	1.450
	.0168	.0094	9.9	2.02	1.450
	.0320	.0090	11.0	2.24	1.380
	.0437	.0088	11.8	2.41	1.350
	.0593	.0088	12.1	2.47	1.350
	.0766	.0087	12.5	2.55	1.340
	.1357	.0083	13.1	2.67	1.350
	.1775	.0097	13.5	2.75	1.490
	.2157	.0105	13.9	2.83	1.620
	.2384	.0108	14.1	2.87	1.660
	.2716	.0111	14.2	2.89	1.710

(Cont'd.)

Number of Shearing	Displacement Inch	Δh Inch	Load Lb.	Shearing Resistance psi	$\frac{\Delta V}{V_o}$ %
Fourth Shearing	0	.0100	0	0	1.54
	.0065	.0100	6.6	1.35	1.54
	.0274	.0096	9.8	2.00	1.48
	.0581	.0094	11.1	2.26	1.45
	.0806	.0092	11.5	2.34	1.42
	.1380	.0092	12.0	2.45	1.42
	.1693	.0100	12.5	2.55	1.54
	.2198	.0109	13.0	2.65	1.68
	.2423	.0109	13.2	2.69	1.68
	.2719	.0113	13.6	2.77	1.74
Fifth Shearing	0	.0100	0	0	1.54
	.0068	.0100	6.9	1.41	1.54
	.0119	.0100	8.7	1.77	1.54
	.0398	.0096	9.6	1.96	1.48
	.0760	.0094	10.6	2.16	1.45
	.1419	.0102	11.5	2.34	1.57
	.1749	.0103	12.0	2.45	1.58
	.2323	.0109	12.5	2.56	1.68
	.2513	.0112	12.9	2.63	1.72
	.2721	.0112	13.2	2.69	1.72
Sixth Shearing	0	.0098	0	0	1.51
	.0572	.0096	9.7	1.98	1.48
	.0780	.0095	10.0	2.04	1.46
	.0953	.0095	10.5	2.14	1.46
	.1543	.0100	11.2	2.28	1.54
	.2221	.0109	11.9	2.44	1.68
	.2688	.0111	13.0	2.65	1.71

Boring No. CB-1 Weight of Sample (gm) 102.7

Depth (ft.) 23-25 Moisture Content (%) 29.2

Size of Sample (In.) .65 X 2.5 Consolidation Pressure (psi) 20

Rate of test (in./hr.) .007

Number of Shearing	Displacement Inch	Δh Inch	Load In.	Shearing Resistance psi	$\frac{\Delta V}{V_o}$ %
First Shearing	.0028	0	9.9	2.02	0
	.0059	0	19.7	4.02	0
	.0118	0	33.2	6.77	0
	.0165	0	40.0	8.15	0
	.0228	0	47.2	9.62	0
	.0265	0	50.0	10.19	0
	.0290	0	51.5	10.50	0
	.0332	0	53.4	10.88	0
	.0403	0	56.2	11.44	0
	.0468	0	56.9	11.60	0
	.0520	.0006	57.0	11.62	.092
	.0537	.0007	57.0	11.62	.108
	.0555	.0003	56.9	11.60	.123
	.0633	.0009	55.8	11.37	.138
	.0688	.0010	55.2	11.25	.154
	.1397	.0025	38.7	7.89	.385
	.1642	.0031	36.0	7.34	.477
	.2027	.0036	33.0	6.73	.554
	.2334	.0041	31.2	6.36	.631
	.2515	.0046	30.2	6.16	.708
Second Shearing	0	.0013	0	0	.200
	.0066	.0013	9.5	1.94	.200
	.0124	.0012	17.4	3.55	.184
	.0285	.0009	19.9	4.06	.138
	.0483	.0006	21.7	4.42	.092
	.1140	.0004	23.2	4.73	.062
	.1244	.0004	23.3	4.75	.062
	.1644	.0005	23.8	4.85	.077
	.2214	.0003	25.0	5.09	.046
	.2789	.0002	25.5	5.20	.031
Third Shearing	0	.0011	0	0	.169
	.0077	.0010	10.6	2.16	.154
	.0187	.0008	15.6	3.18	.123
	.0285	.0007	17.0	3.47	.108
	.0451	.0006	18.5	3.76	.092
	.0725	.0001	19.4	3.95	.015
	.1315	.0001	20.2	4.12	.015

(Cont'd.)

Number of Shearing	Displacement Inch	Δh Inch	Load Lb.	Shearing Resistance psi	$\frac{\Delta V}{V_o}$ %
	.1559	.0001	20.5	4.17	.015
	.1940	.0001	21.0	4.28	.015
	.2233	.0005	21.6	4.40	.077
	.2371	.0006	22.3	4.55	.092
	.3008	.0013	23.8	4.85	.200
Fourth Shearing	0	.0002	0	0	.031
	.0064	.0003	12.7	2.59	.046
	.0208	.0002	15.1	3.08	.031
	.0375	.0001	16.5	3.36	.015
	.0613	-.0002	17.5	3.57	-.031
	.1377	-.0004	18.5	3.78	-.062
	.2208	-.0003	20.0	4.08	-.046
	.2878	+.0004	22.0	4.50	+.062
Fifth Shearing	0	0	0	0	0
	.0565	-.0004	17.0	3.47	-.062
	.0981	-.0006	17.5	3.57	-.092
	.1501	-.0007	18.3	3.73	-.108
	.2193	-.0004	19.7	4.02	-.062
	.2450	0	20.5	4.18	0
	.2672	.0003	21.5	4.38	.046
	.2775	.0003	21.9	4.46	.046
Sixth Shearing	0	.0001	0	0	.015
	.0165	.0001	13.5	2.75	.015
	.0383	-.0002	15.1	3.08	-.031
	.0899	-.0006	16.6	3.38	-.092
	.1645	-.0006	17.6	3.59	-.092
	.2060	-.0006	18.6	3.79	-.092
	.2473	-.0003	19.8	4.04	-.046
	.2592	-.0001	20.3	4.14	-.015
	.2807	+.0002	22.2	4.53	+.031

Boring No. CB-1 Weight of Sample (gm) 102.1

Depth (ft.) 23-25 Moisture Content (%) 30.2

Size of Sample (In.) .65 X 2.5 Consolidation Pressure (psi) 40

Rate of test (in./hr.) .007

Number of Shearing	Displacement Inch	Δh Inch	Load Lb.	Shearing Resistance psi	$\frac{\Delta V}{V_o}$ %
First Shearing	.0030	0	12.5	2.55	0
	.0089	-.0004	32.2	6.56	-.062
	.0173	-.0009	50.6	10.31	-.138
	.0386	-.0011	70.7	14.41	-.169
	.0455	-.0014	73.8	15.04	-.215
	.0515	-.0017	75.6	15.41	-.262
	.0576	-.0018	77.2	15.74	-.276
	.0643	-.0019	77.6	15.82	-.292
	.1453	-.0027	59.1	12.05	-.415
	.1699	-.0026	56.0	11.41	-.400
	.1942	-.0026	53.4	10.88	-.400
	.2308	-.0026	50.6	10.30	-.400
	.2582	-.0025	48.7	9.93	-.384
Second Shearing	0	-.0073	0	0	-1.123
	.0208	-.0077	29.7	6.05	-1.184
	.0348	-.0079	33.0	6.73	-1.215
	.0919	-.0082	36.7	7.48	-1.262
	.1126	-.0082	37.5	7.64	-1.262
	.1472	-.0082	38.3	7.81	-1.262
	.1920	-.0081	39.3	8.01	-1.246
	.2520	-.0079	41.4	8.44	-1.215
	.2572	-.0079	41.5	8.46	-1.215
Third Shearing	0	-.0097	0	0	-1.490
	.0415	-.0103	27.3	5.56	-1.590
	.0670	-.0105	31.0	6.32	-1.620
	.0945	-.0105	32.2	6.56	-1.620
	.1515	-.0105	33.7	6.87	-1.620
	.1842	-.0105	34.5	7.03	-1.620
	.2046	-.0105	35.7	7.28	-1.620
	.2335	-.0101	37.0	7.54	-1.550
	.2541	-.0098	37.8	7.71	-1.510
Fourth Shearing	0	-.0108	0	0	-1.660
	.0151	-.0108	24.5	4.99	-1.660
	.0266	-.0109	26.0	5.30	-1.680
	.0479	-.0112	28.7	5.85	-1.720
	.1524	-.0112	32.0	6.52	-1.720

(Cont'd.)

Number of Shearing	Displacement Inch	Δh Inch	Load Lb.	Shearing Resistance psi	$\frac{\Delta V}{V_o}$ %
	.1952	-.0110	33.8	6.88	-1.690
	.2340	-.0108	36.0	7.34	-1.660
	.2510	-.0108	37.4	7.62	-1.660
Fifth Shearing	0	-.0115	0	0	-1.770
	.0029	-.0115	7.0	1.43	-1.770
	.0518	-.0118	27.5	5.61	-1.820
	.0671	-.0120	28.5	5.81	-1.850
	.1101	-.0121	29.6	6.03	-1.860
	.1548	-.0121	31.0	6.32	-1.860
	.2350	-.0120	34.7	7.07	-1.850
	.2651	-.0117	37.0	7.54	-1.800
Sixth Shearing	0	-.0129	0	0	-1.980
	.0462	-.0129	28.3	5.77	-1.980
	.0810	-.0129	29.2	5.95	-1.980
	.1162	-.0129	30.7	6.26	-1.980
	.1369	-.0130	31.0	6.32	-2.000
	.2146	-.0130	33.5	6.83	-2.000
	.2567	-.0126	36.4	7.42	-1.940
	.2600	-.0125	36.6	7.46	-1.920

Boring No. CB-1 Weight of Sample (gm) ———

Depth (ft.) 29-31 Moisture Content (%) 27.2

Size of Sample (In.) 2.5 X .568 Consolidation Pressure (psi) 10

Rate of test (in./hr.) .007

Number of Shearing	Displacement Inch	Δh Inch	Load l.b.	Shearing Resistance psi	$\frac{\Delta V}{V_o}$ %
First Shearing	.0011	0	3.9	.80	0
	.0016	0	9.0	1.84	0
	.0060	.0001	12.9	2.64	.0176
	.0161	.0003	19.9	4.07	.0528
	.0267	.0003	24.5	4.99	.0528
	.0503	.0005	31.3	6.38	.0880
	.0632	.0007	33.0	6.73	.1230
	.0765	.0010	33.8	6.89	.1760
	.0900	.0014	34.1	6.95	.2460
	.1038	.0017	39.2	8.00	.2990
	.1044	.0020	33.8	6.89	.3520
	.1136	.0025	33.8	6.89	.4400
	.1253	.0031	33.5	6.83	.5450
	.1536	.0050	32.5	6.63	.8800
	.1981	.0055	30.9	6.30	.9680
	.2373	.0060	30.5	6.22	1.0520
Second Shearing	0	.0040	0	0	.7050
	.0026	.0042	1.4	.28	.7390
	.0091	.0046	7.4	1.52	.8100
	.0186	.0050	15.0	3.06	.8800
	.0329	.0055	20.0	4.12	.9680
	.0458	.0056	21.7	4.42	.9850
	.0816	.0056	25.0	5.10	.9850
	.1123	.0057	26.0	5.30	1.0010
	.1532	.0057	26.5	5.40	1.0010
	.1759	.0057	27.0	5.50	1.0010
	.2142	.0058	26.5	5.34	1.0200
	.2182	.0058	26.5	5.34	1.0200
	.2320	.0058	25.0	5.09	1.0200
Third Shearing	0	.0045	0	0	.7920
	.0073	.0045	11.0	2.24	.7920
	.0240	.0045	17.5	3.57	.7920
	.1386	.0042	22.0	4.48	.7390
	.1659	.0040	22.5	4.59	.7050
	.1728	.0042	22.6	4.61	.7390
	.1762	.0045	22.7	4.64	.7920

(Cont'd.)

Number of Shearing	Displacement Inch	Δh Inch	Load Lb.	Shearing Resistance psi	$\frac{\Delta V}{V_o}$ %
	.1829	.0047	23.1	4.71	.827
	.1931	.0047	23.5	4.79	.827
	.2045	.0052	23.6	4.81	.915
	.2205	.0054	23.7	4.84	.950
	.2273	.0055	23.8	4.86	.968
	.2445	.0055	23.9	4.88	.968
Fourth Shearing	0	.0046	0	0	.810
	.0081	.0045	9.9	2.03	.792
	.0317	.0044	16.2	3.30	.775
	.0859	.0041	18.0	3.67	.722
	.1435	.0040	19.8	4.04	.705
	.1534	.0043	20.5	4.18	.756
	.1704	.0048	21.0	4.28	.845
	.2214	.0050	22.0	4.48	.880
Fifth Shearing	0	.0044	0	0	.775
	.0121	.0043	14.5	2.96	.756
	.0386	.0043	16.2	3.30	.756
	.0588	.0043	17.1	3.49	.756
	.0895	.0041	17.9	3.65	.722
	.2360	.0040	20.1	4.08	.705
	.2390	.0046	20.2	4.09	.810
Sixth Shearing	0	.0042	0	0	.739
	.0079	.0042	10.4	2.12	.739
	.0320	.0041	13.9	2.83	.722
	.0679	.0043	15.4	3.14	.756
	.0904	.0042	16.0	3.26	.739
	.1112	.0044	16.3	3.32	.775
	.1584	.0045	16.4	3.33	.792
	.1775	.0043	16.6	3.39	.756
	.2032	.0043	17.2	3.50	.756
	.2429	.0045	17.4	3.54	.792
	.2445	.0045	17.5	3.55	.792

Boring No. CB-1 Weight of Sample (gm) 102.16

Depth (ft.) 29-31 Moisture Content (%) 27.8

Size of Sample (In.) .65 X 2.5 Consolidation Pressure (psi) 20

Rate of test (in./hr.) .007

Number of Shearing	Displacement Inch	Δh Inch	Load Lb.	Shearing Resistance psi	$\frac{\Delta V}{V_o}$ %
First Shearing	.0027	0	9.1	1.86	0
	.0084	-.0001	21.0	4.28	- .0154
	.0158	-.0004	32.2	6.56	- .0615
	.0260	-.0010	47.8	9.74	- .1540
	.0316	-.0013	53.0	10.80	- .2000
	.0600	-.0038	63.0	12.84	- .5850
	.0841	-.0040	59.0	12.03	- .6150
	.0917	-.0043	58.0	11.82	- .6620
	.0999	-.0050	57.0	11.62	- .7700
	.1069	-.0055	56.0	11.41	- .8460
	.1227	-.0059	52.9	10.78	- .9080
	.1391	-.0068	47.4	9.66	-1.0500
	.1832	-.0068	44.5	9.07	-1.0000
	.2255	-.0068	43.5	8.87	-1.0000
Second Shearing	0	-.0091	0	0	-1.4000
	.0031	-.0091	6.6	1.35	-1.4000
	.0102	-.0091	18.2	3.71	-1.4000
	.0198	-.0092	25.5	5.20	-1.4100
	.0524	-.0095	29.5	6.01	-1.4600
	.0689	-.0096	31.2	6.36	-1.4800
	.1342	-.0094	33.3	6.79	-1.4500
	.1480	-.0094	33.7	6.87	-1.4500
	.1616	-.0093	34.2	6.97	-1.4300
	.1688	-.0091	34.0	6.93	-1.4000
	.1827	-.0090	34.1	6.95	-1.3800
	.2034	-.0091	34.8	7.09	-1.4000
	.2342	-.0091	35.8	7.30	-1.4000
	.2377	-.0091	35.8	7.30	-1.4000
Third Shearing	0	-.0107	0	0	-1.6500
	.0047	-.0110	9.7	1.98	-1.6900
	.0082	-.0111	15.7	3.20	-1.7100
	.0259	-.0117	21.2	4.32	-1.8000
	.0424	-.0122	23.0	4.69	-1.8800
	.0474	-.0123	23.3	4.75	-1.8900
	.1036	-.0128	26.0	5.30	-1.9700
	.1067	-.0128	26.5	5.40	-1.9700
	.1206	-.0128	26.7	5.44	-1.9700

(Cont'd.)

Number of Shearing	Displacement Inch	Δh Inch	Load Lb.	Shearing Resistance psi	$\frac{\Delta V}{V_o}$ %
	.1583	-.0129	28.0	5.71	-1.9800
	.1857	-.0129	29.2	5.95	-1.9800
	.2096	-.0124	30.0	6.11	-1.9100
Fourth Shearing	0	-.0121	0	0	-1.8600
	.0063	-.0122	1.0	.20	-1.8800
	.0081	-.0123	9.9	2.02	-1.8900
	.0541	-.0136	21.0	4.28	-2.0900
	.0780	-.0140	22.3	4.55	-2.1500
	.0983	-.0140	23.0	4.69	-2.1500
	.1120	-.0140	24.0	4.89	-2.1700
	.1395	-.0141	24.7	5.03	-2.1700
	.1601	-.0141	25.0	5.10	-2.1700
	.2278	-.0138	29.0	5.91	-2.1200
	.2299	-.0138	29.3	5.97	-2.1200
Fifth Shearing	0	-.0134	0	0	-2.0600
	.0052	-.0135	9	1.83	-2.0800
	.0649	-.0139	20.3	4.14	-2.1400
	.0786	-.0140	21.0	4.28	-2.1500
	.1092	-.0142	21.5	4.38	-2.1800
	.1128	-.0142	22.0	4.48	-2.1800
	.1335	-.0142	22.7	4.63	-2.1800
	.1576	-.0142	23.5	4.79	-2.1800
	.2248	-.0142	28.4	5.78	-2.1800

Boring No. CB-1 Weight of Sample (gm) 104.2

Depth (ft.) 29-31 Moisture Content (%) 26.5

Size of Sample (In.) .65 X 2.5 Consolidation Pressure (psi) 40

Rate of test (in./hr.) .007

Number of Shearing	Displacement Inch	Δh Inch	Load Lb.	Shearing Resistance psi	$\frac{\Delta V}{V_o}$ %
First Shearing	.0020	0	8.5	1.73	0
	.0030	-.0001	18.5	3.77	-.013
	.0075	-.0004	84.5	7.03	-.053
	.0150	-.0011	57.5	11.72	-.146
	.0248	-.0021	80.2	16.35	-.280
	.0318	-.0028	90.2	18.39	-.373
	.0408	-.0034	96.5	19.67	-.453
	.0458	-.0037	99.8	20.34	-.493
	.0600	-.0051	101.1	20.60	-.680
	.0839	-.0052	94.9	19.34	-.690
	.0923	-.0055	92.5	18.85	-.733
	.1033	-.0057	89.5	18.24	-.760
	.1089	-.0059	87.7	17.88	-.787
	.1282	-.0060	83.0	16.92	-.800
	.1363	-.0060	81.0	16.51	-.800
	.1456	-.0062	79.3	16.16	-.827
	.1577	-.0062	76.5	15.59	-.827
	.1648	-.0062	75.5	15.39	-.827
	.1737	-.0064	74.0	15.08	-.853
	.1897	-.0064	71.7	14.61	-.853
	.2031	-.0067	70.7	14.41	-.893
	.2324	-.0067	68.0	13.86	-.893
Second Shearing	0	-.0101	0	0	-1.350
	.0038	-.0104	5.8	1.18	-1.390
	.0170	-.0104	36.0	7.34	-1.390
	.0230	-.0104	37.2	7.58	-1.390
	.0314	-.0104	39.9	8.13	-1.390
	.0439	-.0108	42.4	8.64	-1.440
	.0560	-.0110	44.0	8.97	-1.470
	.0914	-.0112	46.5	9.48	-1.490
	.1230	-.0113	49.0	9.99	-1.510
	.1387	-.0114	49.5	10.09	-1.520
	.1708	-.0114	51.0	10.40	-1.520
	.2050	-.0114	52.5	10.70	-1.520
	.2407	-.0114	54.5	11.11	-1.520

(Cont'd.)

Number of Shearing	Displacement Inch	Δh Inch	Load Lb.	Shearing Resistance psi	$\frac{\Delta V}{V}$ %
Third Shearing	0	-.0137	0	0	-1.830
	.0061	-.0138	10.5	2.14	-1.840
	.0146	-.0138	28.5	5.81	-1.840
	.0440	-.0140	35.0	7.13	-1.870
	.1028	-.0144	39.0	7.95	-1.920
	.1347	-.0145	41.5	8.46	-1.930
	.1543	-.0145	43.8	8.93	-1.930
	.1878	-.0145	46.5	9.48	-1.930
	.2012	-.0145	47.5	9.68	-1.930
	.2624	-.0145	50.6	10.31	-1.930
	.2762	-.0145	50.8	10.35	-1.930
Fourth Shearing	0	-.0157	0	0	-2.090
	.0059	-.0157	13.7	2.79	-2.090
	.0163	-.0155	31.5	6.42	-2.070
	.0837	-.0159	36.0	7.34	-2.120
	.1009	-.0159	36.5	7.44	-2.120
	.1247	-.0159	37.5	7.64	-2.120
	.1482	-.0159	38.5	7.85	-2.120
	.1711	-.0160	42.0	8.56	-2.130
	.1845	-.0160	43.0	8.77	-2.130
	.2419	-.0160	46.7	9.52	-2.130
	.2519	-.0160	47.5	9.68	-2.130
Fifth Shearing	0	-.0162	0	0	-2.160
	.0131	-.0162	15.1	3.08	-2.160
	.0158	-.0170	26.4	5.38	-2.270
	.0280	-.0173	29.5	6.01	-2.310
	.0577	-.0177	32.5	6.63	-2.360
	.0816	-.0178	33.7	6.87	-2.370
	.1465	-.0178	36.2	7.38	-2.370
	.1627	-.0178	38.5	7.85	-2.370
	.1990	-.0178	42.5	8.66	-2.370
	.2395	-.0178	44.8	9.13	-2.370
	.2496	-.0178	46.5	9.47	-2.370
Sixth Shearing	0	-.0178	0	0	-2.370
	.0095	-.0182	22.2	4.53	-2.430
	.0615	-.0192	32.0	6.52	-2.560
	.1146	-.0192	34.0	6.93	-2.560
	.1592	-.0192	38.5	7.85	-2.560
	.2350	-.0192	43.5	8.87	-2.560
	.2430	-.0192	45.7	9.30	-2.560
	.2470	-.0192	46.0	9.37	-2.560